Discovery of a conserved *Plasmodium* antigen on the surface of malaria parasite-infected red blood cells

Eugene Kojo Oteng

Green Templeton College

University of Oxford

A thesis submitted for the degree of

Doctor of Philosophy

Trinity 2013

Dedication

Unto Him who is able… - Jude 1:24

Acknowledgements

I am deeply grateful to my supervisors, Carole Long and Chris Newbold, for their trust and support throughout this project. I would also like to thank my past mentors, Luke Alphey and Betty Pace, and my parents, Dr. and Mrs. Oteng, each of whom have encouraged me to challenge what is thought impossible. Although too numerous to name individually, I would also like to thank my labmates and colleagues whom I am privileged to now call friends. Finally, I would like to acknowledge the National Institutes of Health Medical Scientist Training Program and Oxford-Cambridge Scholars Program for their support particularly Bridget Lampert, Mike Lenardo, Sarah Noujaim, and Richard Siegel.

Abstract: Discovery of a conserved *Plasmodium* antigen on the surface of malaria parasite-infected red blood cells. Eugene Kojo Oteng. Green Templeton College. Submitted for the degree of Doctor of Philosophy. Trinity 2013.

During its intraerythrocytic stages (IE), *Plasmodium falciparum,* the causative agent of the deadliest human malaria, remodels the host red cell membrane with a poorly defined assortment of parasite-encoded proteins that undergo antigenic variation. Despite the requirement for immunologic stealth, exported parasite proteins also mediate strain-independent functions such as endothelial sequestration that are critical for parasite survival and pathogenesis.

This thesis explores the hypothesis that *P. falciparum* displays novel structurally conserved proteins on the IE surface and these proteins may serve as useful antigens for a broadly effective anti-malarial vaccine. In order to test this hypothesis, we developed an *in vitro* selection technique that sequentially incorporates unique *P. falciparum* isolates as the targets for Systematic Evolution of Ligands by EXponential enrichment (Serial-SELEX) to generate nucleic acid molecular probes, aptamers, capable of recognizing conserved cell surface determinants. Ten of 11 enriched aptamers were -parasite selective and three of these aptamers demonstrated strain-independent binding to *P. falciparum.* Aptamer recognition extended beyond the parasites used in Serial-SELEX to other laboratory and recent field isolates. Surprisingly the same three broadly binding aptamer selected against *P. falciparum* also recognized all laboratory-adapted and clinical isolates of *P. vivax and P. knowlesi* tested, strongly supporting our hypothesis that structurally conserved molecules are present on the surface IEs. Competition studies showed that the aptamers bound a single target which was confirmed as an IE membrane protein. Aptamer-mediated affinity purification and tandem mass spectrometry enabled the definitive identification of the aptamer target as PfHSP90. Discovery of a protein conserved between the major human malarias may have implications for vaccine development and validates the Serial-SELEX technique as a powerful tool for antigen discovery.

Contents

Dedication ii

Acknowledgements iii

Chapter 1. Introduction 1

1.1 Malaria Biology 1

1.1.1 Malaria as a global health challenge 1

1.1.2 Discovery of the malaria parasite 1

1.1.3 Lifecycle and major advancements in the understanding of *P. falciparum* biology 2

1.1.4 Differences between *Plasmodium* species 8

1.2 Epidemiology and natural acquisition of immunity to malaria. 10

1.3 Malaria vaccine development 12

1.3.1 Pre-erythrocytic vaccines 12

1.3.2 Blood stage vaccines 14

1.3.3 Transmission blocking vaccines 14

Pfs25 is a parasite surface protein expressed on zygotes, ookinetes, and young oocyts that is a well known transmission vaccine candidate. An early vaccine formulation using Pfs25 as an immunogen was associated with systemic adverse events (112), however, newer formulations promise an improved safety profile. In terms of efficacy, vaccine-induced antibodies have been shown to reduce the transmission of *P. falciparum* in *in vitro* functional assays (113, 114). 15

1.3.4 Targeting IEs as an alternative to invasion-based blood stage vaccines 15

1.4 Proteins displayed on the IE surface 17

1.4.1 PfEMP1 17

1.4.2 New Permeation Pathway (NPP) 18

1.4.3 Other proteins associated with the IE membrane 20

1.5 Aptamers and SELEX 24

1.5.1 Theory and history 24

1.5.2 SELEX technology 25

1.5.3 SELEX against complex targets 29

1.5.4 Clinical applications of aptamers 31

1.6 Aim and scope of the thesis 34

Chapter 2. Materials and methods 35

2.1 Cell culture and basic techniques 35

2.1.1 MACS purification 35

2.1.2 Percoll/sorbitol purification 35

2.1.3 *P. falciparum* culture 36

2.1.4 *P. vivax* culture 36

2.1.5 *P. knowlesi* culture 37

2.1.6 Rodent parasites 37

2.1.7 *P. falciparum* and *P. vivax* isolates from Cambodia 37

2.1.8 *P. falciparum* and isolates from Mali 38

2.1.9 Display of the aptamer target at various stages in the parasite lifecycle 39

2.1.10 Temperature shifts in *P. falciparum* cultures 40

2.1.11 Inoculating *P. falciparum* into RBCs carrying mutant hemoglobin. 41

2.1.12 Growth inhibition assay 41

2.2 SELEX 43

2.2.1 SELEX libraries and primers 43

2.2.4 PCR conditions for SELEX 43

2.2.5 Digestion of phosphorylated strands of dsDNA for SELEX 44

2.2.2 Serial-SELEX 45

2.2.3 Neutral-SELEX 46

2.2.7 High-throughput sequencing 46
2.2.8 Filtering of Illumina sequences 47
2.3 Aptamer and protein characterization 48
2.3.1 DNA end-labeling 48
2.3.2 Aptamer binding assay 49
2.3.3 Aptamer competition assay 49
2.3.4 Protease susceptibility studies 50
2.3.5 Functionalization of streptavidin coated beads 50
2.3.6 Confocal microscopy 51
2.3.7 Flow cytometry 51
2.3.8 Aptamer-mediated affinity purification 52
2.3.9 Mass spectrometry and protein identification 52
2.3.10 Aptamer screen of recombinant proteins 54
2.3.11 Enzyme-linked immunosorbent assay (ELISA) 55
Chapter 3. Development and evaluation: Serial-SELEX to probe for conserved IE determinants 58
3.1 Introduction 58
3.1.1 Harnessing SELEX to probe for conserved IE determinants 58
3.1.2 Evaluating the dynamics of SELEX 59
3.2 Results 60
3.2.1 Monitoring the progression of aptamer selection 60
3.2.2 Validation of selected aptamers 62
3.3 Discussion 80
3.4 Supplemental information 82
3.5 Acknowledgement 83
Chapter 4. Characterization of the binding range of selected aptamers 85

4.1 Introduction **85**

4.2 Results **86**

4.2.1 Development of a quantitative aptamer binding assay 86

4.2.2 A select group of aptamers bind a wide range of *Plasmodium* 86

4.2.3 Parasitized HbAA, HbAS, and HbSS show similar levels of aptamer binding.. 94

4.3 Discussion **97**

4.4 Supplemental information **100**

4.5 Acknowledgements **106**

Chapter 5. Purification, identification, characterization of the aptamer target **108**

5.1 Introduction **108**

5.2 Results **109**

5.2.1 Broadly binding aptamers bind a common protein stably expressed on the IE surface 109

5.2.2 Identification of the aptamer protein target 115

5.2.3 Exploring the possible role of surface PfHSP90 121

5.2.4 Assessment of naturally acquired PfHSP90 antibody responses 121

5.3 Discussion **129**

5.4 Acknowledgements **134**

5.5 Supplemental information **135**

Chapter 6. Conclusions **166**

6.1 Main conclusions 166

6.2 Study limitations 168

6.3 PfHSP90 as a possible universal malaria vaccine target 168

6.4 PfHSP90 as a target for anti-malarial drugs 170

6.4 Using Serial-SELEX to probe for additional conserved IE determinants 172

6.5 Other applications of Serial-SELEX 174

6.6 Final remarks 174

Chapter 7. Bibliography 177

List of Tables

Table 1.1 Overview of final destination and putative function of selected exported parasite derived proteins 21

Table 2.1 SELEX libraries and primers used in study 43

Table 2.2 Components of the λ exonuclease reaction. 44

Table 2.3 Components of the DNA end-labeling reaction 48

Table 3.2. Sequences and guanine-cytosine content of selected aptamers. 67

Table 4.1. Using aptamers to recognize different *P. falciparum* laboratory lines 89

Table 4.2. Aptamer recognition of *P. falciparum* clinical isolates 91

Table 4.3. Aptamer recognition of *Plasmodium vivax* 93

Table 4.4. Aptamer recognition of other *Plasmodium* species 95

Supplemental Table 4.1 Transformation of raw data from an aptamer binding assay: Raw data. 100

Supplemental Table 4.2 Transformation of raw data from a binding assay: Specific activity of aptamer used in the study. 101

Supplemental Table 4.3 Transformation of raw data from an aptamer binding assay: Data normalized by specific activity. 102

Supplemental Table 4.4 Transformation of raw data from an aptamer binding assay: Average value of RDM was used to establish background binding. 103

Supplemental Table 4.5 Transformation of raw data from an aptamer binding assay: Fold difference above background. 104

Supplemental Table 4.6 Calculation of number of aptamer binding sites to indicated cells. 105

Supplemental Table 5.1. Proteins identified in ~250 kDa region excised from oligopreciptiation with RDM. 135

Supplemental Table 5.2. Proteins identified in ~250 kDa region excised from oligopreciptiation with Euge.4.....136
Supplemental Table 5.3. Proteins identified in ~90 kDa region excised from oligopreciptiation with RDM. 139
Supplemental Table 5.4. Proteins identified in 90 kDa region excised from oligopreciptiation with Euge.4.....141
Supplemental Table 5.5. Top 20 human proteins identified in all bands excised from RDM and Euge.7 oligopreciptiations.....143
Supplemental Table 5.6. Top 200 *P. falciparum* proteins identified in all bands excised from RDM and Euge.7 oligopreciptiations.....154

List of Figures

Figure 1.1. Schematic of *P. falciparum* lifecycle. Reproduced from Miller *et al.* (28) 3

Figure 1.2. Illustration of the IE parasite ultrastructure and PEXEL-protein transport. 4

Figure 1.3. Single stranded nucleic acids can fold in complex shapes to bind specific targets 24

Figure 1.4. Schematic of a typical SELEX experiment 25

Figure 3.1 Schematic representation of Serial-SELEX procedure to generate ssDNA aptamer binding to conserved IE determinants. 61

Figure 3.2 Alignment of Serial-SELEX pools reveals enrichment of unique sequences that can be grouped into aptamer families. 65

Figure 3.3 Deep sequencing of the final pools reveals enrichment of multiple aptamers. 66

Figure 3.4 Euge.1 binding curve. 68

Figure 3.5 Euge.2 binding curve. 69

Figure 3.6 Euge.3 binding curve. 70

Figure 3.7 Euge.4 binding curve. 71

Figure 3.8 Euge.5 binding curve. 72

Figure 3.9 Euge.6 binding curve. 73

Figure 3.10 Euge.7 binding curve 74

Figure 3.11 Euge.8 binding curve 75

Figure 3.12 Euge.9 binding curve 76

Figure 3.13 Euge.10 binding curve. 77

Figure 3.14 Euge.11 binding curve. 78

Figure 3.15 RDM binding curve. 79

Supplemental Figure 3.1 Alignment of selected aptamers 82

Figure 4.2 Aptamer binding assay has limited variation. 88

Figure 4.3 Hemoglobin polymorphisms do not affect aptamer binding. 96

Figure 5.1 Reciprocal competition between radiolabeled and unlabeled broadly binding aptamers indicate recognition of a shared determinant. 110

Figure 5.2 Pre-treating IEs with extracellular protease abolishes Euge.4 binding. 112

Figure 5.3 Aptamer-functionalized fluorescent beads recognize an IE surface protein. 113

Figure 5.5. Preliminary purification of aptamer targets. 116

Figure 5.6. Isolation of aptamer specific proteins 117

Figure 5.7. Euge.4 binding to IEs is independent of KAHRP expression. 120

Figure 5.8. Euge.4 specifically recognizes recombinant PfHSP90. 123

Figure 5.9 Euge.4 binds recombinant PfHSP90 with high affinity 124

Figure 5.10 PfHSP90 is detected exclusive on surface of IEs. 125

Figure 5.11 Display of PfHSP90 is unaffected by heat shock pre-treatment 126

Figure 5.12 Broadly-binding aptamers have no effect on the *in vitro* development of *P. falciparum*. 127

Figure 5.13 Prevalence of antigen-specific IgG among 24 Malian adult sera 128

List of Abbreviations

BSA - Bovine serum albumin

Bq – Becquerel

cDNA - Complementary deoxyribonucleic acid

CPM – Counts per minute

Da - Dalton

DNA - Deoxyribonucleic acid

EDTA - Ethylenediaminetetraacetic acid

ELISA – Enzyme-linked immunosorbent assay

FBS - Fetal bovine serum

HEPES - 2-[4-(2-hydroxyethyl)piperazin-1-yl]ethanesulfonic acid

IgG - Immunoglobulin G

PAGE - Polyacrylamide gel electrophoresis

PBS - Phosphate buffered saline

PCR - Polymerase chain reaction

PSM- Peptide-spectrum match

RNA - Ribonucleic acid

RT- Room temperature

SELEX - Systematic evolution of ligands by exponential enrichment

SEM – Standard error of the mean

SDS - Sodium dodecyl sulfate

tRNA - Transfer ribonucleic acid

Chapter 1. Introduction

1.1 Malaria Biology

1.1.1 Malaria as a global health challenge

Malaria continues to exact a devastating toll in terms of both human mortality and socio-economic burden. Each year an estimated 250 million cases of malaria lead to nearly 1 million deaths (1). Fully 86% of those deaths are of children under 5 years of age. In countries with a heavy malaria burden, the disease may account for as much as 40% of public health expenditure, 30-50% of inpatient admissions, and up to 50% of outpatient visits (2). Recently, massive scale-up of control strategies aimed at treatment of infections with artemisinin-based combination therapies and preventative measures aimed at vector abatement have contributed to the downward trend in malaria deaths in several endemic areas (3, 4). Nevertheless, eradication remains a distant goal and worrisome cracks have emerged in our defenses with the development of parasite resistance to all currently used antimalarials including artemisinin and mosquito resistance to DDT and other commonly used insecticides (5–7). Development of a broadly effective malaria vaccine remains a global health priority (8, 9).

1.1.2 Discovery of the malaria parasite

Spurred by Pasteur and Koch's germ theory of disease in 1879, Alphonse Laveran, a student of Pasteur, discovered *Plasmodium* are the protozoa responsible for malaria in 1880 (10, 11). Less than two decades later, Ross identified mosquitoes as the route of

transmission for avian malaria (12) and Grassi and colleagues found that mosquitoes act as the human malaria vector (13). Ross was awarded the Nobel prize in 1902:

> *"for his work on malaria, by which he has shown how it enters the organism and thereby has laid the foundation for successful research on this disease and methods of combating it"* (14).

1.1.3 Lifecycle and major advancements in the understanding of *P. falciparum* biology

The host range for *Plasmodium* includes birds, reptiles, and mammals such as rodents, primates, and humans. Five species of *Plasmodium* are known to infect humans: *P. falciparum*, *P. vivax*, *P. ovale*, *P. malariae*, and *P. knowlesi* which is an increasingly important zoonotic infection. *P. falciparum* is the most intensively studied and deadly of the human malarias. Its lifecycle, depicted in Figure 1.1**,** spans a vertebrate host, an invertebrate vector, and a number of cell types.

Pre-erythrocytic stages. During a blood meal, a female anopheline mosquito injects sporozoites into the subcutaneous tissues of the human host that then migrate to the liver where they infect hepatocytes. A few hundred sporozoites can be deposited by a single mosquito bite (15), the majority of which home to liver sinusoids using multifunctional circumsporozoite protein (CSP) and a unique gliding motility system mediated by thrombospondin-related anonymous protein (TRAP) (16–19). In a rodent model of infection, some 30% of sporozoites deposited proceed to lymph nodes draining the site of sporozoite inoculation where they prime dendritic cells following

destruction (20–23). There is some evidence that a small fraction of sporozoites may develop in the dermis and produce infective merozoites, fully circumventing the hepatic stage (24). Infection with Plasmodium appears to restrict hepatocyte programmed cell death and normal immune surveillance mechanisms (25, 26). Much of this immunosuppressive effect is mediated by CSP which has been shown to inhibit the activation of NF-κB leading to reduced class I major histocompatibility complex (class I MHC) expression on the cell surface (27).

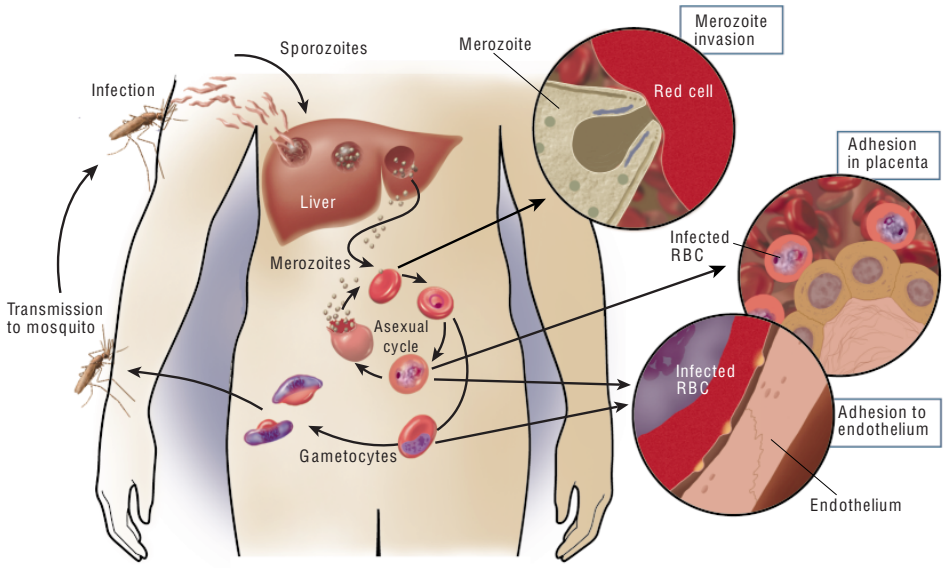

Figure 1.1. Schematic of *P. falciparum* lifecycle. Reproduced from Miller *et al.* (28)

Over the course of about 6-7 days, parasites undergo multiple asexual divisions inside the hepatocyte to become mature schizonts. Schizont rupture releases merozoites that rapidly invade erythrocytes and begin the asexual erythrocyte cycle.

IE stages. Disease – including fever, anemia, lactic acidosis, and in some cases coma

and death (for review see Miller *et al.*, 2002) – occurs only after the parasite leaves the liver and invades red blood cells (RBCs). Erythrocyte invasion is a complex series of highly ordered events that has been extensively reviewed (28, 29). Merozoites display phenotypic variation in which different strains express a variant combination of ligands that bind specific erythrocyte receptors (30). Only a handful of host parasite invasion pairs have been reported, including glycophorin A for EBA-175, glycophorin B for EBL-1, glycophorin C for EBA-140, complement receptor 1 (CD35) for *Pf*RH4, and basigin (CD147) for *Pf*RH5 (31–37). With the notable exception of RH5, all parasite invasion receptors known thus far can be deleted suggesting that invasion is mediated by redundant host-parasite interactions. Recent studies of RH5, however, have challenged that notion. RH5 function cannot be compensated (38, 39) and antibodies directed against RH5 or its host ligand, basigin, efficiently block invasion of a wide variety of *P. falciparum* clones including short-term adapted field isolates (36, 37, 40, 41).

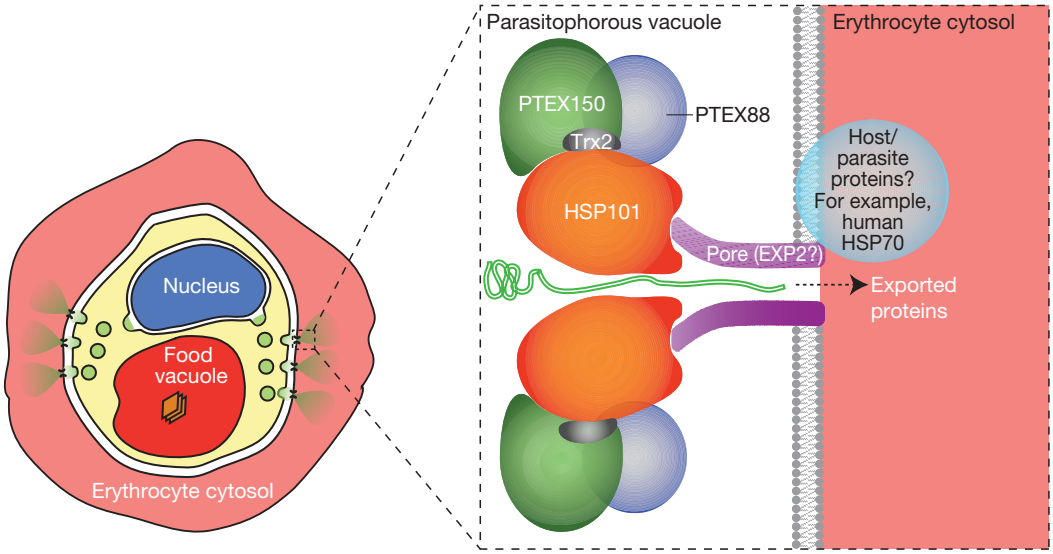

Figure 1.2. Illustration of the IE parasite ultrastructure and PEXEL-protein transport.

Reproduced from de Koning-Ward *et al.* (42)

RBC invasion occurs in less than two minutes whereas intraerythrocytic development takes about 2 days. As it is internalized, the membrane formed initially by invagination of the RBC membrane during merozoite invasion envelops the parasite to become the parasitophorous vacuole (PV) membrane. Once internalized, parasites undergo extensive morphological changes and export proteins that dramatically remodel the host cell membrane and cytoskeleton. Exported proteins must then traverse several membrane systems including the parasite plasma (PP) membrane and the PV membrane to access the highly structured red cell membrane. The parasite's ultrastructure and a model for protein export are shown in Figure 1.2. Transport of selected proteins is facilitated by a conserved *Plasmodium* export element (PEXEL) (43) or host targeting (HT) motif (44). A parasite-encoded aspartic protease, Plasmepsin V, cleaves PEXEL and HT sequences in the endoplasmic reticulum and directs proteins to an ATP-driven translocon complex, PTEX, which injects proteins across the PV into the red cell cytosol (42, 45, 46).

Discovery of PTEX is a major advance in malaria biology. Early models of protein export outside the parasite placed the PP membrane in apposition to the PV membrane. Select fusion of the bi-layers would allow a single step translocation of protein destined for export (47)**,** however**,** no sites have been identified where the PP membrane and PV membrane are fused. A more complex two-step export pattern was also proposed; fusion of transport vesicles at the PP membrane releasing soluble protein through some, in the parasitophorous vacuole or inserting membrane protein into the PPM followed by translocation. A folded polypeptide would likely require a

chaperone to translocate through the membrane.

In support of the two-step model, membrane bound structures 60-100 nm in diameter were described budding from the PP membrane and PV membrane interspace (48). Then in 2009, de Koning-Ward *et al.* reported the identification of the long sought translocon complex. The group identified the *Plasmodium* translocon of exported proteins (PTEX) as the route by which parasite proteins enter the host RBC (30). PTEX is comprised of five proteins: a heat shock protein with ATPase activity, HSP101; a protein of no known function termed PTEX150; the apparent membrane component, EXP2; and two accessory proteins. Proteins known to be exported to the host cytosol were shown to specifically interact with PTEX through reciprocal immunoprecipitation (42, 49). Subsequent studies supporting the proposed model of PTEX function have polypeptides being unfolded by the N-terminus of HSP101 and then passing through EXP which is thought to be the membrane-spanning portion of the translocon (50). The ATP dependence of HSP101 function and its central role in PTEX translocation is consistent with previous studies showing ATP dependence of glycophorin binding protein transport into the host cytosol (51).

Passage through the PTEX affords access to host red cell cytosol where some exported proteins will be trafficked to the RBC surface via either the Maurer's clefts or the tubovesicular network, membrane bound organelles synthesized *de novo* by the parasite (52). Exported proteins may mediate IE adhesions to various host cells (53–56), loss of cellular deformability (57, 58), and antigenic variation (59).

Continued development of the parasite within RBCs is characterized by several rounds of nuclear division resulting in schizont forms containing 16-20 merozoites. Merozoite release is a lytic process regulated at least in part by a parasite kinase and parasite proteases which trigger host proteases (60, 61). These events are apparently downstream of parasite-initiated triggering of host G protein-coupled receptor signaling which ultimately leads to increased activation of host calpain and weakened cytoskeletal membrane through pathological influx of Ca^{2+} (62).

Sexual stages. Whereas the majority of the released merozoites propagate asexually, a small fraction commit to development of crescent shaped gametocytes following invasion. These sexual stage gametocytes are taken up when a female mosquito takes in a blood meal. In the mosquito midgut gametocytes develop into male and female gametes. Fertilization creates a motile ookinete that penetrates the midgut wall where it forms an oocyst. Few oocytes are formed but they are capable of releasing large numbers of sporozoites that migrate to mosquito salivary glands to be transmitted into the next host.

Plasmodium parasites face a variety of innate immune mechanisms and suffer significant losses during their development within the mosquito vector. In 2002, a field-study identified a subpopulation of field Anopheles carrying loci that completely protect mosquitoes from infection. A follow up genetic-mapping survey conducted in West Africa (63) mapped resistance to loci on chromosome 2L to the same genomic

region later associated with studies of East African *A. gambiae* malaria resistance, suggesting a widespread presence of a host factor that controls malaria transmissibility (64). Delineating the genes and molecular mechanisms mediated in mosquito refractoriness has been an area of active research. In addition, non-genetic factors also determine transmission efficacy of the *Plasmodium* within *A. gambiae*. Cirimotich and colleagues report that reactive oxygen species from certain bacteria that constitute the flora of mosquito midgut have an anti-*Plasmodium* effect that can make the mosquito refractory to infection (65).

1.1.4 Differences between *Plasmodium* species

All species of *Plasmodium* share the significant features of the *P. falciparum* lifecycle, however, there are important variations. For example, *P. knowlesi* completes its asexual lifecycle in 24 hours, 48 hours in the case of *P. falciparum, P. ovale,* and *P. vivax,* and 72 hours for *P. malariae.* Importantly, *P. vivax* and *P. ovale* parasites can produce a dormant form, the hypnozoite. This can remain in the hepatocyte for a period from 17 days to over a year before being reactivated to develop as an exo-erythrocytic schizont, provoking a relapse of the disease (66). *P. vivax* is generally unable to invade erythrocytes lacking the Duffy antigen receptor which may explain why in western Africa, where the Duffy negative genotype is predominant, there is no *P. vivax* in that region (67–69). However, it appears that Duffy antigen-independent red cell invasion is possible because *P. vivax* parasites have recently been observed inside Duffy-negative erythrocytes in Madagascar and elsewhere (70, 71)**.** Finally, *P. falciparum* can invade a large percentage of RBCs, whereas *P. vivax* invasion is limited to reticulocytes. Reticulocytes are a rare

subpopulation of immature RBCs and as a as a consequence infection by *P. vivax* rarely leads to high parasitemia and generally causes a milder clinical course than *P. falciparum*.

1.2 Epidemiology and natural acquisition of immunity to malaria.

Malaria occurs throughout much of the tropical regions of the world, with *P. falciparum* predominant in Africa where 90% of all malaria deaths occur (72, 73). *P. vivax* is common in Central and South America and the prevalence of the two species is approximately equal in South and East Asia and the Pacific Islands (67, 74).

Endemicity is generally defined in terms of parasitemia rates and can range from hypoendemic (≤10 percent) to holoendemic (≥75 percent). Parasite prevalence rates are a function of infectious bites by female anopheline vectors which in turn are dependent on vector ecology and epidemiological control measures such as indoor residual spraying. Infection with malaria parasites is not always associated with symptoms as parasites can be found in a high proportion of otherwise healthy individuals. Even as parasites multiply during the lytic asexual stages, there appears to be poor correlation between parasite density and morbidity (75).

If symptoms do develop, they are generally mild and include fever, chills, headache, and occasionally gastrointestinal symptoms such as vomiting or diarrhea which generally resolve often with medication (76). In a small fraction of patients, severe malaria may arise independent of parasite density. Severe malaria is characterized by respiratory distress, severe anemia (Hb < 5 g/dL), or impaired consciousness (Blantyre coma score < 3) characteristic of parasite sequestration in the brain (77).

These syndromes may be present in combination within a given individual and can be accompanied by jaundice, hypoglycemia, and renal failure (76–78).

Despite variation in transmission rates and disease outcomes, it has been consistently observed that patients with repeated infection develop limited, non-sterilizing immunity to malaria. This partial immunity prevents symptomatic and severe illness and controls the blood-stage infection. In hyperendemic regions, immunity is generally insignificant before the age of five but well-developed by the age ten (79, 80). Protection from severe disease, however, seems develop after one or two infections (81). These observations have provided strong rationale for malaria vaccine development with the hope that an effective vaccine would induce in a child a likeness of adult immunity.

1.3 Malaria vaccine development

1.3.1 Pre-erythrocytic vaccines

Every stage of the parasite life cycle in humans presents the host immune system with diverse targets, some of which have been the focus of vaccine development. The rationale for pre-erythrocytic vaccines centers around the seminal observation that vaccination with irradiated sporozoites results in sterile protection in murine models and humans (82, 83). Subsequent studies suggested that much of that immunity could be achieved by immunization with CSP alone (84), although recent work using mice tolerized to CSP and work with protein arrays suggests that other antigens can also confer sterile protection (85, 86). The leading malaria vaccine candidate, RTS,S, utilizes the immunodominant epitope of CSP. This vaccine is being assessed in a Phase 3 trial at 11 sites in seven countries in sub-Saharan Africa. Results from Phase 2 and early Phase 3 cohorts show that RTS,S confers limited, non-sterile protection in 30-50% of participants (87, 88). Analysis of 200 children living in a single site in Kenya found that vaccine efficacy over a 4-year period was 17% (89). Clinical efficacy waned over the course of observation and vaccine efficacy against all episodes of clinical malaria varied by transmission intensity (89), corroborating earlier data from a trial in Mozambique and pooled analysis of data from RTS,S Phase 2 trials (90, 91). Thus it is unclear what role RTS,S might play in achieving the two strategic goals set out by the global malaria research community as part of the Malaria Vaccine Technology Roadmap: a vaccine that is 50% protective against severe disease and death by 2015, and a vaccine that prevents 80% of clinical malaria

episodes by 2025 (8).

The availability of a standardized human challenge model has accelerated the search for alternative vaccine targets and more powerful formulations. Following experimental vaccination, healthy human volunteers are exposed to bites from five infectious *Anopheles stephensi* fed on *P. falciparum* NF54 or the NF54 derivative, 3D7. Nearly 100% of unprotected volunteers develop parasitemia with the average time to detection by thick blood smear 6-7 days. Following microscopically detectable blood-stage infection, volunteers are immediately treated with curative drug regimens to minimize the clinical risk. Vaccine efficacy is generally interpreted as a reduction in liver-stage burden or delay in the time to blood-stage patency. This human challenge model was used to demonstrate the efficacy of RTS,S providing justification for large field trials in naturally exposed populations (92–94). Conversely, the lack of human challenge efficacy was clear indication to halt and re-evaluate a number of other vaccine candidates (95–98) . More recently, Ewer et. al. showed that a prime-boost regimen using chimpanzee-derived simian adenovirus and modified virus Ankara expressing ME-TRAP (a multi-epitope string fused to TRAP) conferred sterile protective immunity and delayed time to patency in 21% and 36% of human volunteers, respectively (99). Interestingly, protection correlated to the strong induction of vaccine-induced CD8+: nearly all other vaccination regimens, including RTS,S, likely act by CD4+ antibody-mediated response (99).

1.3.2 Blood stage vaccines

Vaccines that target the asexual erythrocytic stages are aimed at reducing or preventing infection generally by blocking invasion. It is known that antibodies are a key component of blood-stage immunity because passive transfer of IgG from immune adult Africans to Thai adults (100) or African children (101) rapidly reduces parasitemia and fever. Maternally derived antibodies can protect neonates and infants from *P. falciparum* infection (102). Few blood stage antigens have been tested in humans and none have exhibited significant clinical efficacy in Phase 2 trials (103, 104). One major factor is extreme polymorphism and complexity of invasion pathways. A study of the genetic diversity of AMA-1, a leading vaccine antigen associated with merozoite invasion, identified 214 unique haplotypes among 506 human infections (105). Studies suggesting that AMA-1 haplotypes could be grouped into 5 or 6 genetic populations are supported by the observation that monovalent AMA-1 gives strain-specific immunity (106–108). Hope that a multivalent formulation could provide coverage against most AMA-1 alleles is tempered by the observation that immunization with a simple divalent AMA-1 formulation showed neither overall nor allele-specific efficacy (106). More recent data suggest that a mixture of 4-5 allelic forms of AMA-1 may elicit strain-transcending immunity (107).

1.3.3 Transmission blocking vaccines

Finally, there is renewed interest in transmission blocking vaccines that would direct antibodies to the parasite sexual stages with the aim of interrupting parasite development inside the mosquito midgut (109). The feasibility of this approach is

supported by the observation of transmission-blocking antibodies in individuals living in endemic areas (110, 111). However, there are ethical concerns about deploying a vaccine that would not directly confer protection to individuals but instead protect communities through so-called "herd immunity." Moreover, sexual stage antigens can be difficult to produce and relatively high titers seem to be required to block transmission (112). Nevertheless, the approach enjoys support since it is the scheme most in line with eradication efforts.

Pfs25 is a parasite surface protein expressed on zygotes, ookinetes, and young oocyts that is a well known transmission vaccine candidate. An early vaccine formulation using Pfs25 as an immunogen was associated with systemic adverse events (113), however, newer formulations promise an improved safety profile. In terms of efficacy, vaccine-induced antibodies have been shown to reduce the transmission of *P. falciparum* in variety of functional assays (114, 115).

1.3.4 Targeting IEs as an alternative to invasion-based blood stage vaccines

A strong case can be made for directly targeting IE parasites for vaccination. While malaria parasites invade many human and mosquito cell types, immunity to IE forms is likely essential for controlling disease (116, 117). IEs are responsible for all of the pathology associated with malaria and are a major target of naturally acquired immunity. In endemic areas, imperfect, non-sterilizing immunity develops after repeated infection and is thought to be mediated by antibody responses to IEs as shown by passive transfer experiments (118, 119). Indeed, children who fail to generate an immune response to the infected erythrocyte surface are at increased risk

of developing clinical malaria (117). Cellular as well as innate immune mechanisms may also contribute to acquired protective immunity (120–122). Furthermore, the long-term protective component of the most clinically advanced malaria vaccine, RTS,S, may not be against the liver stages as originally designed but directed against the blood stages via parasite breakthrough and exposure to IEs and subsequent acquisition of blood-stage immunity (90). Experimental infection with low levels of blood-stage parasites appears very efficient at inducing complete protection (123). Although there are confounding issues with this study in humans, subsequent studies in murine models have reported similar results (124).

The current suite of blood-stage vaccine candidates aim to block merozoite invasion of red blood cells, a rapid process that occurs in less than two minutes and involves a complex and often redundant constellation of host receptors and polymorphic parasite ligands. Parasite proteins displayed on the surface of IE may represent a more stable target, as they must be exposed to potential immune effectors in the blood for long periods of time. Moreover, some IE surface proteins may have conserved functions and possibly structure across genetically distinct parasite isolates. Vaccine-induced antibodies against conserved proteins may be especially potent, acting to disrupt parasite biology while mediating opsonophagocytic activity.

1.4 Proteins displayed on the IE surface

1.4.1 PfEMP1

Few parasite proteins have been experimentally localized to the IE surface. *P. falciparum* erythrocyte membrane protein 1 (PfEMP1) is the parasite's main virulence and cytoadherence ligand and also the best characterized IE surface protein (125–127). Display of PfEMP1 allows IEs to adhere to the lining of capillary blood vessels avoiding elimination in the spleen (128, 129). While PfEMP1 expression is crucial for sequestration and therefore pathogenesis, its expression on the RBC surface also exposes it to host immune responses. Consequently, during the course of infection, *P. falciparum* undergoes clonal antigenic variation by switching between its approximately 60 extremely polymorphic *var* genes per haploid genome to evade host immune recognition and response (125, 127). Parasite isolates contain different complements of *var* genes, thus, the global gene repertoire is very large (130, 131). Transcriptional regulation generally allows for only a single *var* gene/PfEMP1 variant to be expressed at any one time (132–134). Epigenetic mechanisms (135–137) and nuclear repositioning (138) may also regulate allelic exclusion. *In vitro*, some parasites switch to expressing a different *var* gene at up to 2%/generation (139). Which *var* gene is selected may be non-random and determined by a structured switching pathway (140).

Periodic switching between *var* genes correlates with immune evasion, alternate adhesive properties of infected erythrocytes, and the periodicity of symptoms of infection (141). Certain *var* genes and *var* gene clusters have been mechanistically

linked to different clinical manifestations of malaria. *P. falciparum* infection during pregnancy leads to the sequestration of IEs in the placenta causing maternal anemia as well as intrauterine growth retardation, premature birth and increased infant mortality (142, 143). A single PfEMP1 variant, VAR2CSA, binds placental chondroitin sulfate A and is strongly associated with placental malaria (54, 144–148). More recently, it has been found that Var/PfEMP1 variants from group A and B/A proteins termed DC8 and DC13 are preferentially expressed in parasites that bind to human brain endothelial cell *in vitro* and are differentially expressed in children diagnosed with severe malaria as compared to those with uncomplicated malaria (149–152). Underscoring the link between clinical manifestations and PfEMP1 display, reduced presentation of PfEMP1 may be the mechanism by which individuals heterozygous for hemoglobin C and S are afforded protection from the most serious complications of malaria (153–155).

1.4.2 New Permeation Pathway (NPP)

It has been known for decades that *P. falciparum* dramatically increases the permeability of the host cell plasma membrane to a wide range of serum solutes 15-20 hours post invasion, presumably to facilitate its rapid growth and division inside metabolically quiescent red blood cells (156–159). Radiotracer uptake and hemolysis studies demonstrate that monosaccharides, amino acids, nucleosides, monocarboxylates, and monovalent inorganic anions all pass through this influx phenomenon which is commonly termed the NPP and is thought to be comprised of an anion-selective channel or set of channels ((160–162), for a review see Sherman 2008). The biological importance of the NPP is unclear for most solutes. However, for

L-glutamate, an amino acid that must be present in the extracellular medium to support *in vitro* culture, the rate of influx through endogenous transporters is insufficient to sustain growth and therefore the NPP may be essential for survival (163). In the case of pantothenic acid, another essential vitamin, the NPP is the sole route of entry into IEs because uninfected mature human erythrocytes lack a functional pantothenate transporter (164, 165). Furthermore, ion channel blockers such as furosemide (166), dantrolene (167), and their derivatives (168, 169) kill parasites by abolishing NPP-mediated flux, limiting access to essential soluble serum nutrients.

Nguitragool *et al.* now report an important breakthrough as they identify parasite-encoded CLAG3 proteins as key determinants of NPP activity (170). They convincingly correlate *clag3* expression with NPP influx and demonstrate that CLAG3 proteins are exposed on the erythrocyte surface. However, it appears unlikely that CLAG3 proteins directly form a channel. These proteins have limited homology to any of the five known anion channel gene families and they lack discernable transmembrane regions. Moreover, *P. falciparum* can tolerate disruption of *clag3* genes and *clag3*-null parasites grow at only subtly reduced rates *in vitro*, observations inconsistent with the central role of the NPP in parasite nutrient acquisition (171). Therefore, despite its likely importance in parasite biology and potential as a drug and vaccine target, the complete molecular composition and genetic origin of the NPP remain elusive.

1.4.3 Other proteins associated with the IE membrane

Other proteins have been localized to the IE membrane and have been implicated in knob formation and anchoring of variant surface antigens. Table 1.1 presents an overview of their subcellular localization and putative function.

Table 1.1 Overview of final destination and putative function of selected exported parasite derived proteins

Protein	Location	Predicted export signal	Putative function, interacting partners, remarkable features	Reference
PfEMP1	MC, RBC membrane, RBC surface	PEXEL-like motif	Cytoadherence ligand. Involved in antigenic variation. Interacts with KAHRP	59,161,162
RIFIN/STEVOR	RBC cytoplasm, RBC surface	RXLXE/D, RXLXQ	May be surface-exposed in late stages. Possibly involved in antigenic variation	163,164
KAHRP	RBC skeleton	RXLXQ	Binds to RBC spectrin–actin and to the ATS of PfEMP1. Essential for knob formation. Deletion decreases RBC rigidity and adhesion under flow conditions	165,166
MESA/PfEMP2	RBC skeleton	RXLXE	Binds to protein 4.1R. May disrupt p55–4.1R interaction	57, 167

Protein	Location	Predicted export signal	Putative function, interacting partners, remarkable features	Reference
RESA/Pf155	RBC skeleton	RXLXGE	Binds to spectrin. Deletion increases heat-induced membrane vesiculation. May stabilize RBC membrane. May prevent invasion of already parasitized RBCs	168-170
PfEMP3	MC, RBC skeleton	RXLXE	Binds to spectrin. Disrupts spectrin–actin–4.1R interaction. Appears to be involved in PfEMP1 trafficking. Repeat region	171, 172
Clag3.1/3.2	IE surface		Possible component of the NPP	159

Efforts to define which of the parasite's estimated 5,000 gene products are exported to the IE surface are still quite nascent despite the advent of *in vitro* culture to recover large amounts of protein and complete sequencing of the *P. falciparum* genome (184, 185). A putative secretome of ~400 proteins has been described based on the presence of an export signal sequence, but it is unclear which proteins exported out of the parasite are eventually trafficked to IE surface (43, 186). There has been some progress in better defining the *Plasmodium* proteome (187–189), but definitive identification of IE surface proteins has proven a challenge due the lack of *Plasmodium*-specific reagents, general low expression of parasite protein relative to amounts of endogenous protein, and differences in expression between well-characterized clones and recent field isolates (175, 188, 190). Furthermore, high-throughput evaluation of the structure of *Plasmodium* membrane proteins remains challenging due to their large multi-domain arrangement and recalcitrance to heterologous expression. Taken together, there are few options to evaluate the identity and structure of IE surface proteins.

A malaria vaccine directed against structurally constrained epitopes would be broadly efficacious and serve as a novel tool for malaria eradication. However, targeted epitope discovery remains a major technical barrier for conventional genomic and proteomic techniques. We propose to address this with an aptamer-based approach.

1.5 Aptamers and SELEX

1.5.1 Theory and history

Nucleic acids were considered simply passive carriers of information until the discovery of the catalytic activity of RNAs (191, 192). Numerous types of RNAs have been discovered which exhibit function without being translated into protein such as rRNAs, tRNAs, ribozymes, riboswitches, and circular RNAs (193–196). These nucleic acids form complex three-dimensional structures to carry out cellular functions once thought only possible with protein (Figure 1.3), lending support to the RNA World hypothesis which proposes that prebiotic RNA molecules catalyzed all biological reactions (197).

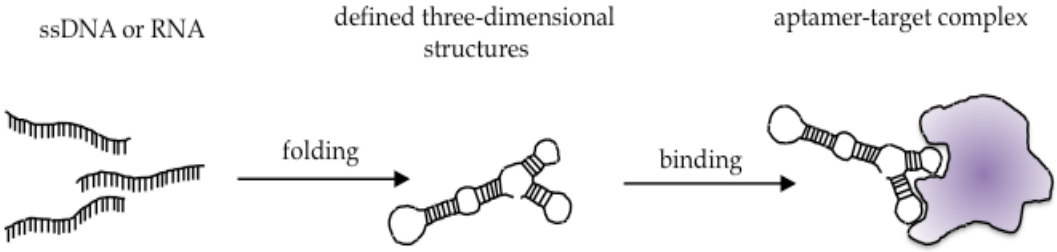

Figure 1.3. Single stranded nucleic acids can fold in complex shapes to bind specific targets

It soon became apparent that the immense combinatorial variety of nucleic acids and ease of manipulation could be harnessed for directed search for nucleic acid

sequences that exhibit predefined properties. Building on the observation that random dsDNA could be screened to identify the binding motif of a DNA binding protein (198), Tuerk and Gold selected synthetic RNA ligands that recognized bacteriophage T4 DNA polymerase (199). Independently, Ellington and Szostak isolated RNA with high affinity for a series of organic dyes used in affinity chromatography (200). The *in vitro* evolution technique developed was called 'Systematic Evolution of Ligands by EXponential Enrichment' (SELEX) and the high-affinity nucleic acids isolated were termed aptamers from the Latin root "aptus" which means "fitting."

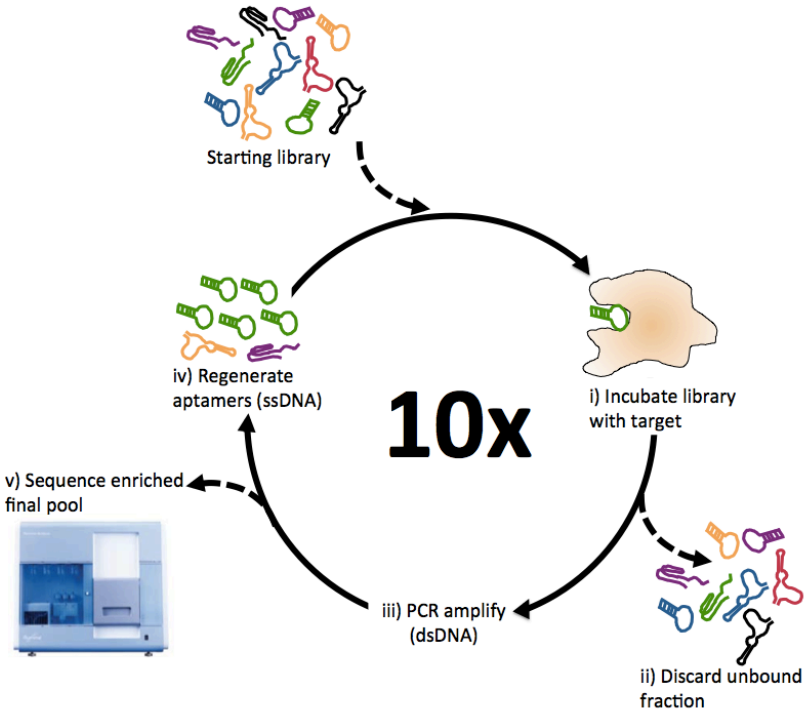

Figure 1.4. Schematic of a typical SELEX experiment.

1.5.2 SELEX technology

The SELEX experiment (illustrated in Figure 1.4) consists of iterative rounds of target binding selection, partitioning binding from non-binders, and nucleic acid

amplification. The experiment requires chemical synthesis of a large randomized nucleic acid library that acts as the substrate for combinatorial selection. A SELEX library features two components: 1) a randomized core of 30-40 bases that generates shape diversity as each molecule is directed to fold into a unique shape due to Watson-Crick and non-canonical interactions. 2) Flanking regions of known sequence that act as primers for aptamer-specific PCR amplification. For RNA selections, a T7 promoter is included in the flanking region so the library can be transcribed. The practical size of the average SELEX library (10^{15} unique sequences) is only a fraction of the theoretical sequence space (4^{40} for a 40N library) but sufficient for *in vitro* selection. As comparison, the total diversity of the human IgM pool is estimated to be on order of 10^{10} (201), phage display libraries are usually on the order of 10^{9} (202), and most small molecule libraries rarely exceed 10^{5} compounds.

The key assumption underpinning SELEX is that there is enough structural diversity present within a library that there exists an aptamer against the target of interest. Isolating that aptamer involves iterative rounds of counterselection, selection, and amplification. Each round includes three stages: (1) the oligonucleotide library is incubated with the target molecule; (2) the oligonucleotide complexes with the target are separated from non-bound oligonucleotides; (3) bound sequences are amplified by PCR. The principals of Darwinian evolution apply as the entire nucleic acid library is incubated with the target of interest and all sequences are forced to compete for target binding. Stringent washing ensures that only sequences that survive this selective pressure will have their genotypes represented in the next round following amplification and regeneration of aptamer as single stranded nucleic acid. Due to the

large size of the initial library and limitations in partitioning efficiency, iterative rounds must be performed to exponentially enrich for target binding sequences. A counterselection step is often incorporated to give more specific enrichment. After a number of rounds of SELEX, final pools are evaluated for sequence enrichment and putative aptamers sequences are further characterized.

Using relatively simple selection schemes, aptamers have been isolated against purified targets ranging from small organic molecules such as amino acids and carbohydrates, to peptides and proteins. Three relevant examples are highlighted below:

As discussed previously, PfEMP1 plays an essential role in malaria pathology by mediating adhesion to the endothelial cells and to non-infected erythrocytes (rosetting) and other cells. Barfod *et al.* recovered an aptamer against the relatively well conserved DBL1α domain of PfEMP1 thought to be involved in rosetting (203). Although selected against recombinant protein, DBL1α-specific RNA aptamers were able to locate the protein on the surface of infected erythrocytes and showed rosette disrupting capacity at low nanomolar concentrations underscoring their potential as an adjunct therapy for severe malaria.

P. falciparum enzymatically digests hemoglobin during its IE developmental stages as a source of amino acids and the toxic heme group released is rapidly sequestered by polymerization into hemozoin (204, 205). Anti-malarial drugs used in the clinic such

as chloroquine and its derivatives act in part by disrupting heme polymerization leading to the buildup of toxic substances (206). Niles *et al.* investigated the pathways for hemoglobin degradation in malaria using heme-binding aptamers previously isolated by SELEX (207). Using hypotonic lysis and resealing conditions, researchers pre-loaded heme binding aptamers into RBCs and found that upon infection, parasite growth in cells was significantly reduced after 72 hours in culture, when compared to the controls. The studies demonstrate aptamers can be used to study parasite-specific metabolic pathways.

To facilitate preclinical evaluation of potential therapeutics in animal models, White *et al.* selected an aptamer against thrombin by alternating between human and porcine thrombin as the protein target (208). Underscoring the utility of the technique, a number of species-specific aptamers were recovered when only porcine thrombin was used as the target of selection. Co-crystal analysis showed the recovered aptamer binds to thrombin exosite-2, and not exosite-1, where aptamers selected against only human thrombin bind (209). Interaction between the toggle aptamer and thrombin buries a total of 1193 $Å^2$ of solvent-accessible surface area contacts and involves a succession of adenine-arginine stacking interactions. Remarkably, the calculated degree of shape complementarity between the toggle aptamer and thrombin is better than most antibody-antigen interactions and rivals that of subunit-subunit interaction between oligomeric proteins which are among the most highly complementary macromolecular surfaces in nature (210).

1.5.3 SELEX against complex targets

Multiple groups have demonstrated that aptamers may be selected against complex targets including protein mixtures such as serum (211), cell and viral surfaces (212–218), and even tumors *in vivo* (219, 220). Cell based selection (Cell-SELEX) is particularly promising because: 1) Careful application of counterselection, selection, and elution parameters obviates the need to know the target ahead of time. This allows for *a priori* characterization of markers for specific disease states, receptors and markers of cellular differentiation, as well as determinants of disease in pathogenic organisms, 2) Aptamer binding cell surfaces target molecules in their native conformation with all post-translational modifications left intact, 3) As long as the binding of one aptamer does not interfere with the binding of another aptamer, aptamers against multiple targets may be simultaneously selected, 4) Aptamers returned from Cell-SELEX often have dissociation constants rivaling antibodies and are thus suitable for target affinity purification and definitive identification (215, 219, 221–223).

The most prominent example of Cell-SELEX and the myriad of possible downstream applications of selected aptamers is Sgc8. Sgc8 was isolated from a SELEX library by positive selection on acute lymphoblastic leukemia cells (T-ALL) and negative selection against a Burkitt's B cell lymphoma line (218). As a result, Sgc8 displays high affinity and selectivity for a membrane protein displayed on most T-ALL cells and shows no affinity for B cell myelomas, B cell lymphomas, or normal human bone marrow cells (218). Aptamer-mediated purification followed by mass spectroscopy identified the transmembrane protein tyrosine kinase 7 (PTK7) as the target of Sgc8

(223).

Hypothesizing that multimerizing Sgc8 would improve its avidity and increase its potential for diagnosis and therapy, the Tan group attached a hydrophobic tail to the end of Sgc8 in order to create highly ordered aptamer functionalized micelles. As predicted, aptamer–micelles showed improved binding at near physiological conditions including dynamic fluid experiments that mimic blood circulation (224).

Taking a different approach to achieve high contrast *in vivo* imaging, Shi *et al.* reported design of a Sgc8 molecular beacon that only fluoresces in the presence of PTK7-expressing tumors (225). Molecular beacons are hairpin shaped aptamers with an internally quenched fluorophore. Binding to a receptor causes a significant conformational change resulting in an activated fluorescence signal. Time-dependent fluorescence imaging of CCRF-CEM (T-ALL type) tumors in a mouse model with Sgc8 molecular beacons gave clear fluorescent images of the tumor site within 15 minutes after injection and at 60 minutes, the beacon was almost cleared from blood and non-target tissues. In contrast, the fluorescent signal from "always on" Sgc8 probes at the tumor site was roughly indistinguishable from non target sites with a very limited signal-to-background ratio (225).

More recently, the Church group developed a logic-gated nanorobot that uses Sgc8 for targeted payload delivery (226). The nanorobot consists of a clamshell made of nanostructured DNA, DNA orgami (227), enclosing a therapeutic payload. Cargo

delivery can be controlled by two different aptamers which effectively form an AND logic gate. In this configuration, the nanorobot is activated only when both aptamers bind their substrates triggering structural rearrangements analogous to that of molecular beacons that open the nanorobot. In one experiment, researchers loaded Sgc8-gated nanobots with a powerful antibody combination known to bind human CD33 and human CDw328 and induce growth arrest in leukemic cells. Upon recognition of surface PTK7 on cells from a patient with aggressive lymphocytic NK-type leukemia, aptamer conformation shift opened the nanobot, allowing the antibody payload to bind to cell-surface receptors ultimately inhibiting the growth of the target cells. Much work remains before the nanobot or other aptamer-based systems can be used in the clinic but there is certainly great potential.

1.5.4 Clinical applications of aptamers

Several properties of aptamers make them attractive diagnostic and therapeutic agents that rival, and in some cases even surpass, antibodies**.** Aptamers fall in the 5-15 kDa range that allows for excellent tissue penetration and organ distribution but they are susceptible to renal filtration. In order to reduce clearance, aptamers can be modified by addition of polyethylene glycol (PEG) and other moieties to increase their bioavailability (228, 229). Degradation by serum nucleases is another concern, particularly for RNA. This can be overcome by using libraries modified with 2'-fluoro- or 2'-amino-pyrimidine (230, 231) to avoid recognition by endonucleases. Chelliserrykattil *et al.* reported selection using 2'-O-methyl modifications is also possible using a mutant T7 RNA polymerase that incorporates modified nucleotides (232)**.** Post-selection base substitution with O'–methyl for O-H residues at the 2'

position are also possible but this approach carries the risk of disrupting aptamer structure and function (233, 234). DNA is relatively stable compared to RNA but addition of a 3' inverted thymidine can dramatically increase its serum lifetime (207). Aptamers display little or no immunogenicity which may be surprising considering the correlation between anti-DNA antibodies and various autoimmune syndromes. On the other hand, defibrotide, a complex mixture of single stranded DNA derived from the controlled depolymerization of porcine intestinal mucosal DNA, has been successfully used to treat a variety of cardiovascular disorders for over two decades with few reported serious adverse effects (235).

The potential of aptamers to be developed into useful therapeutics has been realized in the FDA approval of Mucagen (Pagaptanib), an RNA aptamer to $VEGF_{165}$, as a treatment for age-related macular degeneration (236). In addition, two anti-cancer aptamers are currently in clinical trials with 15 more in the pre-clinical pipeline (237, 238). There is particular promise in developing aptamers for controlling the blood clotting cascade because their therapeutic activity can be controlled or even reversed by complementary sequence antidotes (239) or protein- and polymer-based molecules that capture oligonucleotide (240).

In terms of disease diagnosis, Gold *et al.* described a new aptamer-based multiplexed biomarker discovery technology capable of measuring a thousand proteins using just a minute volume of plasma or serum (241). This new platform has reconfirmed well-known biomarkers and identified dozens of new markers in two large clinical studies

of chronic kidney disease and lung cancer (241, 242).

1.6 Aim and scope of the thesis

The aims of this thesis are to: 1) test whether structurally conserved determinants are displayed on the surface of IEs and 2) to identify such determinants in hopes of developing a broadly effective blood-stage malaria vaccine.

Chapter 2. Materials and methods

2.1 Cell culture and basic techniques

2.1.1 MACS purification

Purification of late-stage parasites by magnetic separation has been previously described (243). Briefly, prior to purification MACS magnet separation columns LS size (Miltenyi Biotec, Auburn CA) were filled with warmed RPMI-1640 (37°C, Gibco, Carlsbad CA). The parasite culture blood was then deposited on the top of the column (typically, 50 mL at 0.5% haematocrit) that was held in place by a Quadro MACS (Miltenyi Biotec) magnetic support. Warmed (37°C) complete medium {CM, (RPMI medium 1640 [pH 7.2], supplemented with 25 mg/mL HEPES, 2 mg/mL sodium bicarbonate, 50 μg/mL gentamicin, and 0.5% Albumax II; Gibco)} was then added until the eluent was free of RBCs. The column was removed from the magnetic support and flushed with an additional 10 mL of CM. The eluent containing purified parasites was centrifuged briefly and the removed parasites used for downstream applications.

2.1.2 Percoll/sorbitol purification

This method has been described previously (244) with minor modification. The cell culture was loaded carefully on top of the Percoll step gradient in a 15-ml tube containing 3 mL of 70% and 30% Percoll (GE Healthcare, Pittsburg PA) in RPMI 1640 in 5% sorbitol (Sigma, St Louis MO), and then centrifuged for 10 min at 10,000 G. Late trophozoite (30-36 hrs post invasion) and late schizont (36-42 hrs post

invasion) parasite were collected at the interface between the Percoll layers, washed twice in CM in preparation for downstream applications.

2.1.3 *P. falciparum* culture

P. falciparum lines were cultured in O^+ erythrocytes at 5% hematocrit in complete medium in an atmosphere of 5% O_2 at 37°C. Cultures were synchronized using a combination of sorbitol hemolysis (17) and gelatin flotation (18). High purity trophozoite-infected cells (approximately 35 hrs post-invasion) were obtained by MACS purification or Percoll/sorbitol gradient. All *P. falciparum* laboratory lines were confirmed negative for *Mycoplasma* contamination using the Mycotrace Detection Kit (PAA Laboratories, Piscataway, NJ). For experiments using KAHRP knockouts, parasite were cultured as described (176).

2.1.4 *P. vivax* culture

Glycerolyte preserved *P. vivax* adapted for growth in *Aotus nancymae* were cultured in McCoy's 5A medium (Invitrogen) supplemented with 2.4 g/L D-glucose, 40 mg/mL gentamycin (Gibco), and 20% heat-inactivated human AB serum (Invitrogen) in an atmosphere of 5% O_2 at 37°C for 18-24 hrs until schizont maturation, which was determined by microscopic examination of Giemsa-stained thin blood films. Blood from PCR negative monkeys was frozen and thawed in parallel as controls.

2.1.5 *P. knowlesi* culture

P. knowlesi (Strain H) was cultured under *in vitro* in an atmosphere of 5% O_2 at 37°C with RBCs collected from Rhesus monkeys (*Macaca mulatta)* and RPMI 1640 (pH 7.2) supplemented with 50 mg/L hypoxanthine and 20% human AB serum (Invitrogen). *P. knowlesi*-infected or uninfected Rhesus monkey RBCs were washed in RPMI 1640 and used directly for binding assays.

2.1.6 Rodent parasites

P. berghei ANKA and *P. yoelii yoelii* 17X were maintained by serial passage in 3- to 4-week-old female BALB/c mice (Jackson Laboratory, Bar Harbor ME). Mouse parasitemias were monitored by light microscopy using air-dried blood smears that were methanol fixed and stained with 10% Giemsa. Blood samples were collected from the tail vein of infected and control mice, rinsed 3 times in the AB buffer and used directly for binding assays.

2.1.7 *P. falciparum* and *P. vivax* isolates from Cambodia

These samples were collected patients presenting to the Sampov Meas Referral Hospital, Pursat province, Cambodia. All patients or the patient's parent or guardian provided written informed consent to participate in the study.

The *P. falciparum* samples were collected in 2009-2010 (245). Patients who met

eligibility criteria (a parasite density of ≥10,000 asexual blood stage *P. falciparum* parasites per uL of blood, no symptoms or signs of severe malaria, age ≥10 years, not pregnant, no other chronic illness) were enrolled for the study (ClinicalTrials.gov identifier NCT00341003). Prior to treatment, a blood sample was collected into an acid citrate dextrose vacutainer (BD Biosciences, San Jose CA). Parasitized erythrocytes were cryopreserved in Glycerolyte 57 (Baxter Healthcare, Deerfield IL) and stored in liquid nitrogen until use.

P. vivax samples were collected in 2009. Patients who met eligibility criteria (any *P. vivax* parasite density with no *P. falciparum* parasites, age ≥2 years, hematocrit ≥25%, not pregnant) were enrolled for the study (ClinicalTrials.gov identifier NCT00663546). Prior to treatment, a blood sample was collected into a heparin vacutainer (BD Biosciences). Parasitized erythrocytes were cryopreserved in Glycerolyte 57 (BD Biosciences) and stored in liquid nitrogen until use.

2.1.8 *P. falciparum* and isolates from Mali

Written informed consent was obtained from Malian adults or the parents or guardians of children if they could read French; if the not, oral consent was obtained and documented by both the adult being consented and a third party witness. This study is registered with ClinicalTrials.gov identifier NCT0066984.

Samples were obtained from children with uncomplicated malaria living in 3

neighboring rural villages (Kenieroba, Bozokin, Fourda) located in the Koulikoro region of Mali, which experiences intense seasonal transmission of *P. falciparum* between June and December. Further details of this study area and the overall cohort have been previously described (246). Uncomplicated malaria was defined as axillary temperature >37.5°C or history of fever in the previous 48 hrs with *P. falciparum* parasitemia (any density) on thick blood smear and no other etiology of febrile illness discernable on clinical examination. Venous blood was collected in the end of the 2009 transmission season in heparin vacutainers (BD Biosciences). Whole blood was processed using Ficoll-Paque PLUS (GE Healthcare); plasma was separated by centrifugation and stored at -80°C until use. Parasitized erythrocytes were cryopreserved in Glycerolyte 57 (Baxter Healthcare) and stored in liquid nitrogen until use.

2.1.9 Display of the aptamer target at various stages in the parasite lifecycle

Merozoite isolation. Merozoites were isolated according to a protocol described previously (247). Briefly, late-stage parasites were isolated (>95% purity) from uninfected RBCs with a MACS magnetic separation column (Miltenyi Biotec, (243)). Parasites were incubated with 10 μM of E64 (Sigma) for 6 to 8 hrs. Schizonts were pelleted at 1,000 G for 5 min. Parasites were resuspended in a small volume of culture medium and filtered through a 1.2-μm Acrodisc 32-mm syringe filter (Pall Corporation, Port Washington NY). Filtered merozoites were assayed immediately for aptamer binding.

Rings. Late trophozoite/schizont stage parasites were obtained by Percoll (GE Healthcare) purification followed by 6 hr incubation with uninfected RBCs. Cells were then treated with 5% sorbitol to lyse any uninvaded cells and returned to culture for 5 hrs before testing.

Trophozoites/schizonts. Parasites were synchronized using 5% sorbitol treatment at 11 a.m. and 5 p.m. on the day prior to binding assay. Between 12 noon and 1 pm on the following day, parasites were enumerated, and then mixed in uninfected blood to 1% final parasitemia and 2% hematocrit and evaluated for aptamer binding.

Gametocytes. For the production of gametocytes**,** *P. falciparum* was maintained in culture using standard procedures (184), and gametocytogenesis was induced as described by Ifediba and Vanderberg (248). To eliminate asexual stage parasites, gametocyte cultures were treated with 50 mM N-acetylglucosamine (Sigma) 6 to 8 days after the culture was initiated. Parasites were synchronized by sorbitol treatment, and gametocytes were purified using either a 70% Percoll gradient (GE Healthcare) or a MACS column (Miltenyi Biotec).

2.1.10 Temperature shifts in *P. falciparum* cultures

Synchronous ring stage parasites (synchronized 4–6 hrs post-invasion) were subjected to a heat shock at 40°C for 2 hrs followed by incubation at 37°C for 8 hrs. Cultures that were kept at 37°C during all phases were used as a non-heat shock control.

2.1.11 Inoculating *P. falciparum* into RBCs carrying mutant hemoglobin.

To evaluate the effect of hemoglobin mutations on display of the aptamer target, trophozoite-infected erythrocytes (*P. falciparum* FCR3*)* were enriched to high purity by Percoll (GE Healthcare), inoculated into hemoglobin A (HbAA), hemoglobin S (glutamate-to-valine substitution in the sixth position of the β-globin chain) hetero- or homozygous (HbAS, HbSS respectively) mutant erythrocytes, and cultured at 1–2% hematocrit. Fresh HbAA, HbAS, and HbSS erythrocytes were collected from adult subjects who had provided written informed consent in accordance with the Declaration of Helsinki and were enrolled at the NIH Clinical Center on clinical protocol NIH 03-H-0015 specifically approved for this study by the Institutional Review Board of the National Heart, Lung, and Blood Institute. Parasitized erythrocytes were always assayed after a single cycle of invasion and growth to the trophozoite stage (~36 hrs).

2.1.12 Growth inhibition assay

Parasite responses to DNA aptamers were tested using a SYBR green growth inhibition assay as described previously (249). Briefly, parasites were diluted to 0.5% parasitemia at a 2% hematocrit, and the parasite suspension (100 μL) was added to wells in duplicate in a 96-well plate containing 100 μL of 2-fold-serially diluted aptamers modified with 3' inverted thymidine to increase serum stability. To each well tRNA (Invitrogen) and salmon sperm DNA (Invitrogen) was also added at a final concentration of 0.1 mg/mL. The parasites were incubated with the aptamers at 37°C for 72 hrs. After incubation, DNA was released and stained with lysis buffer [20 mM

Tris (pH 7.5), 5 mM EDTA, 0.008% saponin, 0.08% Triton X-100] containing SYBR green dye (Invitrogen). The plate was kept in darkness for 30 min and read in a FLUOstar Optima microplate reader (BMG Labtech, Cary NC)

2.2 SELEX

2.2.1 SELEX libraries and primers

Libraries and primers originally designed for recognition of thyroid transcription factor 1 (250), termed LIC, or liver cancer cell lines (251) , LV, are described in Table 2.1. All DNA libraries, PCR primers, and aptamers were obtained from Integrated DNA Technologies (Coralville, IA).

Table 2.1 SELEX libraries and primers used in study

Name	Sequence	Description
LIC-Library	*GGTATTGAGGGTCGCATC* -N_{40} GATGGCTCTAACTCTCCTCT	Primer sites in italics
LIC-Forward	AGAGGAGAGTTAGAGCCATC	Forward primer used for amplification reaction
LIC-Reverse	Phos-GGTATTGAGGGTCGCATC	Reverse primer used for amplification reaction
LV-Library	*ACGCTCGGATGCCACTACAG*-N_{40}-*CTCATGGACGTGCTGGTGAC*	Primer sites in italics
LV-Forward	ACGCTCGGATGCCACTACAG	Forward primer used for amplification reaction
LV-Reverse	Phos-GTCACCAGCACGTCCATGAG	Reward primer used for amplification reaction

2.2.4 PCR conditions for SELEX

Thirty microliter fractions of the bound sequences recovered from Serial- or Neutral-SELEX experiments were divided into 3 x 10 µL aliquots. PCR Supermix (1X Ex Taq Version 2.0, Takara, Mountain View, CA), primers (0.2 µM final concentration) were added to bring the reaction to 100 µL final volume. Reactions were amplified for 13-20 cycles of 0.5 min at 94°C, 0.5 min at 56°C, and 0.5 min at 72°C, followed by 5 min at 72°C and the presence of DNA following PCR was confirmed by electrophoresis on a 4% agarose gel (E-gel, Invitrogen). For the initial amplification

following the first round of SELEX, the entire bound sequence fraction was divided into 4 x 25 μL aliquots and amplified in 100 μL PCR reactions similar to those described above.

2.2.5 Digestion of phosphorylated strands of dsDNA for SELEX

The selective digestion of phosphorylated strand by λ exonuclease (New England Biolabs, Ipswich MA) was utilized to regenerate aptamers as ssDNA following PCR. The reaction mixture described in Table 2.2 was incubated at 37°C for 30 min followed by to 95°C at 10 min.

Table 2.2 Components of the λ exonuclease reaction.

Component	Volume (μL)	End Concentration
10x Digestion Buffer*	10	1 x
PCR product	90	--
Lambda exonuclease (5U/μL)	1	0.05U/μL

* Buffer Components: 67mM Glycine-KOH, 2.5mM $MgCl_2$, 50μg/mL BSA, pH 9.4

2.2.6 Ethanol precipitation for SELEX

Precipitation with ethanol was used to concentrate and purify nucleic acids. Ethanol (2.5 volumes) and NaOAc (3 M, pH 5.2, 0.1 volumes) were added to the solution of nucleic acids. The whole sample was mixed and stored for 2 hrs at -80°C. The

solution was then centrifuged at 16,000 G for 30 min at 4°C. The supernatant was discarded and the pellet was washed again with 70% ethanol. The mixture was centrifuged at 16,000 G for 30 min at 4°C. The supernatant was discarded. The pellet was air-dried and finally dissolved in AB buffer.

2.2.2 Serial-SELEX

For a typical round of SELEX, ssDNA recovered from the previous round was dissolved in 200 μL Aptamer Binding buffer [AB buffer, RPMI-1640 (pH 7.2) supplemented with BSA (1mg/mL, Sigma), yeast tRNA (0.1mg/mL, Invitrogen), sheared salmon sperm DNA (0.1 mg/mL, Invitrogen)] was denatured by heating at 95°C for 5 min and cooled to 4°C before binding. To avoid selecting for aptamers specifically recognizing uninfected RBCs, the library was incubated with 5 x 10^6 uninfected RBCs for 30 min at RT and following centrifugation, unbound sequences were recovered for the selection phase. The remaining sequences were incubated with 10^6 Percoll-purified IEs for 10 min at RT. After washing in AB buffer, IEs were lysed in 100 μL 95°C water, debris pelleted, and the resultant supernatant amplified by PCR. Aptamers were amplified using unmodified forward and phosphorylated reverse primers, treated with λ exonuclease to remove anti-sense strands, and ethanol precipitated. The regenerated single-stranded aptamers were used for the next round of counterselection, selection, and amplification.

For the first round selection, the amount of naive ssDNA library was 10 nmol dissolved in 1 mL of AB buffer and the counterselection step was eliminated. To

enrich for aptamers specific for structures conserved between malaria strains, a unique parasite isolate was used as the target for positive selection in each round. *P. falciparum* strains used (in order) were FCR3, PC26, S35, DIV14, 425, C2A , FAB9, D10, 102/1, and W2-mef. Following 10 rounds of aptamer selection and amplification, the unselected starting library, round 6 pool, and final library were evaluated using the Illumina high-throughput sequencing platform.

2.2.3 Neutral-SELEX

LIC or LV libraries (10 nmol) were diluted 1/10,000 in AB buffer, amplified by PCR and regenerated as ssDNA using λ exonuclease followed by precipitation with ethanol. The recovered ssDNA pools were further subjected to 10 iterative cycles of the dilution and amplification, after which the final pools were interrogated by Illumina high-throughput sequencing.

2.2.7 High-throughput sequencing

Aptamer libraries were constructed using the Illumina Multiplexing Sample Preparation Oligonucleotide Kit protocol with the exception that the DNA was not sheared. Libraries were size-selected to remove unincorporated adapters on a 2% NuSieve Agarose gel (Lonza) run at 120 V for 30 min, stained with SybrGold (Invitrogen), and visualized on a Dark Reader (Clare Chemical, Dolores, CO). To insure that the library was not over amplified, a test amplification was performed where aliquots of a PCR reaction were removed every 2 cycles from 4-16. These

aliquots were evaluated on a 2% agarose gel and an optimal cycle number was selected for a subsequent large-scale amplification. Final libraries were quantitated using qPCR and pooled in an equimolar ratio for sequencing. Paired-end 100 base reads were obtained on a $GA_{ii}x$ using version 4 chemistry or a HiSeq 2000 using version 3 chemistry.

2.2.8 Filtering of Illumina sequences

Multiplexing routinely yielded 2-7x10^6 reads per sample. Sequences were filtered to have an exact match of the primers and a matching multiplexing tag. Only the 40 base randonomized regions were used for further analysis. Identical sequences were collated using an R-script (252)**.** Unique sequences were grouped according to primary sequence similarity using ClustalW2 (http://www.ebi.ac.uk, EMBL-EBL).

2.3 Aptamer and protein characterization

2.3.1 DNA end-labeling

Single stranded DNA aptamers were labeled with a ^{32}P label (Perkin Elmer, Waltham MA) at the 5' end according to the suggested protocol from New England Bioscience. This kit utilizes T4 polynucleotide kinase to catalyze the transfer of the terminal [γ-^{32}P] phosphate of ATP to the 5' hydroxyl terminus of the DNA molecule. Components of the reaction mixture are described in Table 3.1. The reaction mixture was incubated at 37°C for 30 minutes. To minimize losses in the subsequent gel filtration step, 10 μg of yeast tRNA (Invitrogen) and salmon sperm DNA (Invitrogen) was added to the reaction mixture before clean up using NucAway spin columns (Invitrogen) according to manufacturer's instructions.

Table 2.3 Components of the DNA end-labeling reaction.

Component	Volume (μL)	End Concentration
10x T4 polynucleotide kinase buffer*	2	1 x
ssDNA	-	25 pmol
T4 polynucleotide kinase (10 U/μl)	1	0.5U/μL
γ- 32P ATP (370,000 Bq/μl)	1	370,000 Bq
	add H2O to 20μL	

*Buffer Components: 70mM Tris-HCl, 10mM $MgCl_2$, 5mM Dithiothreitol (DTT), pH 7.6

2.3.2 Aptamer binding assay

Binding of individual aptamers to cells was performed in 96 well DNA Lo-Bind deepwell plates (Eppendorf, Hauppauge NY) in triplicate with 5' [^{32}P]-labeled DNA. Five million cells per well were incubated with 100 nM DNA in 25 μL AB buffer in the presence of 1 mg of yeast tRNA (Invitrogen) and salmon sperm DNA (Invitrogen) as a nonspecific competitor. After three washes in 500 μL AB buffer, cells were fixed in 1% paraformaldehyde and the amount of ^{32}P-labeled aptamer associated with cells was determined by liquid scintillation counting. The average binding intensity of two random sequence oligonucleotides was used to determine the level of background binding. A threshold for definitive aptamer binding was set at 5 fold above background. The equilibrium dissociation constants (K_d) of the aptamer–cell interaction were obtained by fitting the Michaelis-Menten equation using Prism version 5.0 (GraphPad Software, La Jolla, CA). The specific binding intensity (Y) versus the aptamer concentration (X) was plotted as function $Y=B_{max}X/(K_d + X)$ where B_{max} is the maximum number of binding sites.

2.3.3 Aptamer competition assay

Unlabeled aptamer competitor was incubated with IEs in 10-fold excess final concentration (750 nM) for 20 min at RT in AB buffer. After incubation, a [^{32}P]-labeled aptamer was added at a final concentration of 75 nM. Binding assay was performed as described. Competition between the labeled and unlabeled version of the same aptamer was used as a positive control.

2.3.4 Protease susceptibility studies

Infected late-stage IEs were washed twice in PBS and incubated at 5% hematocrit with 1mg/mL Pronase E from *Streptomyces griseus* (Sigma) in PBS supplemented with 1 mM $CaCl_2$ and 1 mM $MgCl_2$ for 45 min at 37°C or 1 μg/mL of porcine-modified trypsin (Promega) in PBS for 30 min at 37°C. After extensive washing with AB buffer containing complete Proteinase Inhibitor Cocktail Tablets (Roche), the treated cells were used for aptamer-binding assays. Protease accessibility to erythrocyte cytosol was examined by measuring hemoglobin band intensity in Coomassie-stained SDS-PAGE gels of total cell lysate. Band intensity was quantified with *ImageJ* software (http://rsbweb.nih.gov/) and revealed no detectable hemoglobin degradation.

2.3.5 Functionalization of streptavidin coated beads

A version of Euge.1, Euge.4, Euge.7 and RDM was synthesized with a 3' 15 adenosine tail (15A). 15A-modified aptamers were immobilized to 1 mg hydrophilic magnetic streptavidin-coated beads (New England Biolabs) or 20 μg streptavidin-conjugated fluorescent beads (average diameter 0.5 μm, peak emission 488 nm; Spherotech) using a poly-thymidine capture oligonucleotide (PolyT, Bio-18C-TTTTTTTTTTTTTTT, where18C is a 18-carbon ethylene glycol spacer). Immobilization reactions were carried out with beads, 500 pmol 15A-aptamer, and 500 pmol PolyT in 500 μL PBS for 10 min at RT. Beads were washed twice before use.

2.3.6 Confocal microscopy

Synchronous parasite cultures were purified by MACS and fixed in 1% paraformaldehyde for 10 min before incubation with aptamer-coated fluorescent beads (Spherotech, Lake Forest IL). The cells were washed and used to make thin smears on glass slides and then air-dried prior to fixation in 100% methanol for 5 min. Nuclei were stained with DAPI in Prolong Gold mounting medium (Invitrogen). Fluorescence images were taken on a Leica SP2 confocal microscope under a 100x oil immersion objective with 488 nm excitation**.** Images were processed in Imaris 6.0 (Bitplane AG, Zurich Switzerland) and uniformly deconvoluted using Huygens Essential 3.1 (Scientific Volume Imaging BV, Hilversum, Netherlands). Control experiments using antiserum against the intracellular acidic terminal segment of PfEMP1 [1/400 dilution, (253)] and anti-Spectrin antibody (1/500 dilution, Millipore, Stafford VA) gave no signal, confirming that the parasitized erythrocytes in these experiments were not antibody permeable.

2.3.7 Flow cytometry

Trophozoite-infected erythrocytes (10^6 cells at 1% parasitemia) were stained with aptamer-coated fluorescent beads in FACS staining buffer (FSB; PBS, 2% FBS, and 0.1% sodium azide) for 45 min at room temperature and washed twice with FSB. Nuclei were counterstained with Syto61 (Invitrogen) according to manufacturer's instructions. An Accuri C6 flow cytometer (BD Biosciences) and CFlow software version 1.0 were used to acquire and analyzed up to 500,000 events from each

sample.

2.3.8 Aptamer-mediated affinity purification

All solutions were prepared with Complete Proteinase Inhibitor Cocktail (Roche, Basel, Switzerland). Percoll purified IEs (10^8) were hemolyzed in lysis buffer (7.5 mM Na_2HPO_4, 1 mM EDTA, pH 7.5) and ultracentrifuged at 100,000 G for 45min. The pellet was washed with lysis buffer before solubilization in 1% Lauryldimethylamine-N-Oxide (LDAO, Affymetrix, Santa Clara CA). The membrane faction was incubated with aptamer-functionalized magnetic streptavidin-coated beads (1 mg) in the presence of 5 µg of tRNA and 5 µg of salmon sperm DNA as nonspecific competitors at 4°C for 20 min. Following a series of washes in 0.3 M NaCl, captured proteins were removed from aptamer-coated beads using NuPAGE LDS Sample Buffer (Invitrogen) with 100 mM DTT and analyzed by SDS-polyacrylamide gel electrophoresis (SDS-PAGE) after staining with silver. For large-scale mass spectrometry experiments, protein-aptamer-bead complexes from 10 individual preparations were combined and eluted in NuPAGE LDS Sample Buffer and resolved by SDS-PAGE and visualized with Coomassie stain.

2.3.9 Mass spectrometry and protein identification

Identification of all one-dimensionally gel-separated proteins was performed on reduced and alkylated, trypsin digested samples prepared by standard mass

spectrometry protocols. The supernatant and two washes (5% formic acid in 50% acetonitrile) of the gel digests were pooled and concentrated by speed vacuum (Labconco, Kansas City MO) to dryness directly in 200 µL polypropylene auto-sampler vials (Sun Sri, Rockwood TN). The recovered peptides were re-suspended in 5 µL of Solvent A (0.1% formic acid, 2% acetonitrile, and 97.9% water).

Gel bands were excised, destained in 50% acetonitrile in 25 mM NH_4HCO_3, pH 8.4, lyophilized, and digested with 20 ng/µL of trypsin in 25 mM NH_4HCO_3, pH 8.4 (Promega, Madison WI) overnight at 37°C. The tryptic peptides were extracted from gel slices using 70% acetonitrile containing 5% formic acid. The peptide solution was lyophilized, resuspended in 0.1% trifluoroacetic acid (TFA), and processed with peptide cleanup (ZipTip, Millipore).

Prior to mass spectrometry analysis the re-suspended peptides were chromatographed directly on column, without trap cleanup. The bound peptides were separated at 500 nL/min generating 80-120 Bar pressure, using an AQ C18 reverse phase media packed in a pulled tip, nano-chromatography column (0.100 mm ID x 150 mm L, Precision Capillary Columns, San Clemente CA). The chromatography was performed in-line with an LTQ-Velos Orbitrap mass spectrometer (ThermoFisher Scientific, Waltham MA) and the mobile phase consisted of a linear gradient prepared from solvent A and solvent B (0.1% formic acid, 2% water, and 97.9% acetonitrile) at room temperature. Nano LC-MS (LC-MS/MS) was performed with a ProXeon Easy-nLC II multi-dimensional liquid chromatograph and temperature controlled Ion Max

Nanospray source (ThermoFisher Scientific) in-line with the LTQ-Velos Orbitrap mass spectrometer (ThermoFisher Scientific).

Computer controlled data dependent automated switching to MS/MS by Xcalibur 2.1 software (ThermoFisher Scientific) was used for data acquisition and provided the peptide sequence information. Data processing and databank searching were performed with PD 1.2 and Mascot software (Matrix Science, Boston MA). The data was searched with parallel searches of the PlasmoDB (9.0) and Uniprot KB, Human (12/2012), each with a reverse sequence decoy database. The protein score, which is -10*Log(P) where P is the probability that the observed match is a random event, for each entry was calculated. Proteins were identified using a 1% false discovery rate cutoff and 2 peptide per protein minimums.

2.3.10 Aptamer screen of recombinant proteins

Recombinant full-length human HSP90a, human HSP90a, and PfHSP70 were purchased from Prospecbio (Ness Ziona, Israel). Recombinant C-terminal 193 amino acids of PfHSP90 were purchased from StressMarq Biosciences (Victoria BC, Canada). MSP-1 (3D7 allele of the 19 kDa region), AMA-1 (3D7 allele), Var2CSA (DBL_{3x}) were kindly provided by the PATH /MVI funded reference laboratory at NIH. Polystyrene microtiter plates (Immulon 4HBX flat bottom, ThermoFisher Scientific) were washed with PBS-Tween (PBS-0.1% Tween 20). Individual wells were coated with 100 µL of antigen diluted to 1 µg/mL in coating buffer (0.15M Na_2CO_3, 0.35M $NaHCO_3$, pH 9.6) and incubated overnight at 4° C. Plates were

washed with PBS-Tween, blocked in 5% non-fat dry milk for 1 hour and washed before incubation with 25 μL of [^{32}P]-labeled aptamer in aptamer bind buffer for 20 min at RT. Following a series of washes, aptamers were eluted in 1M NaCl and counted by liquid scintillation. Random oligonucleotide sequences were used as negative controls.

To calculate the equilibrium dissociation constants (K_d) of the interaction between aptamer and immobilized PfHSP90, the aptamer concentration was varied and the specific binding intensity versus the aptamer concentration was fitted to the Michaelis-Menton equation, $Y=B_{max}X/(K_d + X)$, using GraphPad Prism software 5.0 (GraphPad Software).

2.3.11 Enzyme-linked immunosorbent assay (ELISA)

Flat-bottom plates (NUNC Immobilizer, Thermo Fisher Scientific) were washed 3 times with TBS-Tween (TBS-0.1% Tween 20). Individual wells were coated with 1.5 nmol of antigen diluted in coating buffer (0.15M Na_2CO_3, 0.35M $NaHCO_3$, pH 9.6) and incubated overnight at 4°C. Plates were washed with PBS-Tween, blocked in 5% non-fat dry milk for 1 hr and washed before 2 hr incubation with 100 μL test serum diluted 1:200 in ELISA dilution buffer (5% milk in TBS). Wells were then washed 3 times TBS-Tween. Plates were then incubated for 2 hrs with 100 μL of alkaline phosphatase-labeled goat anti-human IgG (1:2,500 in Elisa dilution buffer, Invitrogen) before a final wash. Bound antibodies were detected by adding phosphatase substrate tablets (Sigma) diluted in coating buffer. OD 405 nm was read

20 min after addition of substrate using a Spectramax 190 microplate reader (Molecular Devices, Sunnyvale CA). Twenty-four sera from US residents, never exposed to malaria, were used as negative controls. All samples were tested in duplicate on the same day.

Chapter 3. Development and evaluation: Serial-SELEX to probe for conserved IE determinants

3.1 Introduction

3.1.1 Harnessing SELEX to probe for conserved IE determinants

It is well established that natural immunity to malaria develops after multiple exposures to parasites. Although this largely antibody-mediated protection is imperfect and non-sterilizing, it may point the way toward an effective malaria vaccine. What is yet to be determined is whether this immunity is directed against multiple antigens or against conserved determinants. Discovery of an antigen conserved between genetically distinct parasites at any of the life stages would be important for malaria control efforts but may be especially beneficial if found on IEs, the life stage attributed to all the disease and pathology associated with malaria.

The goal of this chapter is to probe for putative conserved IE determinants using a novel aptamer-based technique we term Serial-SELEX. Whereas the traditional SELEX methodology simply enriches sequences of interest from a large randomized nucleic acid library through repeated cycles of positive and negative selection, we hypothesized that incorporating unique parasite isolates as the targets of iterative positive selections would direct aptamers towards conserved targets.

3.1.2 Evaluating the dynamics of SELEX

We couple our technique with Illumina sequencing, a second-generation sequencing technology that uses massively parallel sequencing of short read lengths to generate throughput on the gigabase scale. Employment of Illumina sequencing allows for unprecedented power to identify even weakly enriched aptamers. Importantly, we can also investigate the dynamics of aptamer selection. Other groups have reported deep biases in the SELEX technique due to pressures imposed by PCR (254) and convergence of the aptamer libraries on a limited number of proteins when presented with complex mixtures of possible targets (211, 215). We investigated the dynamics of SELEX under the heavy selective pressure of Serial-SELEX by interrogating starting libraries, intermediate and final pools using the Illumina sequencing platform. We also conducted control experiments where randomized DNA libraries were subjected to multiple rounds of dilution and amplification, Neutral-SELEX, to test whether PCR bias played a significant role shaping in the dynamics of SELEX.

3.2 Results

3.2.1 Monitoring the progression of aptamer selection

To isolate aptamers against conserved IE surface determinants, two synthetic libraries of 10^{14} ssDNA molecules containing 40 base randomized regions flanked by library-specific primer sequences were subjected to the Serial-SELEX procedure illustrated in Figure 2.1. Final and intermediate rounds were sequenced alongside the starting naïve library and libraries subjected to Neutral-SELEX for comparison. Approximately 2-37 million clones were sequenced in our experiments and 0.5-4 million clones were retained for analysis following strict qualification (Table 3.1). We confirmed that the naïve LV and LIC libraries were diverse, composed almost exclusively (99.6% and 94.9% respectively) of sequences with just a single copy (Table 3.1). Neutral-SELEX experiments where libraries were placed solely under the selective biases imposed by PCR amplification failed to differentially enrich any sequences. Specifically, round 10 pools following Neutral-SELEX consisted almost exclusively of sequences with just a single copy (97.8% for the LV and for 94.9% the LIC). In contrast, subjecting libraries to Serial-SELEX drove the proportion of orphan sequences in the LV and LIC down to 49.0% and 22.3% respectively (Table 3.1). By aligning the 40 base variable regions of unique sequences found in more than 1 copy in final Serial-SELEX pools, we found sequences which could be readily be grouped into large families based on their primary sequence similarity indicating potential co-selection of functionally similar aptamers (Figure 3.2).

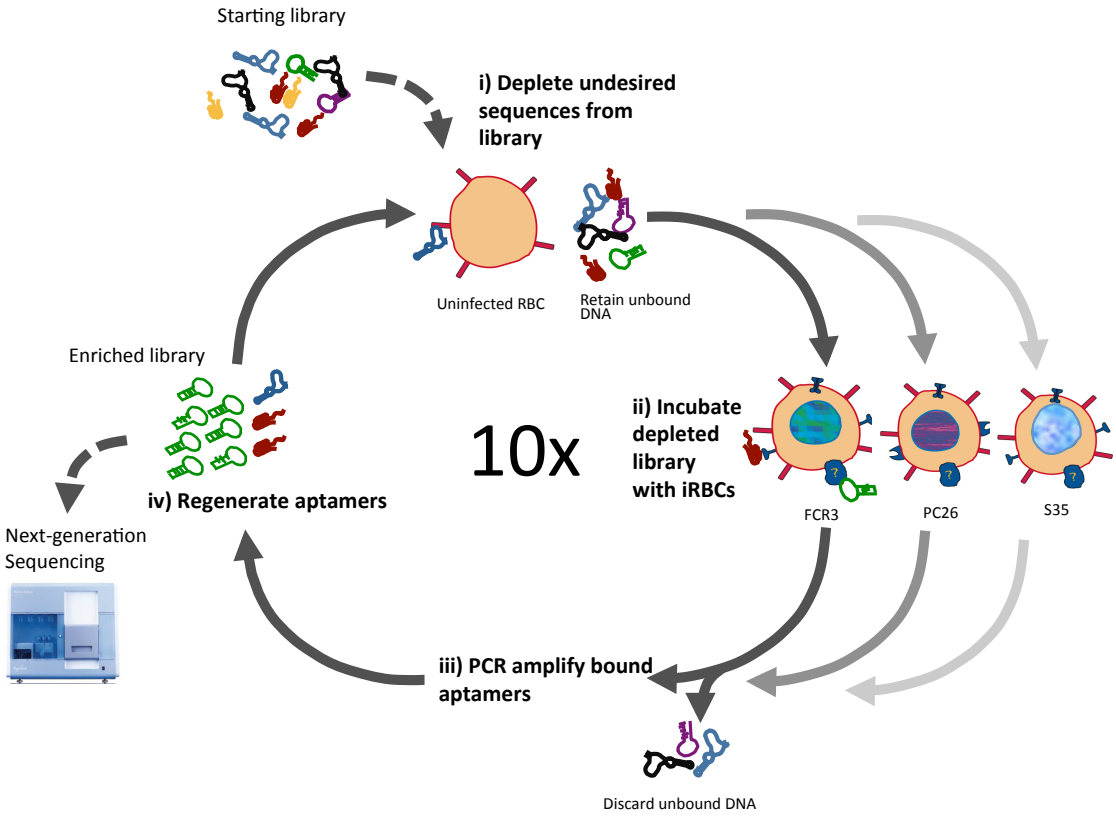

Figure 3.1 Schematic representation of Serial-SELEX procedure to generate ssDNA aptamer binding to conserved IE determinants.

i) A combinatorial ssDNA library, which consists of oligonucleotides with a centrally randomized region of 40 nucleotides flanked by specific primers, is removed of specific binders to uninfected RBC in a negative selection step. ii) The depleted library is incubated with a unique strain of *P. falciparum* to enforce selection of aptamers binding determinants unique to IEs iii) Following thorough washing, bound sequences are amplified by PCR using unmodified forward and phosphorylated reverse primers. iv) Aptamers are regenerated as ssDNA by digesting the phosphorylated reverse of PCR product using lambda exonuclease. The resulting enriched ssDNA pool is used in the next round of the negative selection, positive selection, and amplification. In the last SELEX round the selected ssDNA are analyzed for aptamer enrichment using the Illumina high throughput sequence platform.

Alignment of the 500 most frequent unique sequences from round 6 and 10 from the two parallel Serial-SELEX experiments revealed multiple aptamer families (Figure 3.2). LIC round 10 contained 26 aptamer families including one family, represented by Euge.1, that constituted 58.3% of analyzed sequences (Figure 3.2). LV selection displayed a weaker signature of enrichment; only 6 families could be readily identified in LV round 10, one with a maximum frequency of 32.4%. Interestingly, virtually none of the largest aptamer families in intermediate LV round 6 were found prominently enriched in round 10, underscoring the complex dynamics of SELEX. A similar comparison between intermediate and final LIC Serial-SELEX rounds could not be performed due to the loss of LIC round 6 during Illumina sample preparation.

Liver cancer- or thyroid transcription factor 1-binding aptamers previously derived from our starting libraries were not recovered in the final Serial-SELEX pools (250, 251). Likewise, sequences recovered in the final pool were not previously described in the literature nor found in the human or *Plasmodium* genomes. Taken together, these data suggest that we have enriched multiple aptamers.

3.2.2 Validation of selected aptamers

The most frequent clones from each of 11 of the largest aptamer families were chemically synthesized for further analysis (Table. 3.2). All aptamers were truncated to the 40 base variable regions in order to enhance synthesis efficiency and increase the flexibility of chemical manipulation. We radiolabeled aptamers and showed 10 of 11 aptamers tested have the ability to bind the *P. falciparum* line FCR3 and could

therefore be used as probes of putative conserved surface determinants (Figure 3.4-3.14). We determined the equilibrium dissociation constant (K_d) for the interaction of aptamers with IEs and as shown in Figure 3.4-3.14, we found that selected aptamers have an apparent K_d in the nanomolar range. Binding was sequence dependent as a random sequence control, RDM, showed no appreciable affinity to IEs (Figure 3.15*)*.

Library	SELEX Round	Sample ID	Total Reads	Total Qualified Reads	Qualified Reads With Only 1 Copy	% Qualified Reads With Only 1 Copy	Qualified Reads With More Than 1 Copy	% Qualified Reads With More Than 1 Copy	Unique Qualified Reads After Collapsing Identicals
LIC	--	Unselected Library	5,182,199	646,535	613,496	94.89	33,039	5.11	629,578
LIC	10	Neutral-SELEX	29,904,896	2,939,844	2,789,960	94.90	149,884	5.10	2,862,625
LIC	10	Serial-SELEX	31,131,708	3,492,177	777,804	22.27	2,714,373	77.73	900,980
LV	--	Unselected Library	2,126,732	524,000	522,139	99.64	1,861	0.36	523,056
LV	10	Neutral-SELEX	24,457,128	2,637,540	2,581,622	97.88	55,918	2.12	2,609,398
LV	6	Serial-SELEX	21,142,112	1,861,962	1,670,691	89.73	191,271	10.27	1,761,861
LV	10	Serial-SELEX	37,103,592	3,563,842	1,743,462	48.92	1,820,380	51.08	2,171,540

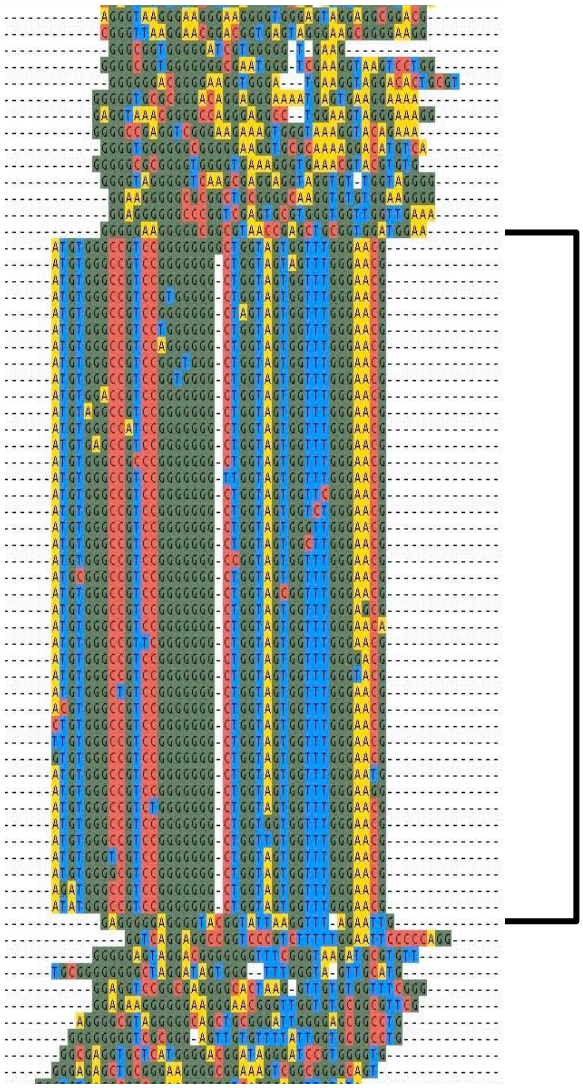

Figure 3.2 Alignment of Serial-SELEX pools reveals enrichment of unique sequences that can be grouped into aptamer families.

Shown is a representative primary sequence alignment (obtained using ClustalW) for visual classification of similarity amoung qualified unique sequence cloned from Serial-SELEX LV round 10.

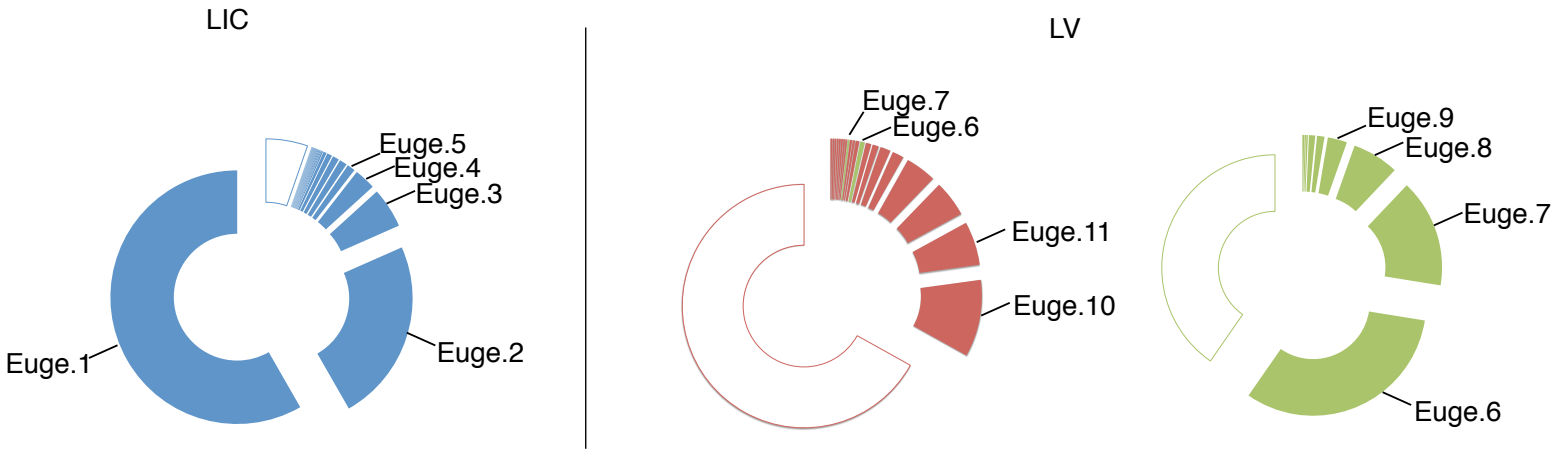

Figure 3.3 Deep sequencing of the final pools reveals enrichment of multiple aptamers.

Doughnut chart represents ~2 million qualified reads from LIC Round 10 (Blue), LV Round 6 (Red), and LV Round 10 (Green). Open pieces represent reads that could not be grouped.

Table 3.2. Sequences and guanine-cytosine content of selected aptamers.

Aptamer	Sequence	% GC
Euge.1	TCGCGGGGTGGGTGGTGTGGGGGAGCGTGTGCGGTTTGGT	70
Euge.2	CGATGGGCGTGCTTGGTTGGTGTGGTTTGGGAACGCGTAT	58
Euge.3	AAACTGTGGTTGGCTCAGGGGTGGTCGGTTGTATGCTATA	50
Euge.4	GGGTGGAGGGGTGGGGGTGGTCGCCTTTTTAGGAAGTTTG	60
Euge.5	CCCTTTTGGAGTTACGAGTCATGGTTTGGTCTGGTTGGCT	50
Euge.6	GTTGGTTTGGTTGGTTTAGTGCATCTTGTATGTTTCACTC	40
Euge.7	GTCTATTACGGGGGGAGGGTGGGTGGAGTAATTGGTTATG	53
Euge.8	TGCTAAGAGGTTGGGTTGTGGTTGGGATGCACTGATTTTT	45
Euge.9	GTTGGTTTGGTTGGTATTTGGGGCCCATCGAGCTTCTTTC	50
Euge.10	GGAGAGGCGCTATCTCAAGTCACATGCCGCGGATCTTGCT	58
Euge.11	TTTGGCTTAAGGTGAAAGATGAGAAATTTCTCGCCGTGTT	40

.

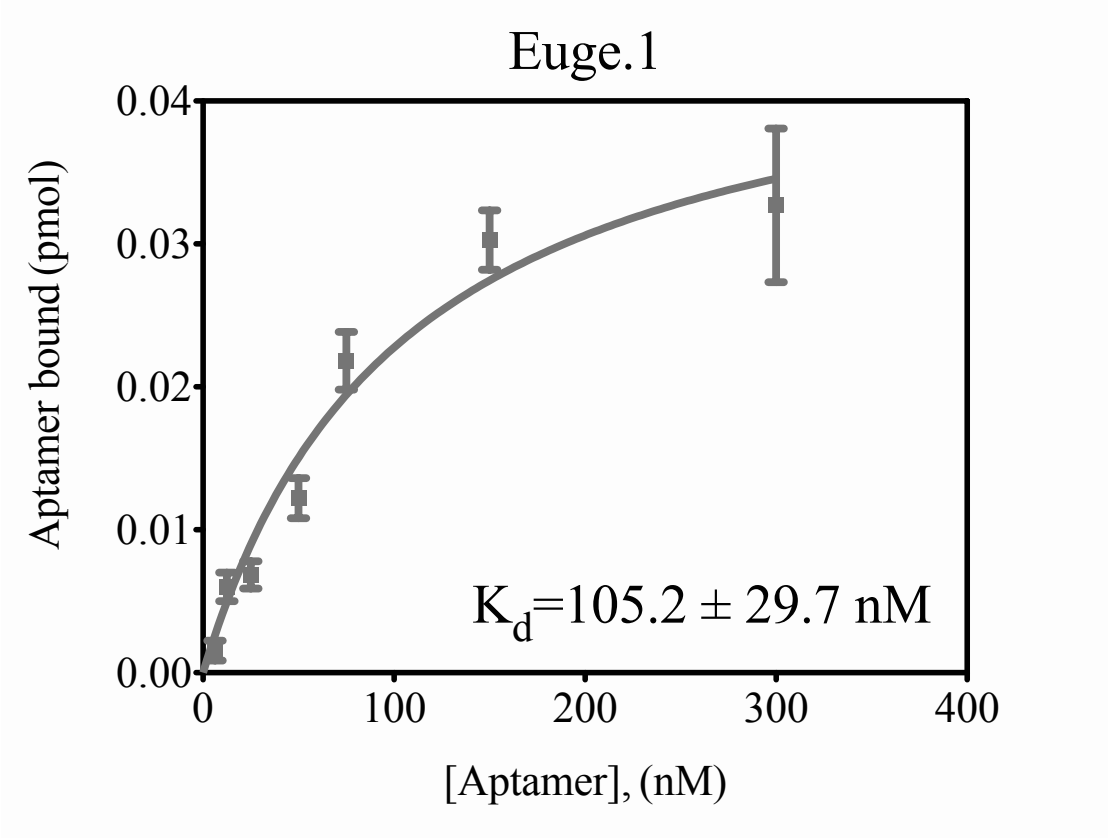

Figure 3.4 Euge.1 binding curve.

IEs (10^6 cells) were incubated with increasing concentrations of radiolabeled aptamer. Standard error values were determined from two independent experiments performed in triplicate.

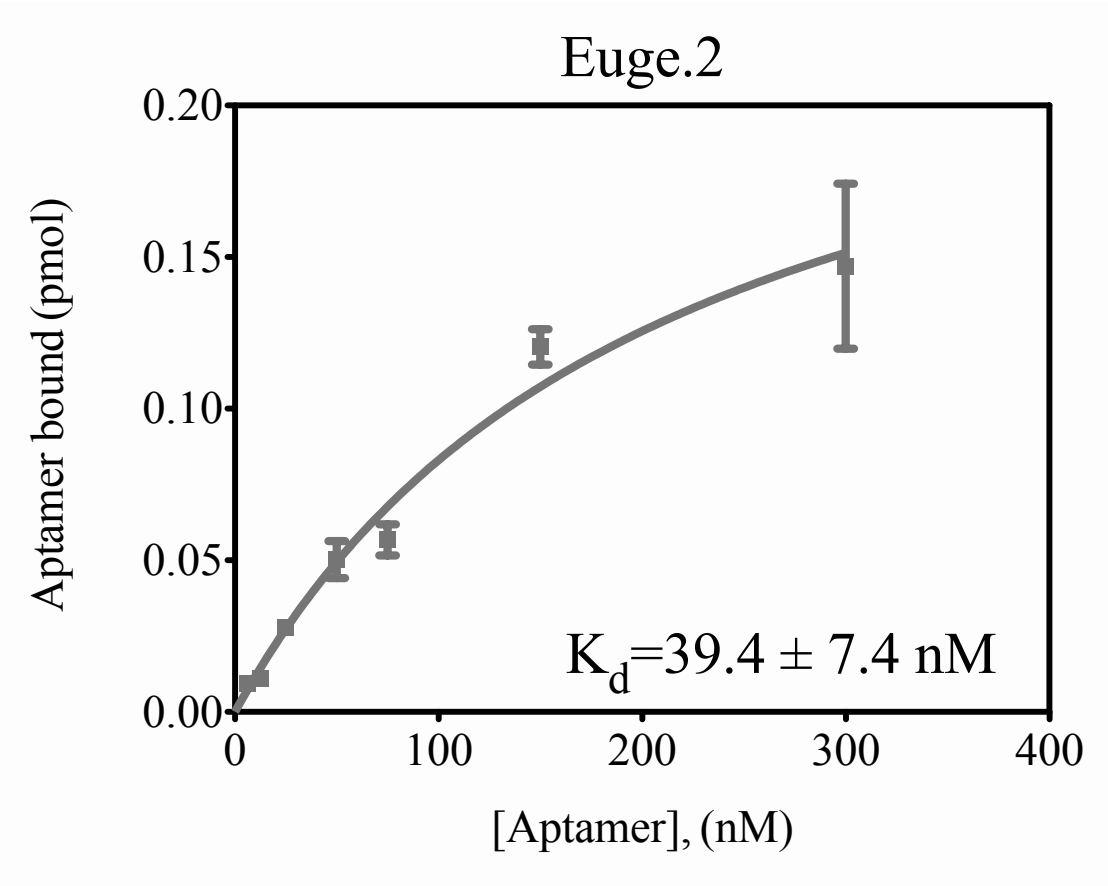

Figure 3.5 Euge.2 binding curve.

IEs (10^6 cells) were incubated with increasing concentrations of radiolabeled aptamer. Standard error values were determined from two independent experiments performed in triplicate.

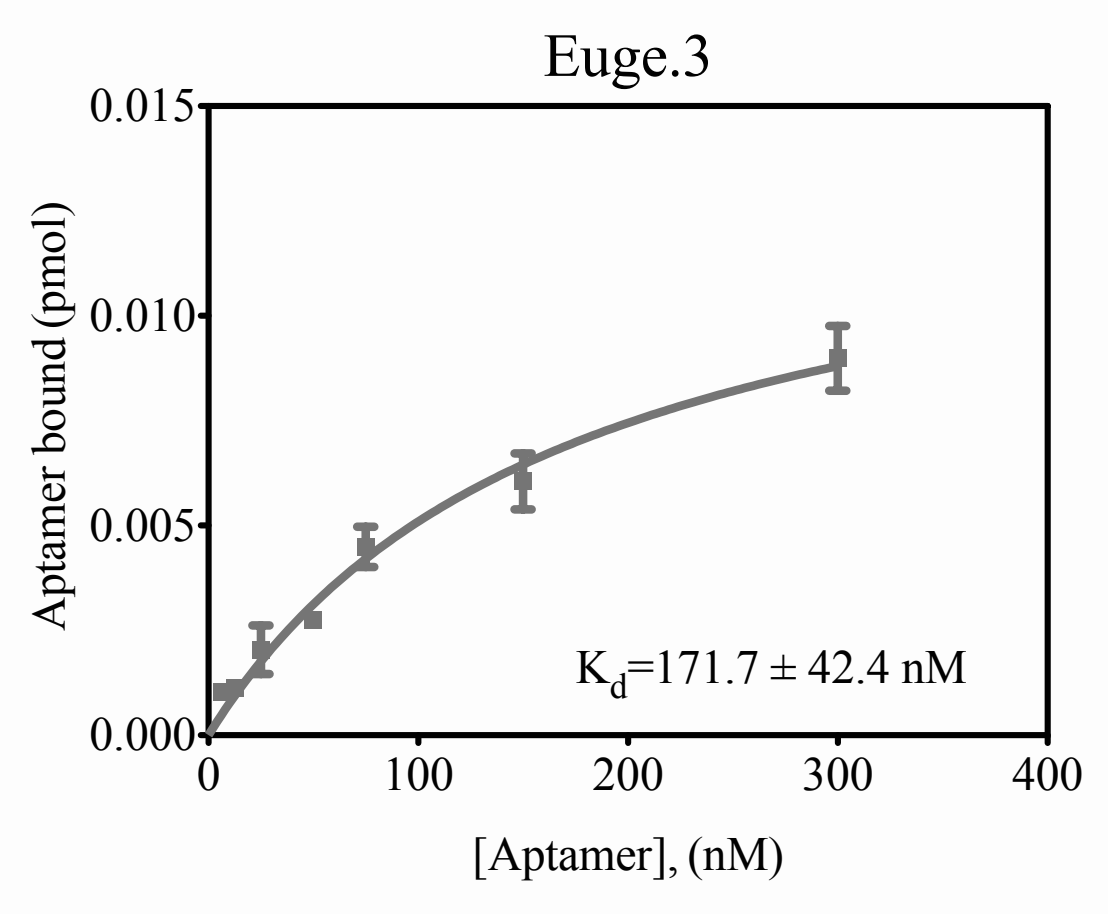

Figure 3.6 Euge.3 binding curve.

IEs (10^6 cells) were incubated with increasing concentrations of radiolabeled aptamer. Standard error values were determined from two independent experiments performed in triplicate.

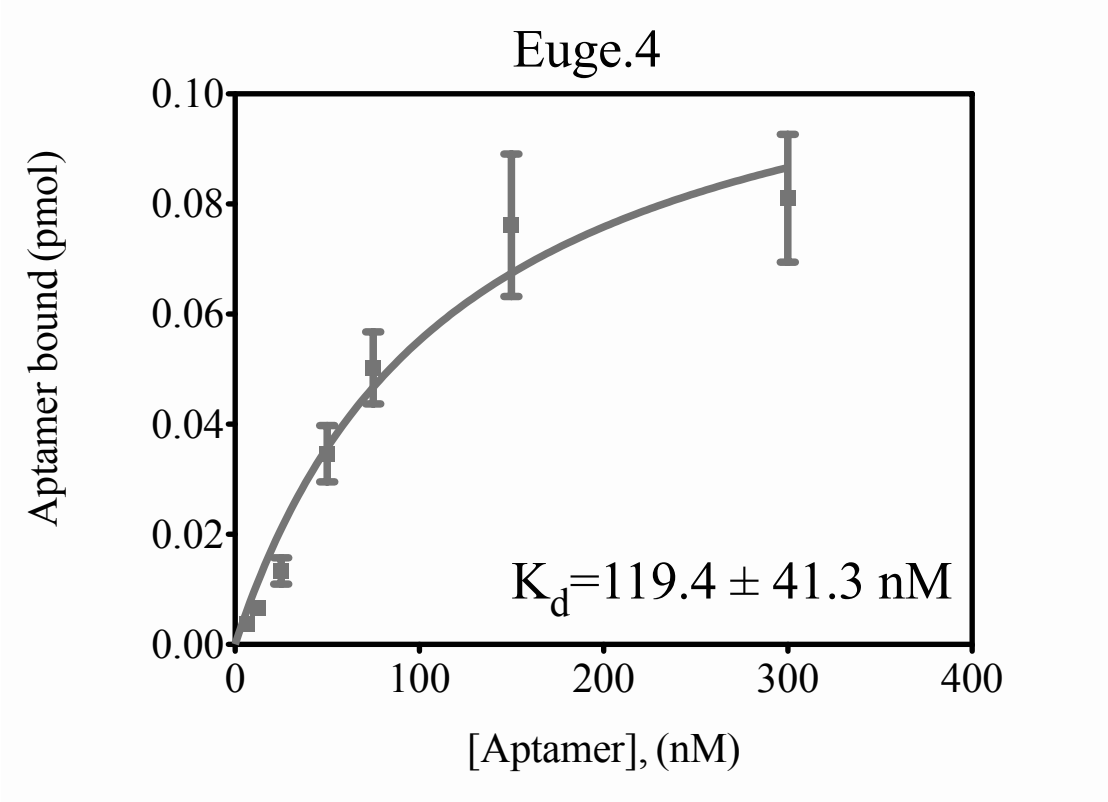

Figure 3.7 Euge.4 binding curve.

IEs (10^6 cells) were incubated with increasing concentrations of radiolabeled aptamer. Standard error values were determined from two independent experiments performed in triplicate.

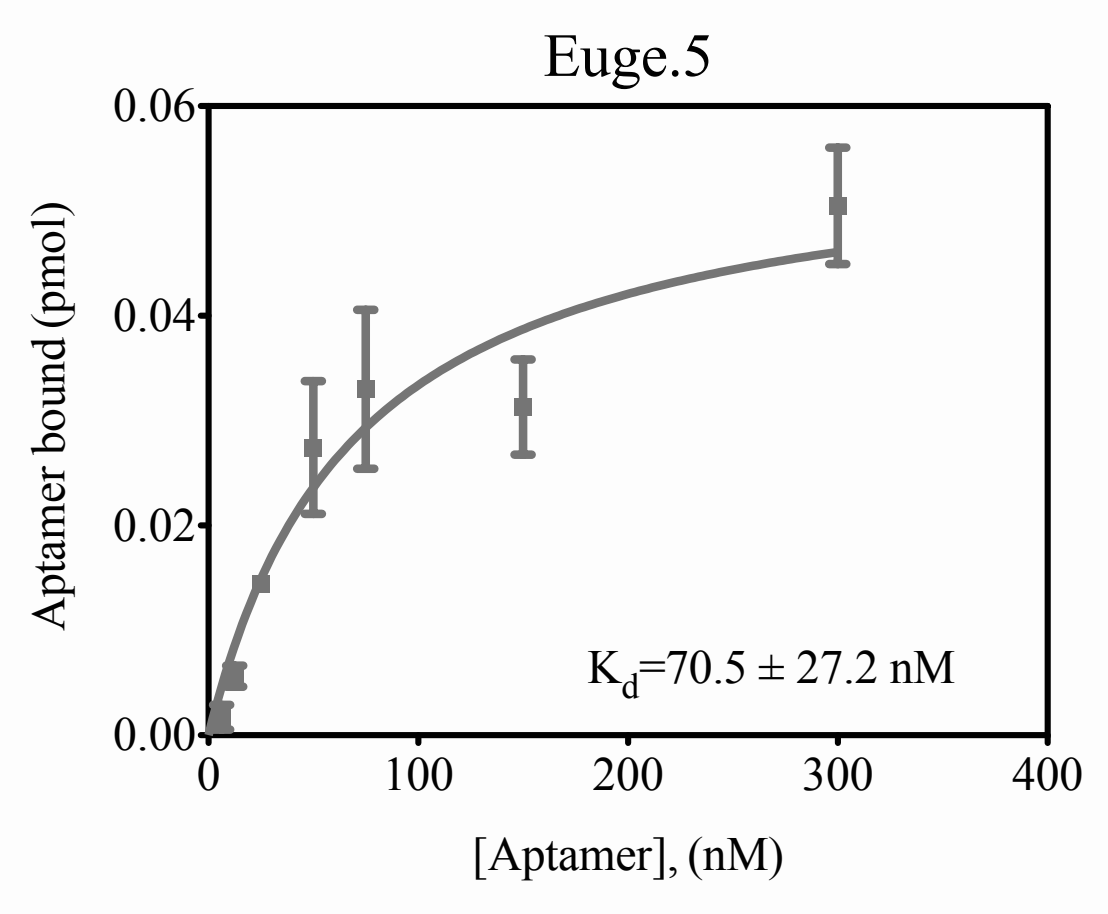

Figure 3.8 Euge.5 binding curve.

IEs (10^6 cells) were incubated with increasing concentrations of radiolabeled aptamer. Standard error values were determined from two independent experiments performed in triplicate.

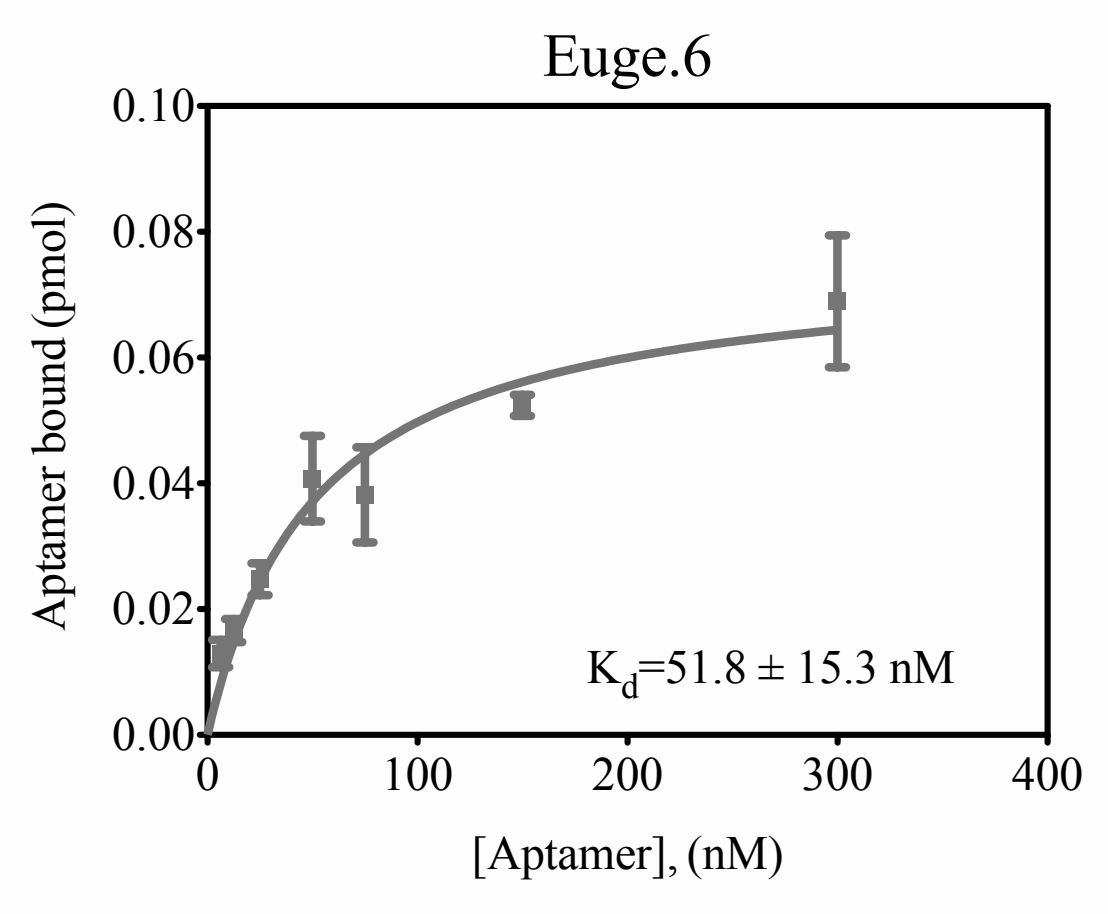

Figure 3.9 Euge.6 binding curve.

IEs (10^6 cells) were incubated with increasing concentrations of radiolabeled aptamer. Standard error values were determined from two independent experiments performed in triplicate.

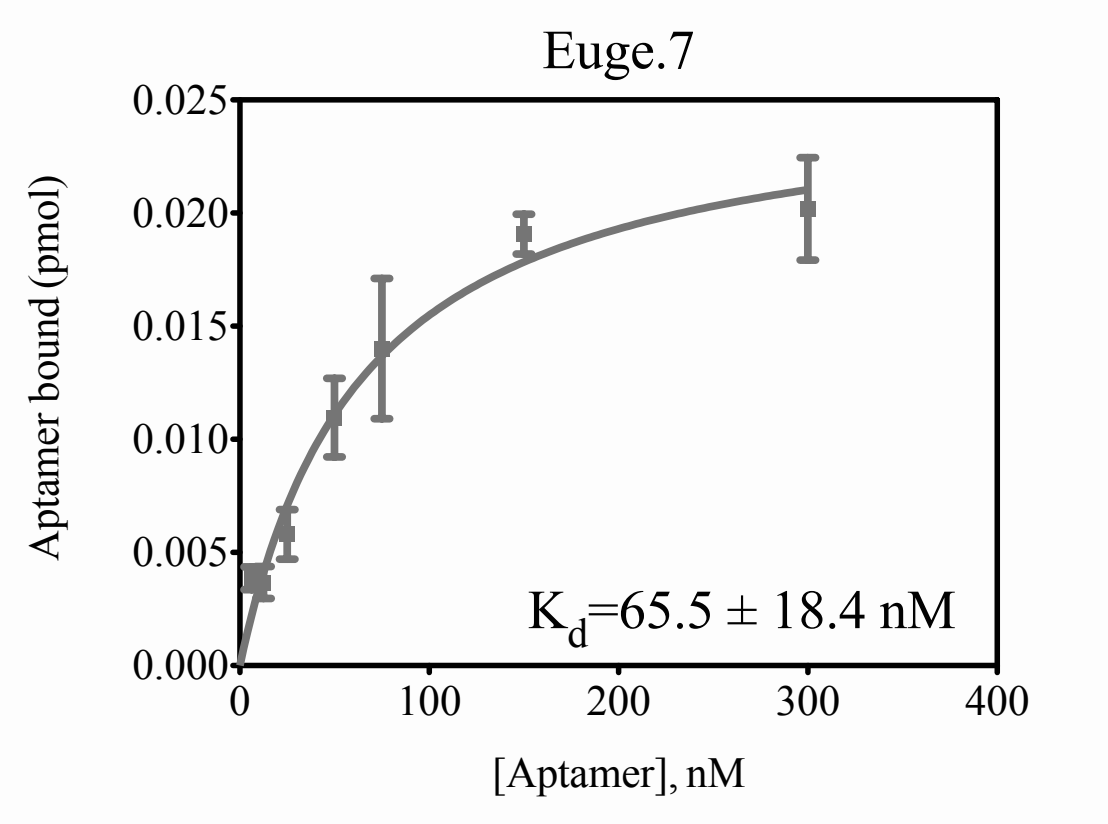

Figure 3.10 Euge.7 binding curve.

IEs (10^6 cells) were incubated with increasing concentrations of radiolabeled aptamer. Standard error values were determined from two independent experiments performed in triplicate.

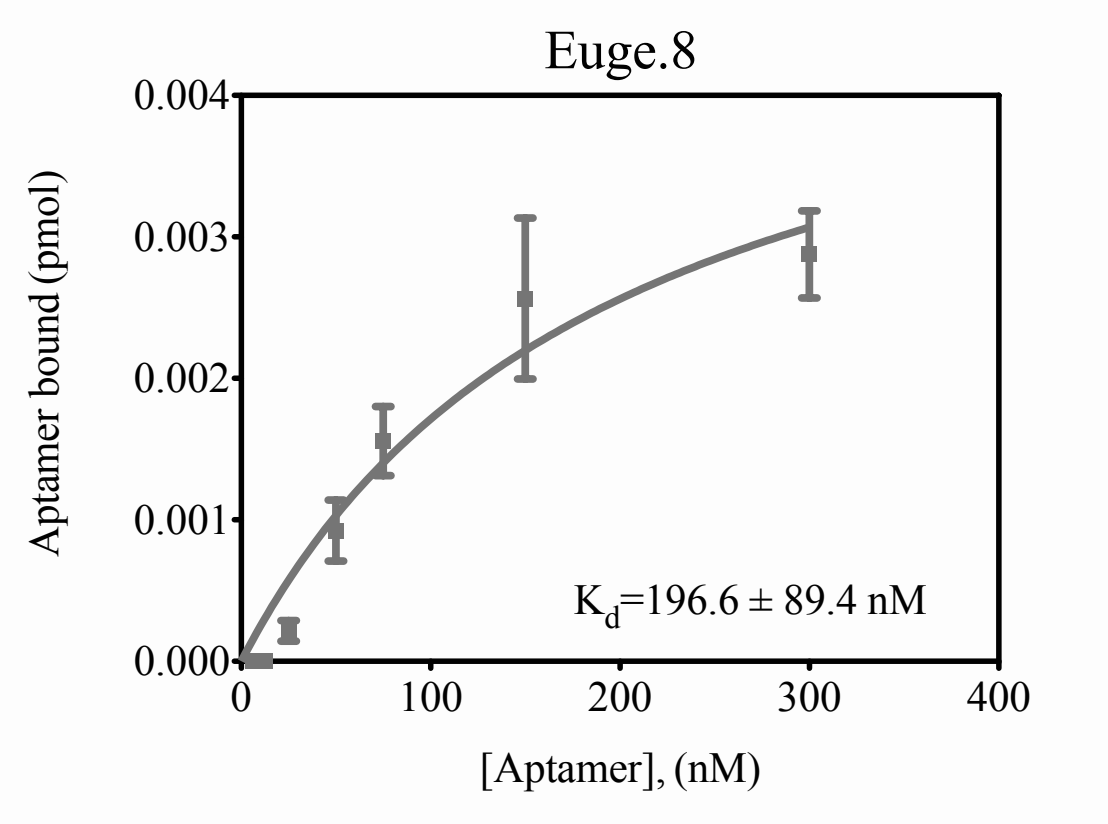

Figure 3.11 Euge.8 binding curve.

IEs (10^6 cells) were incubated with increasing concentrations of radiolabeled aptamer. Standard error values were determined from two independent experiments performed in triplicate.

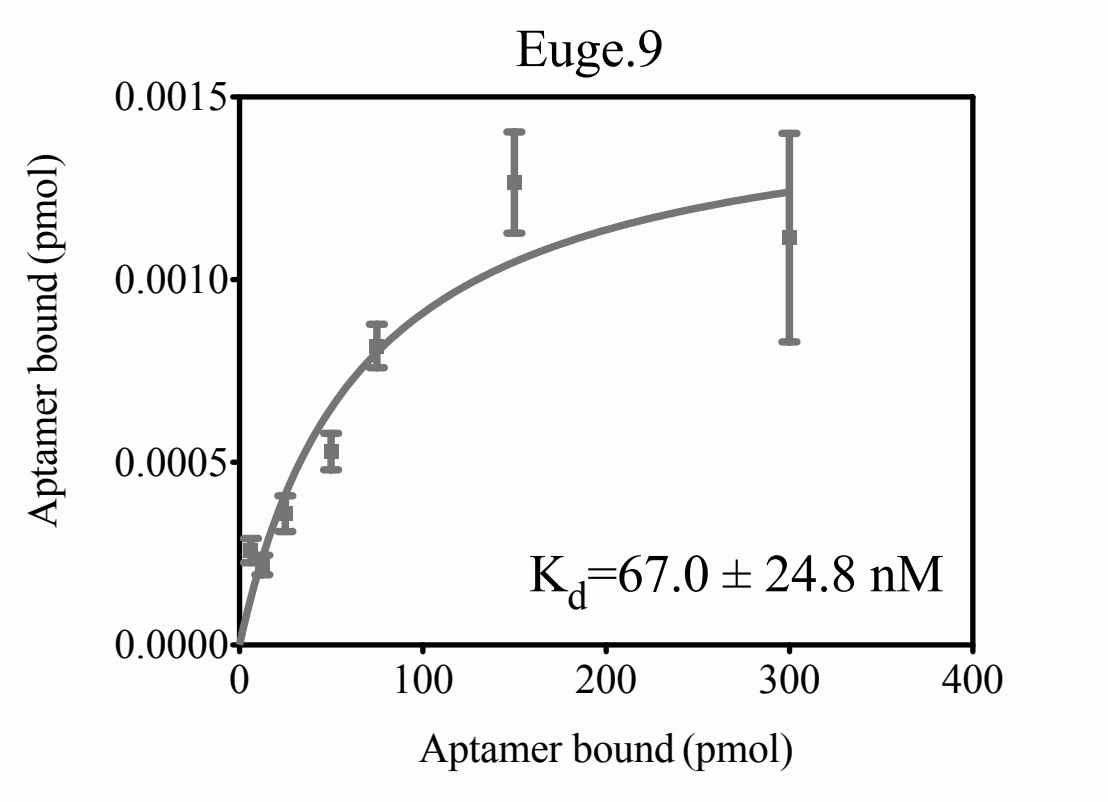

Figure 3.12 Euge.9 binding curve.

IEs (10^6 cells) were incubated with increasing concentrations of radiolabeled aptamer. Standard error values were determined from two independent experiments performed in triplicate.

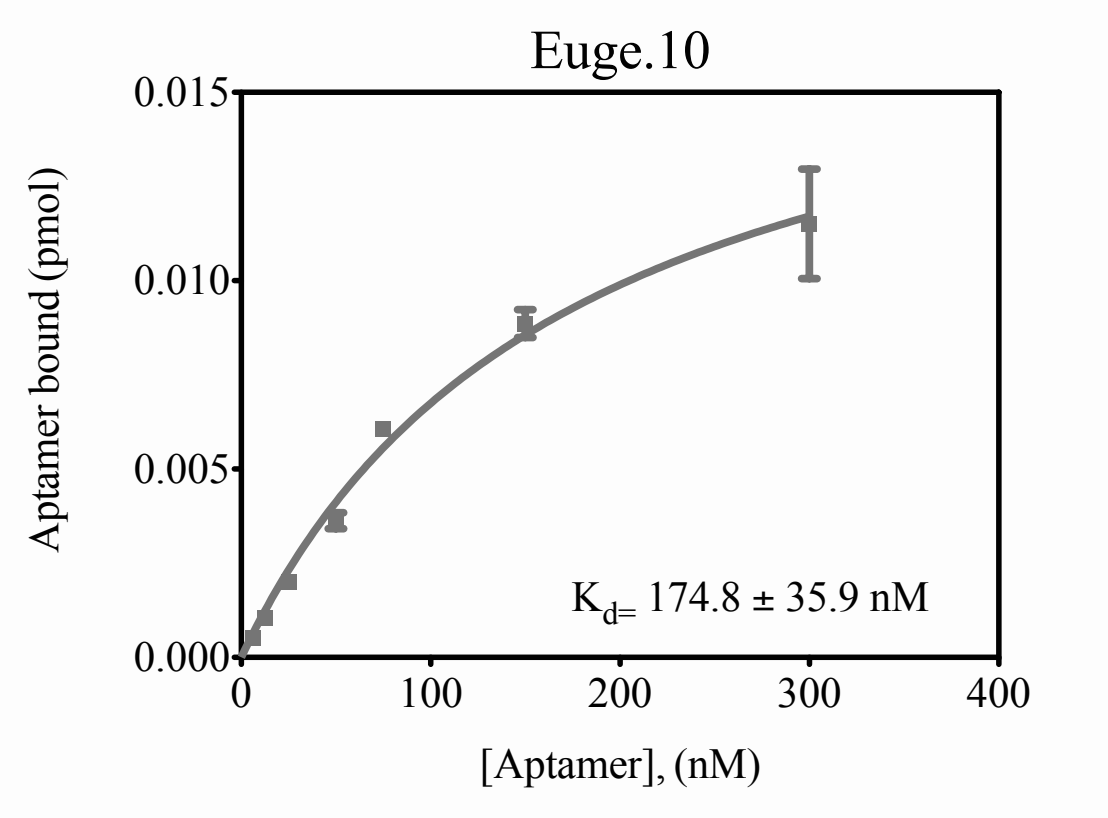

Figure 3.13 Euge.10 binding curve.

IEs (10^6 cells) were incubated with increasing concentrations of radiolabeled aptamer. Standard error values were determined from two independent experiments performed in triplicate.

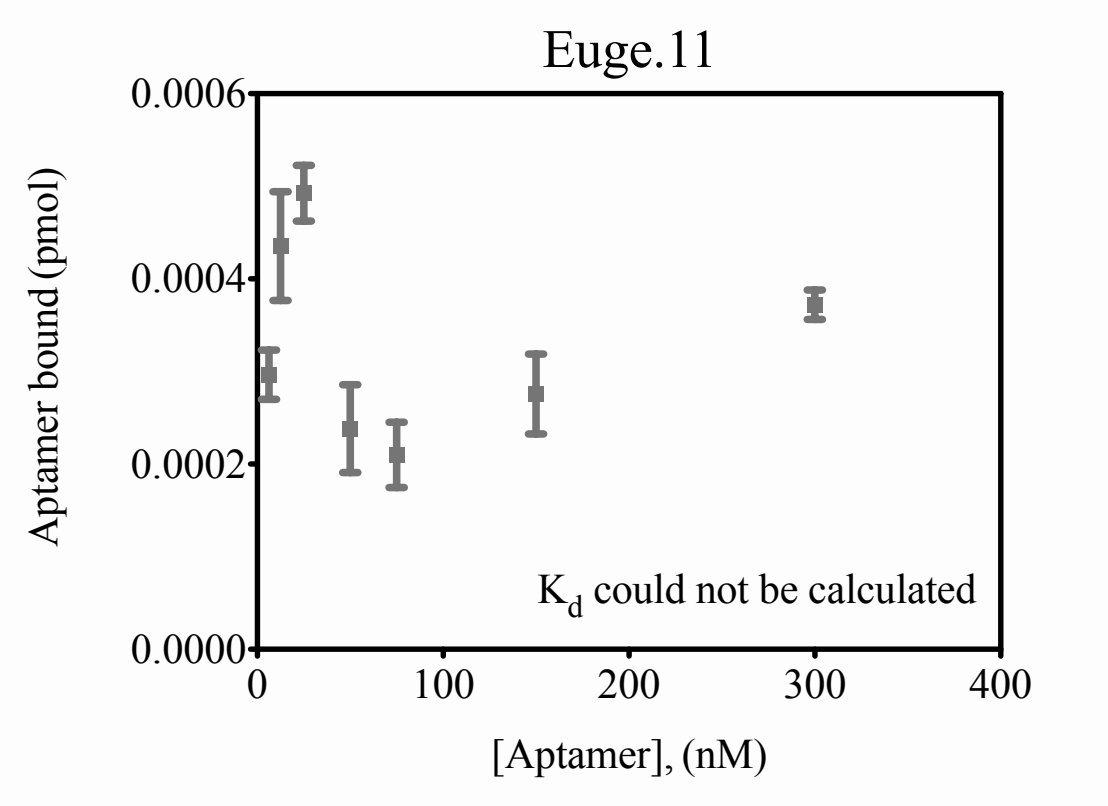

Figure 3.14 Euge.11 binding curve.

IEs (10^6 cells) were incubated with increasing concentrations of radiolabeled aptamer.

Standard error values were determined from an experiment performed in triplicate.

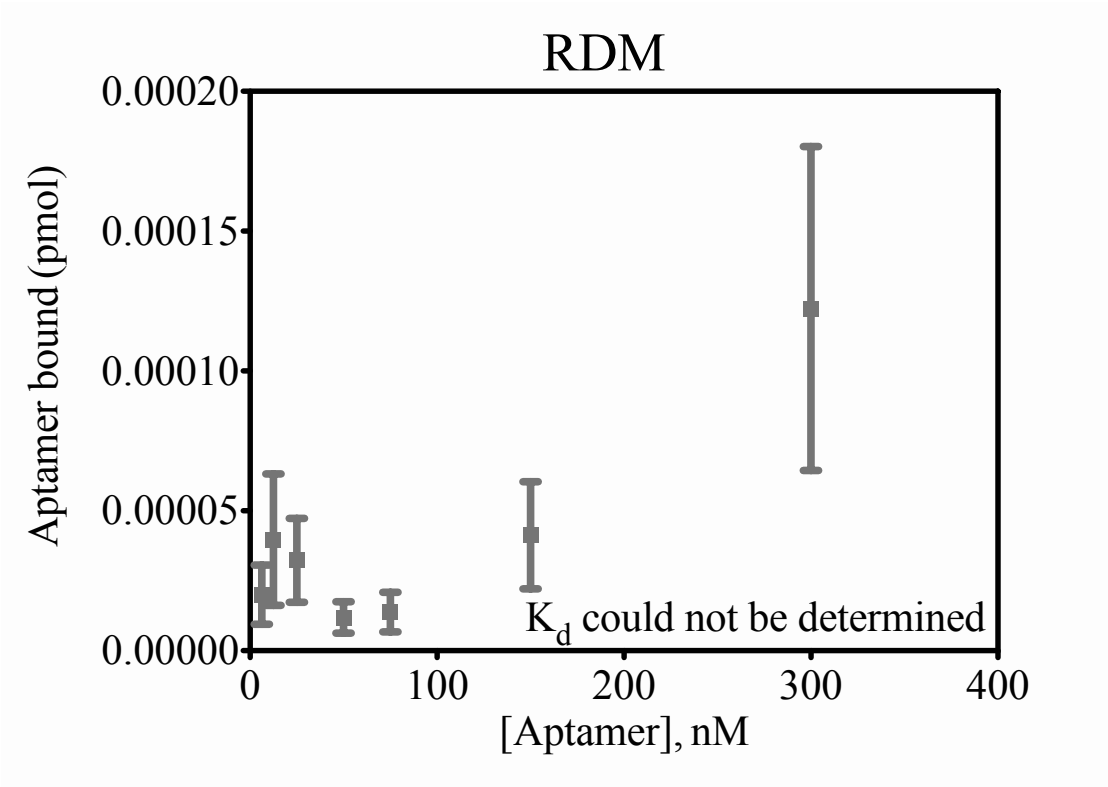

Figure 3.15 RDM binding curve.

IEs (10^6 cells) were incubated with increasing concentrations of radiolabeled aptamer.

Standard error values were determined from an experiment performed in triplicate.

3.3 Discussion

High throughput sequencing was used to monitor the progression of parallel Serial-SELEX experiments aimed at directing aptamers to potential conserved IE determinants. We confirmed that naïve libraries were heterogeneous in sequence (each consisting of 94% or greater unique clones out of an average 585,267 qualified reads) and remained diverse following neutral selection (94% or greater unique clones average 2,785,692 qualified reads). On the other hand, Serial-SELEX enriched multiple aptamer families, most notably Euge.1 by almost 400,000 fold to reach a frequency of 60% of a final analyzed pool fraction. Although we used libraries originally designed for selection against two non-malarial proteins, Serial-SELEX did not recover aptamers previously described in the literature (data not shown). Likewise, recovered sequences have no similarity to sequences in the human or *Plasmodium* genomes. Of the 11 aptamers enriched by Serial-SELEX, 10 demonstrated parasite-specific binding with nanomolar dissociation constants typical of cell selected aptamers (218, 255). Taken together these data suggest that Serial-SELEX enriches for multiple aptamers some of which may presumably recognize a conserved malaria target.

Our experimental design coupled with the resolution of high-throughput sequencing provided a unique glimpse at the dynamics of SELEX. We subjected two libraries that differ only in primer sequences to the pressures of Serial-SELEX and observed dramatically different levels of enrichment: only 22.3% of the final pool from LIC selection remained undifferentiated versus 49.0% in the LV. No aptamer families

were found shared between the two libraries. The within library dynamics are difficult to interpret as leading families of LV round 6 were not found with any degree of prominence in round 10. Complex and possibly stochastic dynamics have been observed against purified and cell surface targets (211, 256). It would thus appear important to carefully monitor SELEX experiments but it seems unlikely that there are uniform optimal conditions for enrichment between different libraries or across different selection pressures.

It is inviting to attribute the apparently stochastic dynamics of SELEX to the nucleotide amplification steps. Previous studies subjecting RNA libraries to non-targeted selection have found biases toward pyrimidine sequences, truncated and less stable molecules (254, 257). A nonspecific bias influencing selections could potentially reduce the likelihood that optimal sequences are identified. To explore this in the context of a DNA library, we subjected two libraries to Neutral-SELEX and show that no particular sequences are differentially enriched. In terms of molecular stability, several sequences enriched by Serial-SELEX including Euge.1 are quite guanine rich (Supplemental Figure 3.1) and likely form complex guanine-quartet structures common to other selected aptamers (214, 258–260). This suggests there is not a strong intrinsic amplification bias toward less complicated molecules. Given the lack of bias in our DNA-based studies, it seems reasonable that the observed bias in RNA selections may be explained by the additional reverse transcription step required to amplify RNA libraries.

3.4 Supplemental information

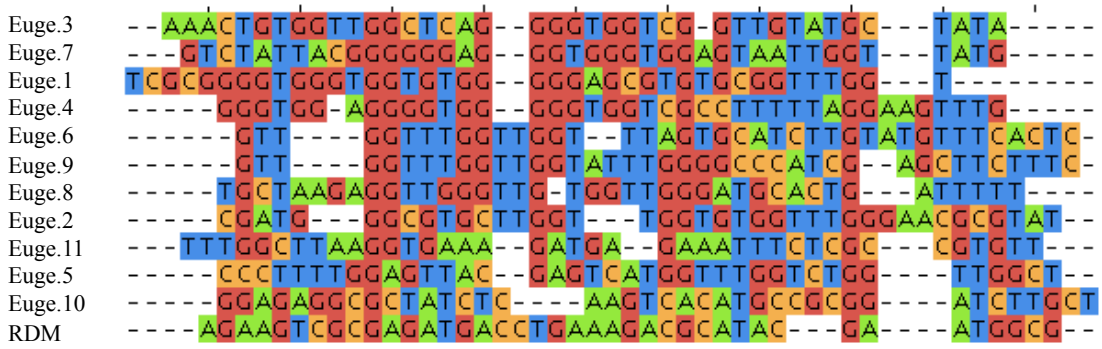

Supplemental Figure 3.1 Alignment of selected aptamers.

Shown are 40 base variable region of aptamers selected by SELEX and random sequence control (RDM).

3.5 Acknowledgement

High throughput sequencing was performed by the NIH Intramural Sequencing Center. Mariam Quinones Ph.D of the Bioinformatics and Computational Biosciences Branch of the National Institutes of Allergy and Infectious Disease/NIH assisted with the filtering and qualification of Illumina sequences.

Chapter 4. Characterization of the binding range of selected aptamers

4.1 Introduction

This chapter focuses on evaluating the binding characteristics of aptamers enriched by Serial-SELEX. Based on the counterselection and selection steps employed, we expect that some aptamers will discriminate against uninfected RBCs while recognizing IEs used in the positive selection steps. The incorporation of multiple parasite isolates is expected to drive enrichment of aptamers that recognize determinants conserved between geographically diverse IEs. Identification of a broadly binding aptamer would strongly support our hypothesis that structurally conserved determinants are displayed on the surface of IEs.

4.2 Results

4.2.1 Development of a quantitative aptamer binding assay

We developed a simple aptamer binding assay, illustrated in Figure 4.1, that allowed us to efficiently and quantitatively measure the cell binding of 11 aptamers described previously (Supplemental Table 4.1-5). We validated the assay by independently testing the binding of radiolabeled Euge.7 to IEs over the course of weeks and observed that the aptamer binding phenotype is relatively stable (Figure 4.2).

4.2.2 A select group of aptamers bind a wide range of *Plasmodium*

Next, we examined the breadth of aptamer binding by screening radiolabeled aptamers against a variety of cell types. Consistent with the incorporation of a negative selection step against RBCs, we found that all members of the panel failed to recognize uninfected RBCs (Table 4.1). Serial-SELEX should enrich for aptamers capable of recognizing IEs used as targets for positive selection. To that end, we screened aptamers against a panel of 7 lines used in Serial-SELEX including the highly drug-resistant line W2-mef (Table 4.1). We identified three aptamers, Euge.1, Euge.4, and Euge.7 that recognize all target lines whereas other aptamers showed a more strain-restricted binding phenotype. We extended our study to 8 laboratory lines not used in Serial-SELEX and found that Euge.1, Euge.4, and Euge.7 recognized all lines tested (Table 4.1).

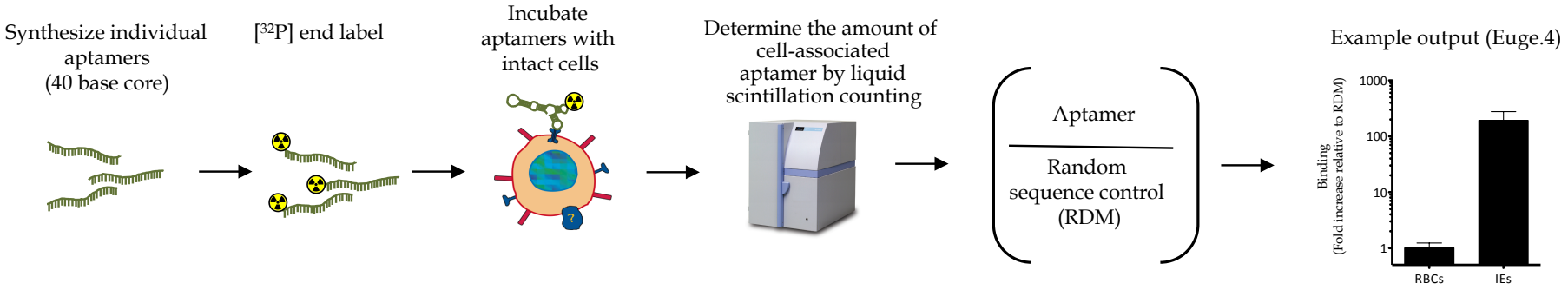

Figure 4.1 Schematic of the aptamer binding assay.

The 40 base randomized regions from individual aptamers recovered from SELEX were synthesized, end-labeled with [^{32}P], and incubated with intact cells. Following incubation and wash, cells were lysed and the amount of cell-associated aptamer was quantified by liquid scintillation. The assay's output was fold difference above background. Background was defined as the level of binding of a random sequence control to IEs. Samples were always tested in triplicate.

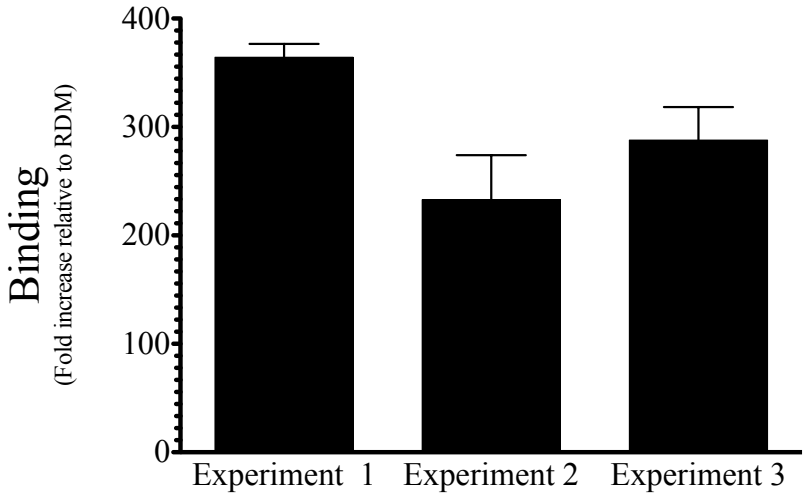

Figure 4.2 Aptamer binding assay has limited variation.

Shown are the results from three independent binding experiments using Euge.7 and IEs (FCR3 strain). The assays were performed approximately a week apart. Error bar indicate the SEM of experiments performed in triplicate.

Table 4.1. Using aptamers to recognize different *P. falciparum* laboratory lines

	Euge.1	Euge.2	Euge.3	Euge.4	Euge.5	Euge.6	Euge.7	Euge.8	Euge.9	Euge.10	Euge.11
Human Uninfected RBCs	1	1	3	2	2	1	1	1	1	1	1
FCR3*	124	14	29	173	6	5	297	18	10	5	2
FVO*	69	13	34	379	8	6	396	20	23	1	4
S35*	9	1	1	12	2	2	36	3	1	2	1
PC26*	26	3	4	23	4	1	116	9	2	5	1
C2A*	28	4	4	55	11	2	149	13	3	5	1
Div30*	8	2	1	20	1	2	33	4	2	1	1
W2-mef*	24	5	14	218	4	2	16	4	7	2	2
3D7	9	4	2	54	2	2	36	6	4	1	2
Indo China	122	11	21	154	8	3	357	14	7	5	1
102/1	34	3	3	55	6	2	161	10	3	6	1
D10	21	4	4	88	3	2	93	8	3	2	2
KMW2	8	2	1	27	2	1	30	4	1	1	1
HB3	24	12	41	78	8	3	203	9	9	5	3
L32	6	1	2	11	1	1	6	1	1	1	1
DD2	5	1	1	36	--	--	9	1	1	--	--

The binding capacity of radiolabeled aptamers (100 nM) to IEs infected with indicated strains of *P. falciparum* is given as the fold difference above background. Background was defined as the level of binding of a random sequence control to IEs. Cells highlighted in red exceed the threshold for definitive aptamer binding set at 5 fold above background. * Strains used for Serial-SELEX.

To rule out whether aptamer binding was due to artifact generated by parasite laboratory adaptation (261, 262), we tested clinical isolates from malaria-infected patients in Cambodia and Mali. Euge.1, Euge.4, and Euge.7 recognized all *P. falciparum* clinical isolates tested (Table 4.2). Taken together, these data confirm our hypothesis that structurally conserved determinates are displayed on IEs.

Table 4.2. Aptamer recognition of *P. falciparum* clinical isolates

	Euge.1	Euge.2	Euge.3	Euge.4	Euge.5	Euge.6	Euge.7	Euge.8	Euge.9	Euge.10	Euge.11
CP887	36	4	2	100	2	1	122	3	3	1	2
CP845	16	2	1	16	2	2	28	2	3	1	7
CP877	34	6	2	61	4	2	118	4	5	1	12
CP819	31	3	3	98	2	1	54	4	3	2	1
CP830	5	1	1	39	1	1	12	2	2	1	1
KN-1254	116	19	93	265	21	6	307	29	32	8	3
KN-1314	41	5	16	171	7	4	118	8	12	4	1
KN-1068	19	2	20	18	4	8	45	4	7	2	2
KN-0490	56	1	4	25	--	--	6	1	1	--	--
KN-0430	151	23	117	823	--	--	757	23	32	--	--

The binding capacity of radiolabeled aptamers (100 nM) to IEs infected with indicated strains of *P. falciparum* is given as the fold difference above background. Background was defined as the level of binding of a random sequence control to IEs. Cells highlighted in red exceed the threshold for definitive aptamer binding set at 5 fold above background. CP lines are derived from Cambodian infections and KN from Malian infections.

The identification of a subset of aptamers that recognize all strains of *P. falciparum* tested raises the question of whether these aptamers may bind other species of *Plasmodium*. To address this question, we determined the binding potential of Euge.1, Euge.4, Euge.7 and a representative strain-restricted aptamer, Euge.9, to five *Aotus*-adapted *P. vivax* clones (Table 4.3). Euge.1, Euge.4, and Euge.7 recognized *Aotus*-adapted clones but showed no obvious affinity for uninfected *Aotus* RBCs prepared in parallel. Aptamer recognition of *P. vivax* to real human clinical samples was also tested. We found that Euge.4 and Euge.7 could bind *P.vivax* clinical isolates whereas Euge.1 displayed measurable affinity but failed to meet our strict criterion for definitive binding (Table 4.3).

Finally, we tested aptamer binding to additional species of *Plasmodium*. The results (Table 4.4) show that Euge.1, Euge.4, Euge.7, Euge.9 recognize *P. knowlesi*-infected IEs but not any of the murine lines or corresponding uninfected RBC controls screened.

Table 4.3. Aptamer recognition of *Plasmodium vivax*

	Euge.1	Euge.4	Euge.7	Euge.9
Aotus Uninfected RBCs	1	1	2	1
NIH-1993	10	71	18	3
Brazil-1 CDC	17	32	83	2
Chesson	8	28	47	1
Vietnam-IV	12	33	49	2
Indo-1	19	31	92	2
Pv-0320	4	40	35	1
Pv-0274	4	14	11	2

The binding capacity of radiolabeled aptamers (100 nM) to IEs infected with indicated strains of *P. vivax* is given as the fold difference above background. Background was defined as the level of binding of a random sequence control to IEs. Cells highlighted in red exceed the threshold for definitive aptamer binding set at 5 fold above background. NIH-1993, Brazil-1 CDC, Chesson, Vietnam-IV, and Indo-1 are *Plasmodium vivax* adapted for culture in *Aotus nancymae*. Pv-0320 and Pv-0274 are *Plasmodium vivax* lines are derived from microscopy-confirmed Cambodian infections.

4.2.3 Parasitized HbAA, HbAS, and HbSS show similar levels of aptamer binding

In addition to the genotype of the invading parasite, display of malaria parasite proteins on the IE surface is also dependent on the hemoglobin environment. The structural hemoglobinopathies S (HbAS) and C (HbAC) affect the trafficking system that directs parasite-encoded proteins to the surface of infected erythrocytes leading to abnormal display of PfEMP1 (154, 155). To test whether display of the aptamer targets are similarly affected, we inoculated isogenic parasite lines into HbAA, HbAS, and HbSS cells and measured aptamer binding. Figure 4.3 shows that Euge.1, Euge.4, and Euge.7 binding is unaffected by the hemoglobin type in the target cell.

Table 4.4. Aptamer recognition of other *Plasmodium* species

	Euge.1	Euge.4	Euge.7	Euge.9
Rhesus Uninfected RBCs	2	2	3	3
Plasmodium knowlesi	28	61	22	7
Mouse Uninfected RBCs	1	1	2	1
Plasmodium yoelii	1	2	2	1
Plasmodium berghei	2	2	2	1

The binding capacity of aptamers to IEs infected with the indicated strain of Plasmodium is given as the fold difference above background. Background was defined as the level of binding a random sequence control to IEs. Cells highlighted in red exceed the threshold for definitive aptamer binding set at 5 fold above background. *Plasmodium knowlesi* (Strain H) were adapted for culture in Rhesus *macaque* (*Macaca mulatta)* whereas *P. berghei (*ANKA) and *P. yoelii yoelii* (17X) were grown in BALB/c mice.

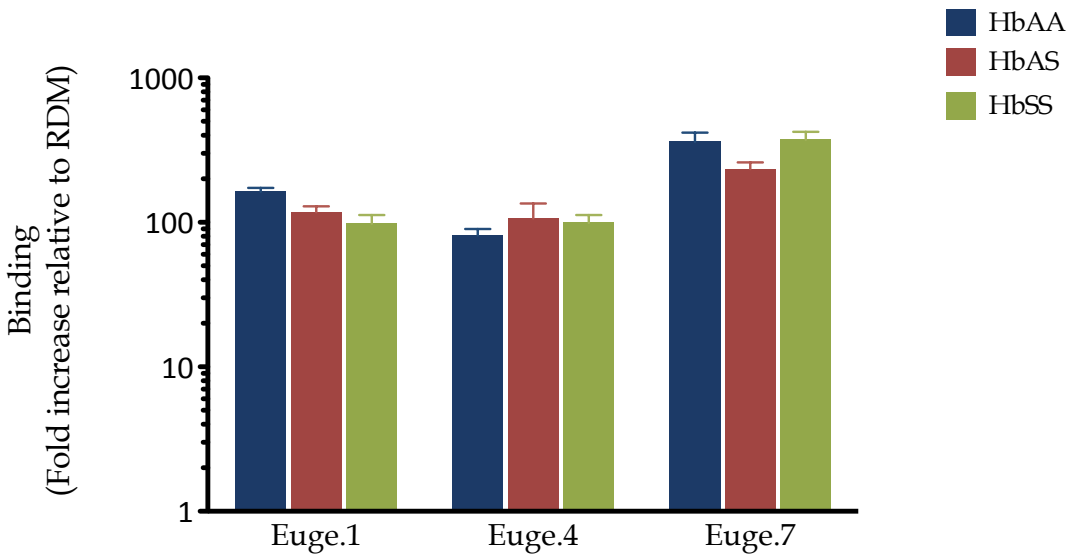

Figure 4.3 Hemoglobin polymorphisms do not affect aptamer binding.

HbAA, HbAS, HbSS erythrocytes parasitized with *P. falciparum* (FCR3 strain) were tested with the indicated radiolabeled aptamers (100 nM). The assay was performed 3 times in triplicate and error bars represent the SEM.

4.3 Discussion

Examination of the breadth of aptamer binding highlighted 3 aptamers (Euge.1, Euge.4, Euge.7) that recognized all 25 laboratory-adapted clones and clinical isolates of *P. falciparum* tested including the drug resistant line W2-mef. Remarkably, these aptamers also recognized all tested laboratory and clinical isolates of *P. vivax* and *P. knowlesi* but failed to recognize either of the murine malaria parasites, *P. chabaudi* or *P. berghei*. Aptamer binding was not affected by either the host determinants displayed on the cell nor the hemoglobin type within the cell.

Discovery of an epitope common between *P. vivax* and *P. falciparum* is unexpected. Whereas cross-reactive pre-erythrocytic or blood stage immunity can be elicited between strains of avian parasites and between species of murine parasites (263, 264), there is no definitive evidence of cross-species immunity between *P. falciparum* and *P. vivax* (265, 266). Sera from patients with microscopically confirmed single infections of *P. vivax* are unreactive to *P. falciparum* antigens (267), however, sera from subjects self-reporting infection only with *P. vivax* do appear to possess cross-reactive antibodies to *P. falciparum* possibly suggesting an undiagnosed prior infection (268–270). A monoclonal antibody raised against AMA-1 from *P. vivax* recognizes the *P. falciparum* homolog but with 100-fold weaker affinity than its cognate ligand (271). Observations in the field that individuals previously exposed to *P. vivax* have some clinical tolerance and lower-than-expected rates of infection following exposure to *P. falciparum* (272–275) may be better explained by innate

mechanisms to attenuate superinfection than active cross-species immunity (276). Immune evasion may be aided by the fact the aptamer target is relatively low abundance. Using Euge.4 as a target marker and assuming 1:1 binding we calculate that there are roughly 25,000-100,000 copies of aptamer target per IE. This is fraction of the 100,00 band 3 anion exchanger and Glycophorin A.

The stark contrast between the wide breadth of aptamer binding and the strain-specificity of most anti-malaria immune responses may be explained by the possibility that cross-reactive aptamers recognize non-immunodominant determinants. Serial-SELEX is performed *in vitro* completely independent of the positive and negative factors that determine whether an immune response will be produced against a particular epitope (277, 278) . In addition, aptamers may act as finer probes than antibodies. FDA scientists recently reported that thrombin-binding aptamers were able to detect small changes in conformation of epitopes in heat-treated thrombin that did not affect specific activity or binding to anti-thrombin antibodies (279).

It is curious that there is limited relationship between the degree of aptamer enrichment by Serial-SELEX and the breadth of aptamer binding. Serial-SELEX clearly enriches broadly binding aptamers: Euge.1 is a member of the dominant aptamer family from the final LIC pool and Euge.7 is representative of the second largest family of the LV pool. However, it is unclear why broadly binding aptamer, Euge.4, comprised just 3% of the final LIC pool. The fact that Euge.6 was differentially enriched from LV round 6 to round 10 but failed to bind isolates used in

the later rounds of selection highlights the complex dynamics of SELEX and the importance of individually validating aptamers for target cell binding.

We have identified three broadly binding aptamers but it is as yet unclear how many unique IE determinants are targeted. The three aptamers contain little primary sequence similarity aside from a guanine-rich motif common to many selected DNA aptamers (214, 258–260) including some of the strain-restricted aptamers tested. Further work is required to elucidate the aptamer target or targets.

4.4 Supplemental information

Supplemental Table 4.1 Transformation of raw data from an aptamer binding assay: Raw data.

	Replicate #	Aptamers												
		RDM*	Euge.1	Euge.2	Euge.3	Euge.4	Euge.5	Euge.6	Euge.7	Euge.8	Euge.9	Euge.10	Euge.11	RDM*
RBCs	1	157	548	252	385	818	1018	224	424	209	202	222	461	423
RBCs	2	307	546	206	442	701	438	339	322	702	494	333	547	211
RBCs	3	281	838	480	2813	1075	499	468	722	424	1233	305	440	814
KN-1254	1	728	82569	11493	65543	350162	17947	5377	233217	23190	19490	6490	3406	449
KN-1254	2	863	58013	7393	53533	224265	15677	4021	260958	28035	19682	3741	2504	590
KN-1254	3	1120	53257	7298	55067	142043	17234	5404	262492	27069	27511	3675	2994	397
KN-1314	1	494	10039	2011	6993	116365	3231	1822	87075	7620	6927	1530	603	399
KN-1314	2	487	14958	1734	7787	100842	2644	2474	47860	4156	5275	1476	635	358
KN-1314	3	490	25849	1581	7871	121677	7049	2516	78006	4079	5549	1514	811	685

The binding capacity of radiolabeled aptamers to IEs infected with the indicated strain of *Plasmodium* is given as CPMs. *Two preparations of RDM were tested independently.

Supplemental Table 4.2 Transformation of raw data from a binding assay: Specific activity of aptamer used in the study.

Aptamer	CPM/pmol
RDM*	105686
Euge.1	76248
Euge.2	61829
Euge.3	85843
Euge.4	123411
Euge.5	108107
Euge.6	104208
Euge.7	112539
Euge.8	125172
Euge.9	95913
Euge.10	74800
Euge.11	117146
RDM*	78943

*Two preparations of RDM were tested independently.

Supplemental Table 4.3 Transformation of raw data from an aptamer binding assay: Data normalized by specific activity.

	Replicate #	Aptamers												
		RDM*	Euge.1	Euge.2	Euge.3	Euge.4	Euge.5	Euge.6	Euge.7	Euge.8	Euge.9	Euge.10	Euge.11	RDM*
RBCs	1	0.0005	0.0024	0.0013	0.0015	0.0022	0.0031	0.0007	0.0012	0.0006	0.0007	0.0010	0.0013	0.0018
RBCs	2	0.0010	0.0024	0.0011	0.0017	0.0019	0.0013	0.0011	0.0009	0.0019	0.0017	0.0015	0.0015	0.0009
RBCs	3	0.0009	0.0036	0.0026	0.0108	0.0029	0.0015	0.0015	0.0021	0.0011	0.0042	0.0013	0.0012	0.0034
KN-1254	1	0.0023	0.3574	0.0613	0.2520	0.9363	0.0548	0.0170	0.6839	0.0611	0.0671	0.0286	0.0096	0.0019
KN-1254	2	0.0027	0.2511	0.0395	0.2058	0.5997	0.0479	0.0127	0.7652	0.0739	0.0677	0.0165	0.0071	0.0025
KN-1254	3	0.0035	0.2305	0.0390	0.2117	0.3798	0.0526	0.0171	0.7697	0.0714	0.0947	0.0162	0.0084	0.0017
KN-1314	1	0.0015	0.0434	0.0107	0.0269	0.3112	0.0099	0.0058	0.2553	0.0201	0.0238	0.0067	0.0017	0.0017
KN-1314	2	0.0015	0.0647	0.0093	0.0299	0.2696	0.0081	0.0078	0.1403	0.0110	0.0181	0.0065	0.0018	0.0015
KN-1314	3	0.0015	0.1119	0.0084	0.0303	0.3254	0.0215	0.0080	0.2287	0.0108	0.0191	0.0067	0.0023	0.0029

The binding capacity of radiolabeled aptamers to IEs infected with the indicated strain of *Plasmodium* is given as pmol. *Two preparations of RDM were tested independently.

Supplemental Table 4.4 Transformation of raw data from an aptamer binding assay: Average value of RDM was used to establish background binding.

	Replicate #	RDM*	RDM*	Average Binding RDM
RBCs	1	0.0005	0.0018	0.0014
RBCs	2	0.0010	0.0009	
RBCs	3	0.0009	0.0034	
KN-1254	1	0.0023	0.0019	0.0024
KN-1254	2	0.0027	0.0025	
KN-1254	3	0.0035	0.0017	
KN-1314	1	0.0015	0.0017	0.00187
KN-1314	2	0.0015	0.0015	
KN-1314	3	0.0015	0.0029	

The binding capacity of radiolabeled aptamers to IEs infected with the indicated strain of *Plasmodium* is given as pmol. *Two preparations of RDM were tested independently.

Supplemental Table 4.5 Transformation of raw data from an aptamer binding assay: Fold difference above background.

	Replicate #	Aptamers										
		Euge.1	Euge.2	Euge.3	Euge.4	Euge.5	Euge.6	Euge.7	Euge.8	Euge.9	Euge.10	Euge.11
RBCs	1	1.6983	0.9631	1.0598	1.5663	2.2251	0.5079	0.8903	0.3945	0.4977	0.7013	0.9299
RBCs	2	1.6921	0.7873	1.2167	1.3422	0.9574	0.7687	0.6761	1.3252	1.2171	1.0520	1.1034
RBCs	3	2.5970	1.8345	7.7433	2.0583	1.0907	1.0612	1.5160	0.8004	3.0377	0.9635	0.8875
KN-1254	1	148.2011	25.4390	104.4918	388.3090	22.7195	7.0616	283.6073	25.3546	27.8098	11.8742	3.9791
KN-1254	2	104.1262	16.3639	85.3449	248.6967	19.8459	5.2807	317.3422	30.6518	28.0837	6.8446	2.9253
KN-1254	3	95.5897	16.1536	87.7905	157.5173	21.8169	7.0970	319.2077	29.5956	39.2547	6.7238	3.4977
KN-1314	1	24.5449	6.0634	15.1864	175.7789	5.5716	3.2595	144.2403	11.3487	13.4638	3.8132	0.9596
KN-1314	2	36.5716	5.2282	16.9107	152.3301	4.5594	4.4259	79.2804	6.1897	10.2528	3.6786	1.0105
KN-1314	3	63.1996	4.7669	17.0931	183.8031	12.1554	4.5010	129.2174	6.0750	10.7854	3.7733	1.2906

The binding capacity of radiolabeled aptamers to IEs infected with the indicated strain of *Plasmodium* is given as fold difference above background.

Background was defined as the level of binding RDM to IEs.

Supplemental Table 4.6 Calculation of number of aptamer binding sites to indicated cells.

	Replicate #	Euge.4 pmol	Euge.4 molecules bound per cell*
RBCs	1	0.0022	331
RBCs	2	0.0019	286
RBCs	3	0.0029	437
KN-1254	1	0.9363	140,913
KN-1254	2	0.5997	90,255
KN-1254	3	0.3798	45,620
KN-1314	1	0.3112	37,468
KN-1314	2	0.2696	32,460
KN-1314	3	0.3254	65,297

* $5x10^6$ cells per sample

4.5 Acknowledgements

We thank Hans Ackerman, M.D. D.Phil., Gregory Kato, M.D., Mary Hall C.I.P., James Nichols, R.N., John Baird, Darlene Allen and the NIH Clinical Center phlebotomy staff for management of protocol NIH 03-H-0115, subject recruitment, and blood drawing. We also thank Rick Fairhurst, M.D. Ph.D, Julianna Sa Ph.D, and Alvaro Molina-Cruz Ph.D for providing parasite isolates.

Chapter 5. Purification, identification, characterization of the aptamer target.

5.1 Introduction

We have previously subjected two randomized oligonucleotide libraries of up to 10^{15} unique sequences to Serial-SELEX and validated high-affinity parasite-specific aptamers. Screening individual sequences for IE binding highlighted 3 aptamers that recognize an unprecedented breadth of *Plasmodium* species. Here we go on to characterize the target of these broadly binding aptamers as a single IE membrane protein using biochemical and imaging techniques. Definitive identification was achieved by affinity purifying the target using aptamers and subjecting the recovered protein to mass spectrometry. Finally, we go on to explore the role of the aptamer target in parasite biology and its association with naturally acquired immunity to malaria.

5.2 Results

5.2.1 Broadly binding aptamers bind a common protein stably expressed on the IE surface.

SELEX has the potential to enrich for aptamers against multiple targets, however, convergence on a single target within a complex mixture has been observed (211, 215). We tested whether Euge.1, Euge.4, and Euge.7 recognize unique IE determinants using an aptamer competition assay. Figure 4.1 shows that all three aptamers compete with each other for IE binding suggesting they likely recognize a shared determinant.

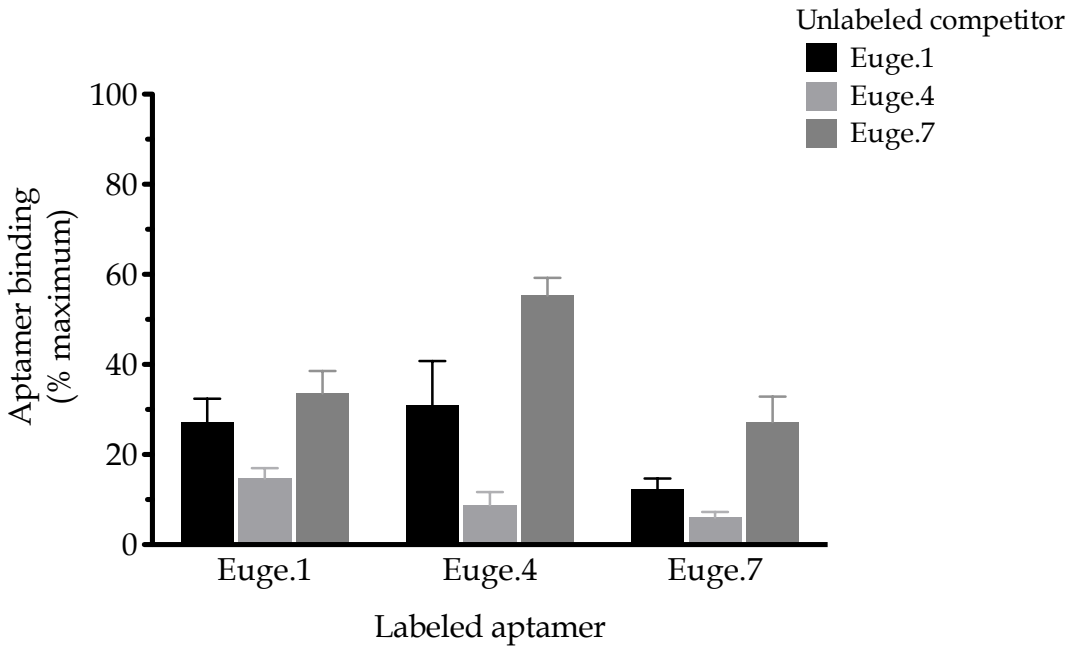

Figure 5.1 Reciprocal competition between radiolabeled and unlabeled broadly binding aptamers indicate recognition of a shared determinant.

Indicated aptamers were tested at 75nM. Maximum binding was defined as the level of binding of aptamer to IEs pre-incubated with random sequence control (750 nM). Error bars represent the SEM from assays performed three times in triplicate.

As a test of whether the shared aptamer target is a membrane protein on the cell surface, we treated IEs with extracellular protease before incubation with radiolabeled aptamer. As shown in Figure 5.2, after treating the cells with trypsin or pronase-E, Euge.4 lost its binding to treated IEs. Similar results were observed for tests with Euge.1 and Euge.7 (data not shown). It can be deduced that the binding entity of the aptamer had been removed by the proteinases, indicating that the target molecule was most likely a membrane protein. To further confirm the IE surface localization, 0.5 μm fluorescent-beads were functionalized with Euge.4 and were shown to bind the surface of IEs in an aptamer-specific and protease-sensitive manner (Figure 5.3).

Next we used Euge.4 to determine the relative levels of target protein at various stages of parasite development. We confirmed the aptamer target was displayed at ring and trophozoite/schizont stages (Figure 5.4). The aptamer signal against free merozoites and late stage gametocytes was above background but did not meet our stringent threshold for definitive binding (Figure 5.4).

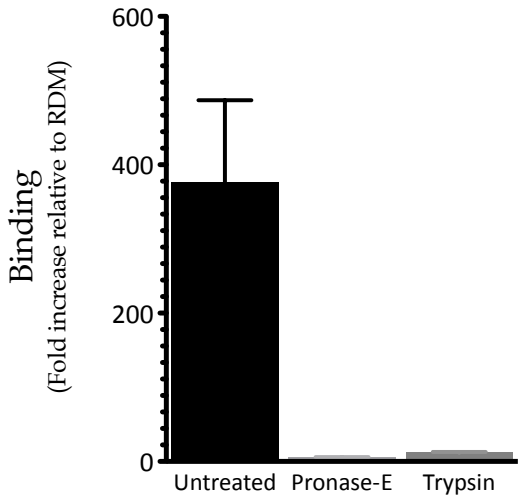

Figure 5.2 Pre-treating IEs with extracellular protease abolishes Euge.4 binding.

The final concentration of the aptamers in the binding buffer was 100 nM.

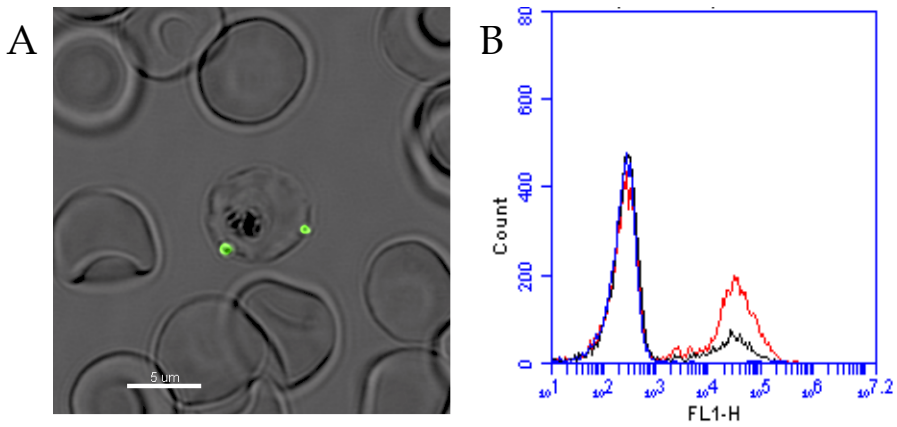

Figure 5.3 Aptamer-functionalized fluorescent beads recognize an IE surface protein.

(A) Fluorescence confocal images of parasite cultures by Euge.4-functionalized fluorescent beads. Beads were only found associated with IEs (evidenced by the presence of hemozoin) consistent with the parasite-specific binding of Euge.4. (B) Flow cytometry assay for the binding of the aptamer-functionalized fluorescent beads to IEs. The red curve represents the binding Euge.4-functionalized fluorescent beads to untreated IEs whereas the black curve indicated Euge.4-bead binding to IEs pre-treated with trypsin. The blue curve represents the background binding of RDM-functionalized beads. Euge.4-bead binding is attenuated by pre-treatment with extracellular protease.

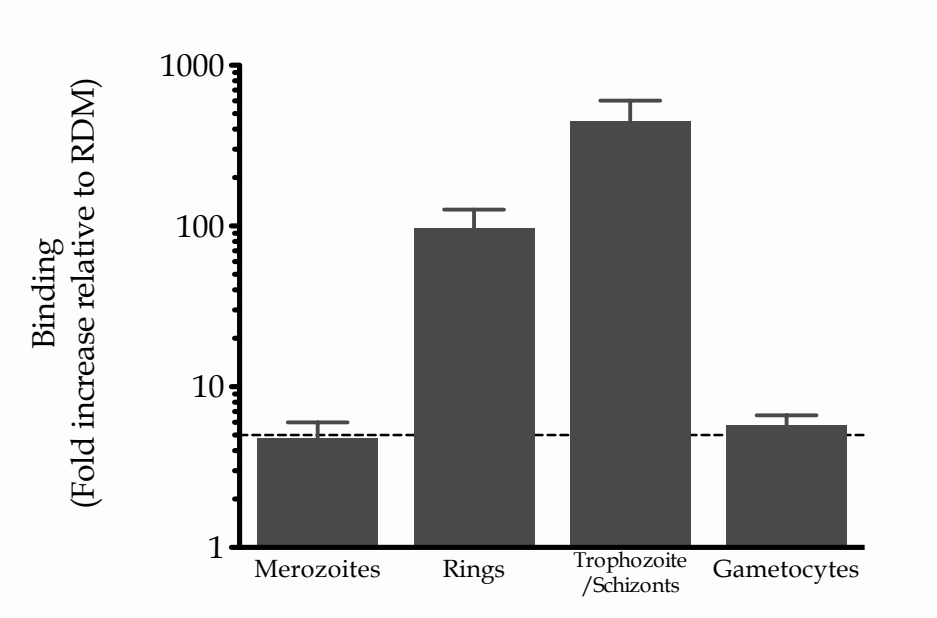

Figure 5.4. Time course for the display of the aptamer target.

Tightly synchronized *P. falciparum* (FCR3 strain) cultures were purified at the stages indicated and incubated with radiolabeled Euge.4 (100nM). The amount of parasite-associated aptamer was counted and expressed as fold increase above random sequence control (background). Dotted line indicates 5 fold above background. Assays were performed 3 times in triplicate and error bars indicate the SEM.

5.2.2 Identification of the aptamer protein target

An affinity purification procedure was used to isolate the target of cross-reactive aptamers. IE membrane extracts were incubated with streptavidin magnetic beads functionalized with aptamers. Aptamer-bead complexes were washed extensively, and bound proteins were eluted and then resolved by SDS-PAGE before staining. Figure 5.5 shows the affinity purification profile of RDM, Euge.1, Euge.4, and Euge.7. Strikingly, Euge.1, Euge.4, and Euge.7 exhibited identical profiles different from that of RDM. The broadly binding aptamers appeared to specifically interact with a number of proteins, most notably high-molecular-weight polypeptides corresponding to 90 kDa and ~250 kDa. Scale up of the purifications yielded bands that were visible by Coomassie staining. Once again, large-scale purification with Euge.4 (Figure 5.6 A) and Euge.7 (Figure 5.6 B) yielded an identical banding pattern with prominent bands corresponding to 90 kDa and ~250 kDa that were not isolated by control purification with RDM.

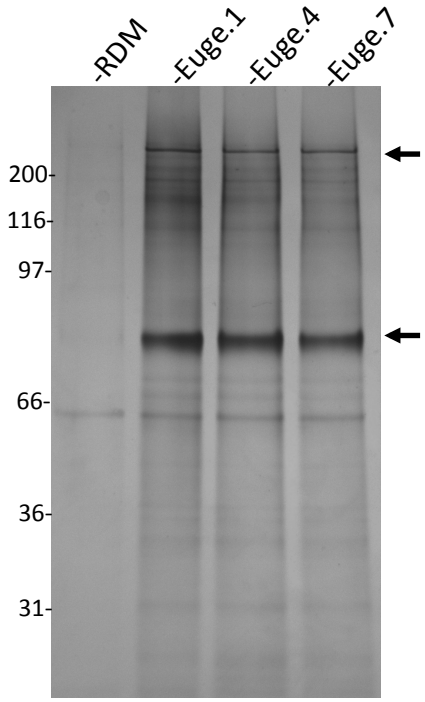

Figure 5.5. Preliminary purification of aptamer targets.

Shown is a silver-stained gel depicting proteins affinity purified from membrane extracts by the indicated aptamers.

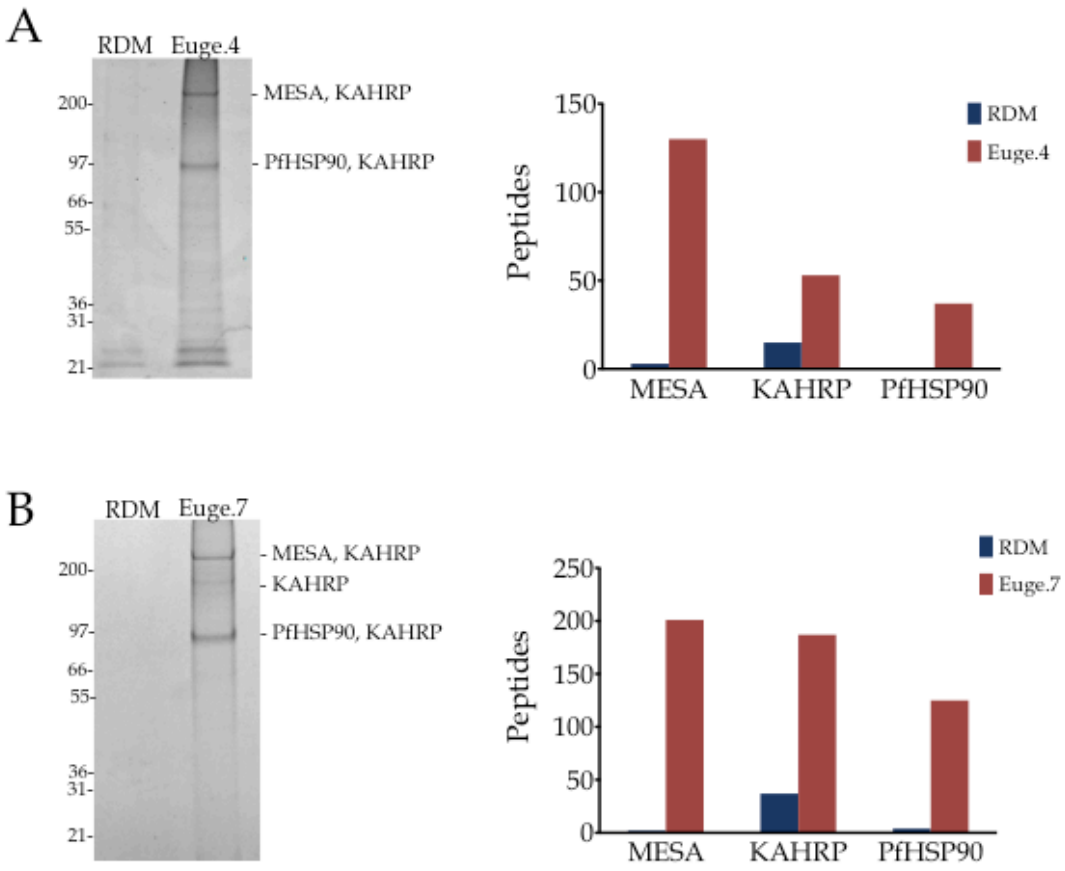

Figure 5.6. Isolation of aptamer specific proteins.

A, B, Left, Coomassie-stained SDS–PAGE gels of material eluted from oligoprecipitations performed using aptamers Euge.4 (A), Euge.7 (B) with control purifications with RDM run in parallel on parasite lysates from 3D7. Right, the total number of peptide representing the top three parasite proteins detected from all visible bands unique to pull-downs using broadly binding aptamers. Data are representative of duplicate experiments.

SDS-PAGE bands visually unique to Euge.4 and Euge.7 pull-downs were excised along with the corresponding gel regions of the negative control and analyzed by LC-MS/MS (liquid chromatography coupled with tandem mass spectrometry) based sequencing (Figure 5.6 A,B and Supplementary Table 5.1-6).

Dozens of parasite and human proteins were identified by mass spectrometry. We focused our search for an aptamer target using three lines of reasoning. First, the target protein was assumed to be of parasite origin because aptamer binding is restricted to parasitized cells and mature enucleated red blood cells lack the machinery for *de novo* protein synthesis. Second, broadly binding aptamers should differentially enrich a target protein such that a large number of total peptides and unique peptides should be recovered. Third, the aptamer target should be consistently recovered in duplicate experiments and also found in pull-downs with Euge. 4 or Euge.8 as these aptamers compete for red cell binding and likely share a binding site. Based on these criteria, mature parasite-infected erythrocyte surface antigen (MESA, PF3D7_0500800), knob-associated histidine-rich protein (KAHRP, PF3D7_0202000), and heat shock protein 90 (PfHSP90, PF3D7_0708400) were identified as the top three parasite protein hits specifically and consistently purified in duplicate experiments with both Euge.4 and Euge.7. MESA and KAHRP have been reliably localized to the cytoplasmic face of the IE membrane (177, 178, 280) in line with their role in trafficking, knob formation, and display of PfEMP1 (56, 176). We formally ruled out KAHRP as a possible aptamer target by showing that the level of aptamer binding to KAHRP negative knockouts was similar to binding of the KAHRP

positive parental line (Figure 5.7).

We next investigated PfHSP90 as a possible aptamer target because HSP90 has been localized to the plasma membrane in a variety of cancer cells (281–284) and pathogens (285–287). To test whether PfHSP90 is a target of broadly binding aptamers, we screened recombinant PfHSP90 and related proteins for aptamer binding. As shown in Figure 5.8, Euge.4 recognized recombinant PfHSP90 (K_d=65.0 ± 7.0 nM) but failed to bind either PfHSP70, human HSP90 (hHSP90), human HSP70 or leading malaria vaccine candidates MSP-1, AMA-1, or VAR2CSA. Euge.4 recognition of PfHSP90 was sequence specific because a random sequence control showed almost no signal (Figure 5.8). We found that Euge.4 bound recombinant PfHSP90 with high affinity (Figure 5.9) with a calculated dissociation constant (K_d=65.0 ± 7.0 nM) similar to the interaction between Euge.4 and intact IEs.

We next investigated the localization of PfHSP90 using an antibody specific for PfHSP90 which does not cross-react to human, yeast, or *Dictyostelium* Hsp90 homologues (288). Fluorescently labeling anti-PfHSP90 antibody allowed direct detection of PfHSP90 exclusively on the IE surface (Figure 5.10).

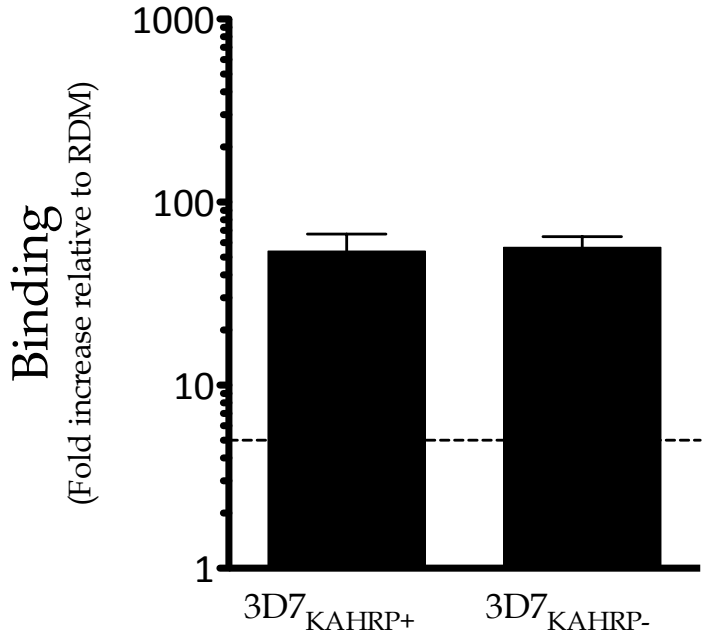

Figure 5.7. Euge.4 binding to IEs is independent of KAHRP expression.

Mean ± SEM level of Euge.4 binding to intact isogenic KAHRP^{+} and KAHRP^{-} lines is indicated. Two independent experiments were performed in triplicate.

5.2.3 Exploring the possible role of surface PfHSP90

Cytoplasmic HSP90 is a key molecular chaperone able to keep target proteins in a folding-competent state enabling the specific signaling required for responses to cellular stress induced by temperature changes or drug exposure (289). On tumor cells, surface HSP90 appears to mediate tumor invasiveness and metastasis (283, 290). To explore the function of surface PfHSP90, we pre-treated cells with a 2 hour heat shock known to induce PfHSP90 cytoplasmically (291, 292) and measured surface displayed PfHSP90 using Euge.4. Figure 5.11 shows that unlike cytoplasmic PfHSP90, the level of surface displayed PfHSP90 is unaffected by heat shock suggesting an alternate role in parasite biology. As a test of whether surface PfHSP90 was important for parasite development, we incubated aptamers with parasites over the course of asexual development but we failed to observe any difference in parasite growth between cultures treated with PfHSP90 binding aptamers and those treated with random sequence control (Figure 5.12).

5.2.4 Assessment of naturally acquired PfHSP90 antibody responses

Despite being displayed on the IE surface, PfHSP90 may not be under substantial immune selection pressure. Consistent with this notion, we found that malaria-experienced Malians have little or no antibody against the recombinant C-terminal fragment of PfHSP90, in contrast to blood stage candidate AMA-1 (Figure 5.13) and other recombinant protein available as ELISA-coating antigen (36). Mammals may be tolerant to proteins with extensive structural homology with host protein and indeed

PfHSP90 shares 70% homology to hHSP90 and 64% homology to rabbit HSP90. Nevertheless, antibodies to PfHSP90 are readily inducible by vaccination of rabbits (geometric mean endpoint titre is 409,600, n=2), confirming the antigen is not inherently non-immunogenic in mammals (L. Rietveld, personnel communication).

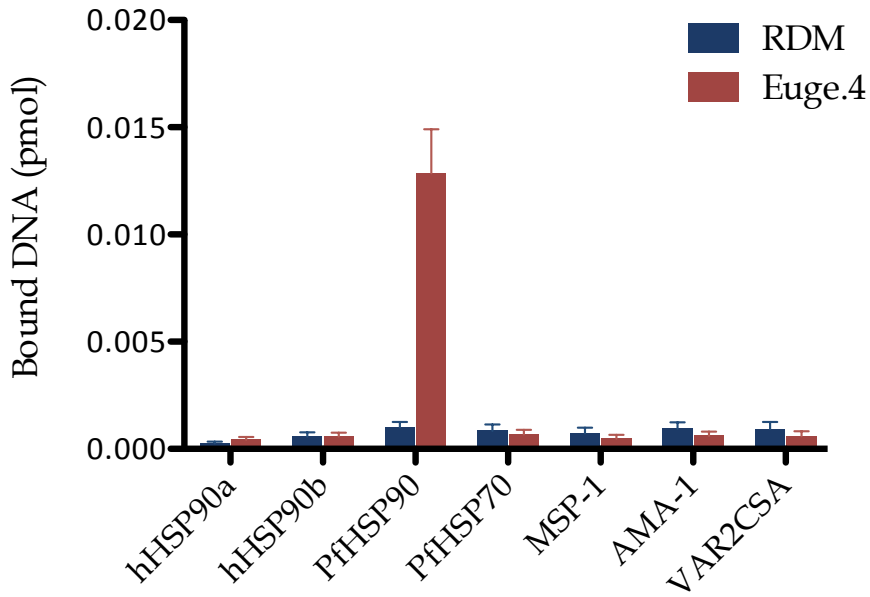

Figure 5.8. Euge.4 specifically recognizes recombinant PfHSP90.

ELISA-type screen of recombinant proteins using radiolabeled aptamer identified PfHSP90 as the target of Euge.4. Importantly, there is a lack of Euge.4 binding to the two human homologues of HSP90, hHSP90a and hHSP90b.

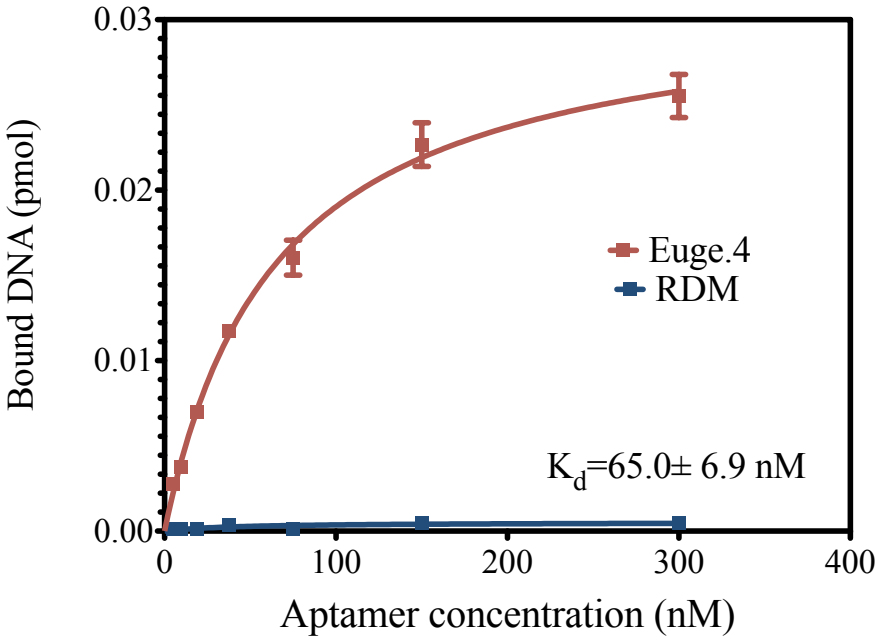

Figure 5.9 Euge.4 binds recombinant PfHSP90 with high affinity.

A constant amount of immobilized PfHSP90 was incubated with increasing concentrations of radiolabeled Euge.4. In separate well, the nonspecific binding was determined using radiolabeled RDM in separate experiments. Error bars represent standard error from triplicate analyses.

-

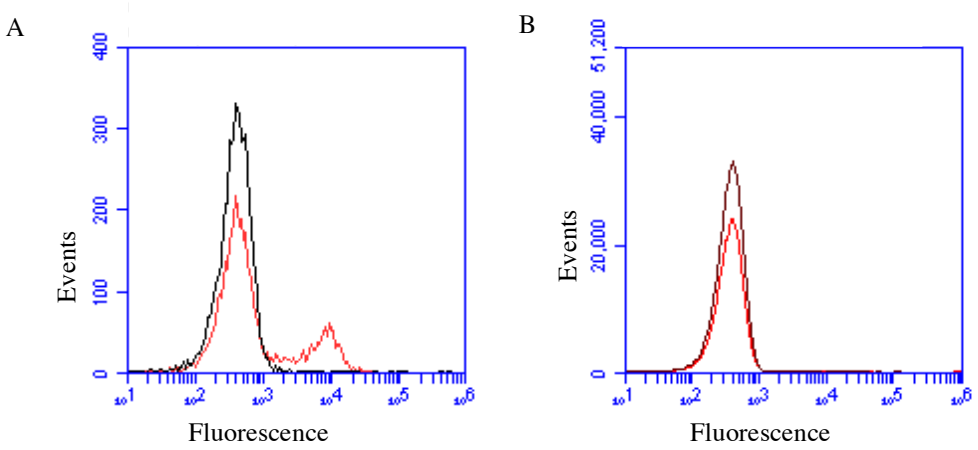

.

Figure 5.10 PfHSP90 is detected exclusive on surface of IEs.

Flow cytometry analysis of Alexa 647-labeled anti-PfHSP90 polyclonal antibody binding to intact IEs (A) or uninfected RBCs (B). The red curve represents the anti-PfHSP90 antibody whereas the black curve represents the background binding of isotype control.

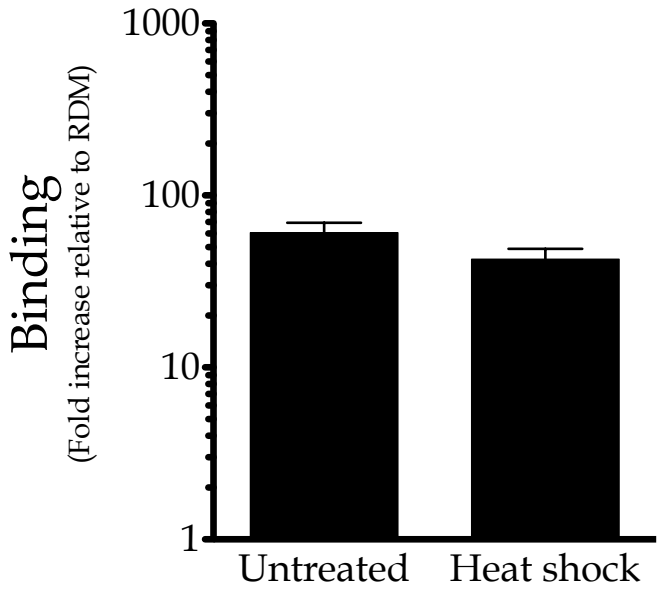

Figure 5.11 Display of PfHSP90 is unaffected by heat shock pre-treatment.

Surface PfHSP90 levels were measured as a function of Euge.4 binding to IEs. Mean ± SEM levels are indicated. Two independent experiments were performed in triplicate.

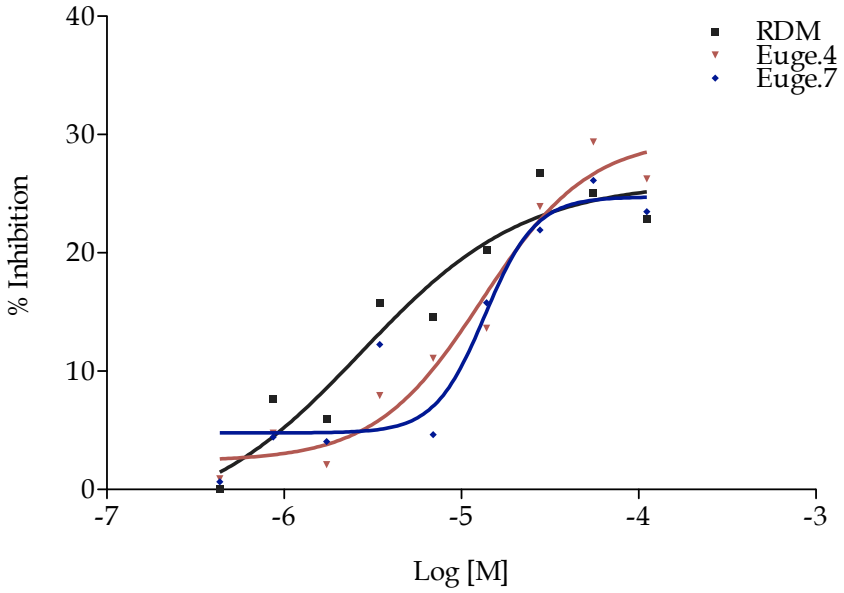

Figure 5.12 Broadly-binding aptamers have no effect on the *in vitro* development of *P. falciparum*.

Aptamers were modified with a 3' inverted-thymidine to increase serum stability and incubated with asynchronous parasites for 72 hours. Percent growth inhibition relative to untreated controls is indicated. Data is represented of two independent experiments performed in triplicate.

\

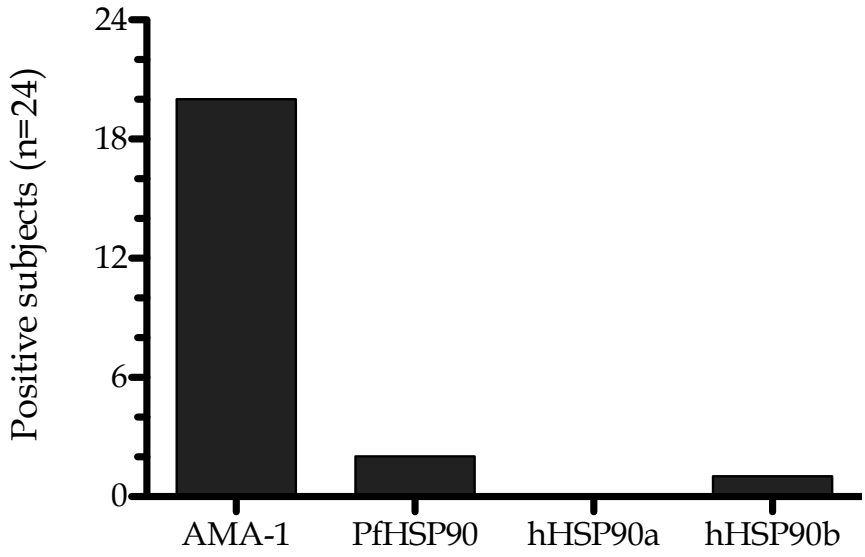

Figure 5.13 Prevalence of antigen-specific IgG among 24 Malian adult sera.

The threshold for positivity was defined as the mean OD 405 nm plus 3 standard deviations of results for 6 malaria-naïve US adults.

5.3 Discussion

In this chapter, we identify PfHSP90 as the target of broadly binding aptamers isolated by Serial-SELEX. We confirm PfHSP90 is displayed on the red cell surface across various stages of intraerythrocytic development and despite its stable display, PfHSP90 somehow escapes immune recognition in malaria-exposed individuals.

HSP90 is a highly conserved molecular chaperone which regulates the conformational states of dozens of proteins including the signal transduction circuitry governing cell proliferation, differentiation, and stress response (293, 294). Full-length HSP90 encodes an N –terminus ATPAse, a central acidic hinge region, and C-terminal domain involved in dimerization and substrate binding through cryptic ATPase activity (295, 296).

P. falciparum possesses three HSP90 genes, but only one of the genes – the one implicated as the aptamer target – encodes for an HSP90 protein possessing the EEVD motif important for ATPase activity and the ability to interact with substrates (297, 298). PfHSP90 mRNA is synthesized soon after invasion in the early ring stage, peaking at the trophozoite stage (299). The protein is detected at all the stages of the erythrocytic lifecycle (300). The protein has a high degree of conservation across Plasmodium with nearly all the sequenced homologs (P. falciparum, vivax, knowlesi, cynomolgi, chabaudi, berghei, and yoelli) showing >90% identity with each other. The three rodent species are particularly closely interrelated with over 99% identity –

essentially the same. Nearing the N-terminus there is a ~25aa sequence that is very heavy in polar amino acids and is present in all the parasites from primates/human but not the rodent ones. Non-synonymous single nucleotide polymorphisms between primate/human and rodent parasite are found throughout the protein and could serve as the basis for aptamer discrimination.

HSP90 and its co-chaperones have been detected on the plasma membrane of fibrosarcoma (281), melanoma (282), breast cancer (283), glioblastoma (284), and developing neuronal cells (301). Multiple lines of evidence indicate extracellular HSP90 plays a key role in tumor metastasis (283, 290) as cell surface-restricted HSP90 inhibitors significantly retard tumor cell migration and integrin/extracellular matrix-dependent cytoskeletal reorganization and reduce tumor colonization *in vivo* (302). HSP90 has been localized to the surface of some *Candida* and shown to be an immunodominant antigen of infection where sustained antibody response correlated closely with a good prognosis and lack of or falling levels of antibody were associated with fatality (303). Monoclonal antibodies against HSP90 administered in conjunction with standard treatment showed improvement over just treatment alone in patients with culture-confirmed invasive candidiasis in a large placebo-controlled trial (304).

It was previously thought that all of the known chaperone proteins encoded by the malaria parasite are contained within the parasite (288). More recently, the export of PfHSP40 into erythrocytes has been demonstrated using a green fluorescent protein-tagged PfHSP40 protein (44). Furthermore, Maier *et al.* (2008) described an HSP40

protein encoded by PF10_0381 that associates with extra-parasitic KAHRP and subsequently plays an important role in the formation of knobs on the erythrocyte surface. Similar results were obtained for another member of the PfHSP40 family, PF3D7_0201800 (49). Here we show that despite lacking an obvious export signal, some HSP90 of parasitic origin is routed to the erythrocyte surface. Pexel-independent export has been observed for a number of proteins, most notably PfEMP1 (59, 305). Interestingly, many members of the host chaperone system such as hHSP90a and Hop60 have been found in IE membrane-associated complexes (288).

HSP90 is essential in all eukaryotes and the specific requirement of PfHSP90 in *P. falciparum* survival is supported by the fact that HSP90 inhibitors kill parasites (306, 307). We are unable to assign a specific role for surface displayed PfHSP90. Surface PfHSP90 is not upregulated in response to heat shock like cytoplasmic PfHSP90 (291, 292) and it appears aptamers against PfHSP90 do not affect parasite survival. The latter observation comes with the caveat that, based on the kinetics of similar studies (207), the serum-stabilized aptamers used in the study were likely degraded by end of the extended course of the growth inhibition assay. Increasing the valency of the aptamers may potentiate an effect (308) as would shortening the course of the assay but it would seem more feasible to simply repeat the assay using anti-PfHSP90 antibody and appropriate controls.

Despite our inability to assign a specific role for surface displayed PfHSP90, the potential of PfHSP90 as a vaccine candidate is demonstrated by its stable display

throughout a large part of the parasite lifecycle and its conservation across many strains and species of *Plasmodium.* Furthermore, Dubois *et al.* found that vaccination with protein extracts containing PfHSP90 provided nearly complete protection from subsequent homologous *P. falciparum* blood stage challenge in the squirrel monkey model. The protection level was correlated with a specific IgG ratio directed against a 90 kDa protein with an isoelectic point between pH5-6 which was most likely PfHSP90 (309, 310).

Generating cross-reactive responses against hHSP90 would be a major concern. PfHSP90 shares 64% identity with its human counterpart, both proteins possess conserved ATP-binding motifs (300), and the human protein can complement deletion of genes encoding HSP90 in yeast (311). Yet there are important differences between PfHSP90 and hHSP90. The complementation of yeast with human or *falciparum* HSP90 confers differential inhibitor sensitivities (311). These differences may serve as the structural basis for Euge.4 discrimination between human and *falciparum* HSP90. Importantly, antibodies generated against the C-terminal PfHSP90 do not recognize hHSP90 suggesting a vaccine against PfHSP90 may be possible.

The reason for the lack of anti-PfHSP90 and anti-hHSP90 antibody in naturally exposed Malians is unclear. The fact that anti-PfHSP90 antibody binds to both the ELISA antigen and native parasites indicate the ELISA PfHSP90 coating antigen is in the correct conformation. The ELISA coating antigen is only the commercially available C-terminal 193 amino acids of PfHSP90 and it may be that antibody

responses may be detectable against the full-length protein. Anti-HSP90 titers have been detected in a small Thai cohort with acute *falciparum* malaria (312) and there is some evidence the naturally occurring polyreactive antibodies bind hHSP90 and other conserved protein in healthy individuals (313). We found that antibody responses against *falciparum* and human HSP90 are minimal in malaria naïve healthy US volunteers (data not shown). The reason underlying the discrepancy between our data and published results is unclear but considering its potential as a near-universal malaria vaccine immunogen, further investigation of natural and vaccine-induced immune responses to PfHSP90 is warranted.

5.4 Acknowledgements

We thank Rich Eastman Ph.D for performing the growth inhibition assay. Bo Peng assisted with the optimization of the aptamer-fluorescent bead binding assay.

5.5 Supplemental information

Supplemental Table 5.1. Proteins identified in ~250 kDa region excised from oligopreciptiation with RDM.

Accession	MW (kDa)	Protein	Σ Coverage	Σ# PSMs	Σ# Peptides	Score
IGKC_HUMAN	11.6	(P01834) Ig kappa chain C region	35.85	5	3	274.59
CYTA_HUMAN	11.0	(P01040) Cystatin-A	35.71	4	3	143.70
ALBU_HUMAN	69.3	(P02768) Serum albumin	31.69	26	17	944.47
CALL5_HUMAN	15.9	(Q9NZT1) Calmodulin-like protein 5	28.08	3	3	113.84
DCD_HUMAN	11.3	(P81605) Dermcidin	22.73	7	3	233.41
HBB_HUMAN	16.0	(P68871) Hemoglobin subunit beta	21.77	3	3	107.19
B3AT_HUMAN	101.7	(P02730) Band 3 anion transport protein	21.19	19	11	652.38
HORN_HUMAN	282.2	(Q86YZ3) Hornerin	17.72	17	12	647.83
PF3D7_0730900	244.0	Plasmodium exported protein, unknown function	14.27	11	9	501.43
IGHG1_HUMAN	36.1	(P01857) Ig gamma-1 chain C region	13.64	3	3	141.31
FABP5_HUMAN	15.2	(Q01469) Fatty acid-binding protein, epidermal	13.33	2	2	97.29
PLAK_HUMAN	81.7	(P14923) Junction plakoglobin	13.15	11	8	379.87
ANXA2_HUMAN	38.6	(P07355) Annexin A2	11.80	4	4	115.49
DSG1_HUMAN	113.7	(Q02413) Desmoglein-1	10.01	13	9	472.11
PF3D7_0202000	71.3	knob-associated histidine-rich protein (KAHRP)	9.79	18	5	492.87
SEMG1_HUMAN	52.1	(P04279) Semenogelin-1	9.52	3	2	146.43
DESP_HUMAN	331.6	(P15924) Desmoplakin	6.93	17	16	627.85
PF3D7_0500800	168.2	mature parasite-infected erythrocyte surface antigen (MESA)	2.93	3	3	162.19

Supplemental Table 5.2. Proteins identified in ~250 kDa region excised from oligopreciptiation with Euge.4.

Accession	MW (kDa)	Description	Σ Coverage	Σ# PSMs	Σ# Peptides	Score
HBB_HUMAN	16.0	(P68871) Hemoglobin subunit beta	62.59	12	8	602.97
PF3D7_0500800	168.2	mature parasite-infected erythrocyte surface antigen (MESA)	60.53	359	116	13188.98
HBA_HUMAN	15.2	(P69905) Hemoglobin subunit alpha	58.45	11	5	418.40
ANK1_HUMAN	206.1	(P16157) Ankyrin-1	45.88	137	53	3975.68
STOM_HUMAN	31.7	(P27105) Erythrocyte band 7 integral membrane protein	44.10	14	10	727.86
SPTA1_HUMAN	279.8	(P02549) Spectrin alpha chain, erythrocyte	40.51	122	69	4536.42
DCD_HUMAN	11.3	(P81605) Dermcidin	35.45	4	4	128.90
PF3D7_1211800	42.8	polyubiquitin (PfpUB)	32.81	3	2	134.40
B3AT_HUMAN	101.7	(P02730) Band 3 anion transport protein	30.63	63	20	2311.00
HORN_HUMAN	282.2	(Q86YZ3) Hornerin	30.32	33	23	1417.93
PF3D7_1126200	17.9	40S ribosomal protein S18, putative	30.13	3	3	153.29
PF3D7_0201900	273.5	erythrocyte membrane protein 3 (EMP3)	29.78	5	4	204.82
PF3D7_0507100	46.2	60S ribosomal protein L4, putative	27.01	11	9	485.70
PF3D7_1465900	24.7	40S ribosomal protein S3, putative	26.24	5	4	228.56
PF3D7_0202000	71.3	knob-associated histidine-rich protein (KAHRP)	25.54	128	20	3176.59
PF3D7_0617800	14.1	histone H2A (H2A) -- Pf3D7_06_v3:748416-748814(-)	24.24	4	2	95.48
PF3D7_0730900	244.0	Plasmodium exported protein, unknown function	22.61	31	22	1244.01
PF3D7_1105000	11.4	histone H4 (H4) -- Pf3D7_11_v3:221818-222129(-)	21.36	2	2	90.28
PF3D7_1462800	36.6	glyceraldehyde-3-phosphate dehydrogenase (GAPDH)	21.07	6	4	358.42
PF3D7_1357000	48.9	elongation factor 1-alpha	20.09	5	5	312.08
PF3D7_0708400	86.1	heat shock protein 90 (HSP90)	18.52	10	10	632.51
SPTB1_HUMAN	246.3	(P11277) Spectrin beta chain, erythrocyte	17.64	30	26	1408.17
PF3D7_0818900	73.9	heat shock protein 70 (Hsp70)	16.84	10	8	490.78
LACRT_HUMAN	14.2	(Q9GZZ8) Extracellular glycoprotein lacritin	16.67	2	2	64.69
PF3D7_0516200	16.1	40S ribosomal protein S14, putative	15.89	3	2	121.51
G3P_HUMAN	36.0	(P04406) Glyceraldehyde-3-phosphate dehydrogenase	15.82	4	4	185.70
PF3D7_1037300	33.7	ADP/ATP transporter on adenylate translocase	15.61	4	3	238.03
PF3D7_1341200	21.7	60S ribosomal protein L18, putative	13.04	2	2	130.96

Accession	MW (kDa)	Description	Σ Coverage	Σ# PSMs	Σ# Peptides	Score
GTR1_HUMAN	54.0	Solute carrier family 2 facilitated glucose transporter member 1	12.20	8	7	285.69
	High	GTR1_HUMAN	1	1	CID	40
PF3D7_1324900	34.1	L-lactate dehydrogenase (LDH)	11.71	3	3	165.68
PF3D7_0917900	72.3	heat shock protein 70 (Hsp70-2)	11.50	5	5	284.80
ATPB_HUMAN	56.5	(P06576) ATP synthase subunit beta, mitochondrial	11.15	3	3	90.02
PF3D7_0520000	22.1	40S ribosomal protein S9, putative	10.05	2	2	108.30
EPB42_HUMAN	77.0	(P16452) Erythrocyte membrane protein band 4.2	9.70	5	5	251.54
PF3D7_0516900	28.0	60S ribosomal protein L8, putative	9.23	4	2	187.57
PF3D7_0930300	195.6	merozoite surface protein 1 (MSP1)	9.13	12	10	528.02
PF3D7_0401800	60.2	Plasmodium exported protein (PHISTb)	8.21	3	3	229.37
PF3D7_1456800	76.4	V-type H( )-translocating pyrophosphatase, putative	7.95	6	5	278.84
PF3D7_1027800	44.2	60S ribosomal protein L3, putative	7.77	3	3	148.02
PF3D7_0106300	139.3	calcium-transporting ATPase (ATP6)	7.25	6	6	328.99
ALBU_HUMAN	69.3	(P02768) Serum albumin	6.90	6	5	312.39
FLOT1_HUMAN	47.3	(O75955) Flotillin-1	6.56	3	2	149.68
ANXA2_HUMAN	38.6	(P07355) Annexin A2	6.19	2	2	61.32
PF3D7_0204700	56.4	hexose transporter (HT)	5.95	2	2	131.10
PF3D7_0532400	61.0	Plasmodium exported protein (PHISTb), unknown function	5.68	2	2	123.12
FILA2_HUMAN	247.9	(Q5D862) Filaggrin-2	5.65	10	5	317.38
ACTB_HUMAN	41.7	(P60709) Actin, cytoplasmic 1	5.60	2	2	125.96
PF3D7_0922500	45.4	phosphoglycerate kinase (PGK)	5.53	2	2	94.77
PF3D7_0709000	48.6	chloroquine resistance transporter (CRT)	5.42	6	3	229.69
41_HUMAN	97.0	(P11171) Protein 4.1	4.51	2	2	163.10
PF3D7_0523000	162.1	multidrug resistance protein (MDR1)	4.44	5	5	276.24
PF3D7_1212700	166.0	eukaryotic translation initiation factor 3 subunit 10	4.43	5	5	233.86
DSG1_HUMAN	113.7	(Q02413) Desmoglein-1	4.29	4	4	146.71
PF3D7_0823800	76.6	DnaJ protein, putative	3.82	3	2	168.90
PF3D7_1420700	112.5	surface protein, Pf113 (Pf113)	3.72	2	2	136.06
PF3D7_1451100	93.5	elongation factor 2	3.61	3	3	134.17
PF3D7_1011800	131.5	QF122 antigen	3.60	4	3	249.89
PF3D7_1224300	97.2	polyadenylate-binding protein, putative (PABP)	3.09	2	2	91.93

Accession	MW (kDa)	Description	Σ Coverage	Σ# PSMs	Σ# Peptides	Score
PF3D7_1222300	95.0	endoplasmin homolog precursor, putative	3.05	2	2	145.18
PF3D7_1447900	118.9	multidrug resistance protein 2 (MDR2)	2.64	2	2	134.62
PF3D7_0302500	167.1	cytoadherence linked asexual protein 3.1 (CLAG3.1)	2.47	3	3	201.40
PF3D7_1211900	140.2	non-SERCA-type Ca2 -transporting P-ATPase (ATP4)	1.98	2	2	125.89
DESP_HUMAN	331.6	(P15924) Desmoplakin	1.92	5	5	223.50
PF3D7_1036900	192.6	conserved Plasmodium protein, unknown function	1.78	3	2	232.67

Supplemental Table 5.3. Proteins identified in ~90 kDa region excised from oligopreciptiation with RDM.

Accession	MW (kDa)	Description	Σ Coverage	Σ# PSMs	Σ# Peptides	Score
CYTA_HUMAN	11.0	(P01040) Cystatin-A	69.39	4	4	162.33
ALBU_HUMAN	69.3	(P02768) Serum albumin	49.10	35	25	1369.27
IGKC_HUMAN	11.6	(P01834) Ig kappa chain C region	35.85	11	3	310.87
HORN_HUMAN	282.2	(Q86YZ3) Hornerin	30.21	54	26	1800.52
B3AT_HUMAN	101.7	(P02730) Band 3 anion transport protein	26.78	27	15	994.12
DCD_HUMAN	11.3	(P81605) Dermcidin	22.73	4	2	203.35
FABP5_HUMAN	15.2	(Q01469) Fatty acid-binding protein, epidermal	20.00	3	3	90.69
HBB_HUMAN	16.0	(P68871) Hemoglobin subunit beta	15.65	2	2	93.26
PF3D7_0202000	71.3	knob-associated histidine-rich protein (KAHRP)	13.30	47	10	1061.52
HSPB1_HUMAN	22.8	(P04792) Heat shock protein beta-1	13.17	4	2	128.18
ACTB_HUMAN	41.7	(P60709) Actin, cytoplasmic 1	8.27	3	3	121.22
FILA2_HUMAN	247.9	(Q5D862) Filaggrin-2	8.20	10	5	266.28
IGHG1_HUMAN	36.1	(P01857) Ig gamma-1 chain C region	7.88	2	2	131.61
DSG1_HUMAN	113.7	(Q02413) Desmoglein-1	7.72	9	7	346.25
ARGI1_HUMAN	34.7	(P05089) Arginase-1	6.83	3	2	76.74
ANXA2_HUMAN	38.6	(P07355) Annexin A2	6.19	2	2	85.91
SPB3_HUMAN	44.5	(P29508) Serpin B3	5.64	2	2	83.66
TRFL_HUMAN	78.1	(P02788) Lactotransferrin	5.35	4	3	131.22
PF3D7_1224300	97.2	polyadenylate-binding protein, putative (PABP)	3.09	2	2	68.84
FILA_HUMAN	434.9	(P20930) Filaggrin	1.65	3	3	99.33

Supplemental Table 5.4. Proteins identified in 90 kDa region excised from oligopreciptiation with Euge.4.

Accession	MW (kDa)	Description	Σ Coverage	Σ# PSMs	Σ# Peptides	Score
HBB_HUMAN	16.0	(P68871) Hemoglobin subunit beta	49.66	7	6	222.41
PF3D7_0708400	86.1	heat shock protein 90 (HSP90)	49.13	42	27	1655.01
CYTA_HUMAN	11.0	(P01040) Cystatin-A	44.90	3	3	161.97
PF3D7_1211800	42.8	polyubiquitin (PfpUB) -- Pf3D7_12_v3:526109-527780(+)	44.62	3	3	104.96
PF3D7_1016300	95.8	glycophorin binding protein (GBP)	36.53	3	2	87.35
STOM_HUMAN	31.7	(P27105) Erythrocyte band 7 integral membrane protein	36.46	10	8	393.44
HORN_HUMAN	282.2	(Q86YZ3) Hornerin	35.65	71	31	2875.99
DCD_HUMAN	11.3	(P81605) Dermcidin	35.45	6	4	284.91
PF3D7_0202000	71.3	knob-associated histidine-rich protein (KAHRP)	34.86	349	33	5970.82
B3AT_HUMAN	101.7	(P02730) Band 3 anion transport protein	32.49	94	21	3126.23
ALBU_HUMAN	69.3	(P02768) Serum albumin	25.78	16	12	739.97
THIO_HUMAN	11.7	(P10599) Thioredoxin	20.95	2	2	115.73
FABP5_HUMAN	15.2	(Q01469) Fatty acid-binding protein, epidermal	20.00	3	3	76.80
HBA_HUMAN	15.2	(P69905) Hemoglobin subunit alpha	19.01	3	2	185.45
LEG7_HUMAN	15.1	(P47929) Galectin-7	18.38	3	2	139.81
ANK1_HUMAN	206.1	(P16157) Ankyrin-1	15.68	26	20	947.46
PF3D7_1465900	24.7	40S ribosomal protein S3, putative	15.38	3	3	117.33
CASPE_HUMAN	27.7	(P31944) Caspase-14	14.46	3	3	211.65
ANXA2_HUMAN	38.6	(P07355) Annexin A2	14.45	6	5	215.44
PF3D7_0818900	73.9	heat shock protein 70 (Hsp70)	14.33	8	7	286.43
G3P_HUMAN	36.0	(P04406) Glyceraldehyde-3-phosphate dehydrogenase	13.73	5	4	204.70
DSG1_HUMAN	113.7	(Q02413) Desmoglein-1	13.54	19	12	818.62

Accession	MW (kDa)	Description	Σ Coverage	Σ# PSMs	Σ# Peptides	Score
PF3D7_0500800	168.2	mature parasite-infected erythrocyte surface antigen,erythrocyte membrane protein 2 (MESA)	12.41	18	14	645.82
GGCT_HUMAN	21.0	(O75223) Gamma-glutamylcyclotransferase	12.23	2	2	90.46
PF3D7_1451100	93.5	elongation factor 2 -- Pf3D7_14_v3:2090902-2093400(+)	11.30	6	6	251.27
PF3D7_0401800	60.2	Plasmodium exported protein (PHISTb), unknown function (PfD80)	10.89	7	5	276.01
FILA2_HUMAN	247.9	(Q5D862) Filaggrin-2	10.83	13	10	589.47
PF3D7_1357000	48.9	elongation factor 1-alpha -- Pf3D7_13_v3:2265817-2267148(-)	10.61	3	3	149.72
PF3D7_0617900	15.4	histone H3 variant, putative (H3.3)	10.29	2	2	66.52
CATA_HUMAN	59.7	(P04040) Catalase	9.87	7	5	315.98
PF3D7_1462800	36.6	glyceraldehyde-3-phosphate dehydrogenase (GAPDH)	9.20	3	3	99.19
PF3D7_0730900	244.0	Plasmodium exported protein, unknown function	9.10	3	3	121.46
DESP_HUMAN	331.6	(P15924) Desmoplakin	8.25	21	19	960.39
ZA2G_HUMAN	34.2	(P25311) Zinc-alpha-2-glycoprotein	7.38	2	2	87.87
PF3D7_0507100	46.2	60S ribosomal protein L4, putative	7.30	2	2	96.64
PF3D7_0917900	72.3	heat shock protein 70 (Hsp70-2)	7.06	5	3	125.96
GTR1_HUMAN	54.0	Solute carrier family 2, facilitated glucose transporter member 1	6.71	4	3	230.09
PLAK_HUMAN	81.7	(P14923) Junction plakoglobin	5.91	4	4	153.34
ACTB_HUMAN	41.7	(P60709) Actin, cytoplasmic 1	5.60	2	2	96.66
EPB42_HUMAN	77.0	(P16452) Erythrocyte membrane protein band 4.2	4.63	2	2	104.86
PF3D7_1456800	76.4	V-type H( )-translocating pyrophosphatase, putative	3.63	2	2	92.72
PF3D7_1224300	97.2	polyadenylate-binding protein, putative (PABP)	3.09	3	2	148.39

Supplemental Table 5.5. Top 20 human proteins identified in all bands excised from RDM and Euge.7 oligopreciptiations.

Protein	Reference	Accession	RDM		Euge.7	
			# Total Peptides	# Unique Peptides	# Total Peptides	# Unique Peptides
Band 3 anion transport protein OS=Homo sapiens GN=SLC4A1 PE=1 SV=3	B3AT_HUMAN	P02730	36	10	234	33
Ankyrin-1 OS=Homo sapiens GN=ANK1 PE=1 SV=3	ANK1_HUMAN	P16157	6	5	206	47
Spectrin alpha chain, erythrocytic 1 OS=Homo sapiens GN=SPTA1 PE=1 SV=5	SPTA1_HUMAN	P02549	30	15	82	49
Hemoglobin subunit beta OS=Homo sapiens GN=HBB PE=1 SV=2	HBB_HUMAN	P68871	36	8	108	10
Spectrin beta chain, erythrocytic OS=Homo sapiens GN=SPTB PE=1 SV=5	SPTB1_HUMAN	P11277	1	1	33	29
Hemoglobin subunit alpha OS=Homo sapiens GN=HBA1 PE=1 SV=2	HBA_HUMAN	P69905	38	6	79	6
Serum albumin OS=Homo sapiens GN=ALB PE=1 SV=2	ALBU_HUMAN	P02768	17	7	17	4
High mobility group protein B1 OS=Homo sapiens GN=HMGB1 PE=1 SV=3	HMGB1_HUMAN	P09429	55	2	44	2
Solute carrier family 2, facilitated glucose transporter member 1 OS=Homo sapiens GN=SLC2A1	GTR1_HUMAN	P11166	3	1	43	8
Erythrocyte membrane protein band 4.2 OS=Homo sapiens GN=EPB42 PE=1 SV=3	EPB42_HUMAN	P16452	1	1	19	7
Histone H4 OS=Homo sapiens GN=HIST1H4A PE=1 SV=2	H4_HUMAN	P62805	31	8	26	5
Zinc finger protein 292 OS=Homo sapiens GN=ZNF292 PE=1 SV=3	ZN292_HUMAN	O60281	29	2	30	2
Leiomodin-3 OS=Homo sapiens GN=LMOD3 PE=2 SV=1	LMOD3_HUMAN	Q0VAK6	8	1	37	2
Uncharacterized protein C9orf174 OS=Homo sapiens GN=C9orf174 PE=1 SV=2	CI174_HUMAN	Q9P1Z9	31	2	27	3
Erythrocyte band 7 integral membrane protein OS=Homo sapiens GN=STOM PE=1 SV=3	STOM_HUMAN	P27105	20	4	33	8
Titin OS=Homo sapiens GN=TTN PE=1 SV=4	TITIN_HUMAN	Q8WZ42	24	5	23	5
Vomeronasal type-1 receptor 2 OS=Homo sapiens GN=VN1R2 PE=2 SV=2	VN1R2_HUMAN	Q8NFZ6	12	1	21	1
Histone H2A type 1-A OS=Homo sapiens GN=HIST1H2AA PE=1 SV=3	H2A1A_HUMAN	Q96QV6	17	3	15	3

Protein	Reference	Accession	RDM		Euge.7	
			# Total Peptides	# Unique Peptides	# Total Peptides	# Unique Peptides
Protein 4.1 OS=Homo sapiens GN=EPB41 PE=1 SV=4	41_HUMAN	P11171	2	2	5	5
Golgin subfamily A member 6-like protein 2 OS=Homo sapiens GN=GOLGA6L2 PE=4 SV=1	F8WBV9_HUMAN	F8WBV9	2	1	11	1
Flavin reductase (NADPH) OS=Homo sapiens GN=BLVRB PE=1 SV=3	BLVRB_HUMAN	P30043			1	1
Dystonin OS=Homo sapiens GN=DST PE=1 SV=4	DYST_HUMAN	Q03001	16	2	21	3
Elongation factor 1-alpha 1 OS=Homo sapiens GN=EEF1A1 PE=1 SV=1	EF1A1_HUMAN	P68104	9	5	9	2
Desmoglein-1 OS=Homo sapiens GN=DSG1 PE=1 SV=2	DSG1_HUMAN	Q02413	4	4	14	9
Heterogeneous nuclear ribonucleoprotein L OS=Homo sapiens GN=HNRNPL PE=1 SV=2	HNRPL_HUMAN	P14866	20	1	13	1
Desmoplakin OS=Homo sapiens GN=DSP PE=1 SV=3	DESP_HUMAN	P15924	44	37	13	11
55 kDa erythrocyte membrane protein OS=Homo sapiens GN=MPP1 PE=1 SV=2	EM55_HUMAN	Q00013	0	0	11	6
Recombining binding protein suppressor of hairless-like protein OS=Homo sapiens GN=RBPJL	RBPJL_HUMAN	Q9UBG7	19	1	21	1
Blood group Rh(CE) polypeptide OS=Homo sapiens GN=RHCE PE=1 SV=2	RHCE_HUMAN	P18577	1	1	13	2
Uncharacterized protein C8orf86 OS=Homo sapiens GN=C8orf86 PE=2 SV=1	CH086_HUMAN	Q6ZUL3	12	1	16	1
Transcriptional repressor CTCFL OS=Homo sapiens GN=CTCFL PE=1 SV=2	CTCFL_HUMAN	Q8NI51	24	1	11	1
Hornerin OS=Homo sapiens GN=HRNR PE=1 SV=2	HORN_HUMAN	Q86YZ3	16	8	41	11
Uncharacterized protein OS=Homo sapiens PE=4 SV=1	C9JWB5_HUMAN	C9JWB5	24	1	23	1
Terminal uridylyltransferase 4 OS=Homo sapiens GN=ZCCHC11 PE=1 SV=3	TUT4_HUMAN	Q5TAX3	13	2	12	2
ADP-ribosylation factor 1 OS=Homo sapiens GN=ARF1 PE=1 SV=2	ARF1_HUMAN	P84077	1	1	7	4
Protein-glutamine gamma-glutamyltransferase 2 OS=Homo sapiens GN=TGM2 PE=1 SV=2	TGM2_HUMAN	P21980	1	1	1	1
Transcriptional adapter 2-beta OS=Homo sapiens GN=TADA2B PE=1 SV=2	TAD2B_HUMAN	Q86TJ2	5	1	20	1
Histone H3.1t OS=Homo sapiens GN=HIST3H3 PE=1 SV=3	H31T_HUMAN	Q16695	8	2	8	1

Protein	Reference	Accession	RDM		Euge.7	
			# Total Peptides	# Unique Peptides	# Total Peptides	# Unique Peptides
Paladin OS=Homo sapiens GN=PALD1 PE=1 SV=3	PALD_HUMAN	Q9ULE6	7	1	4	1
Endoplasmin OS=Homo sapiens GN=HSP90B1 PE=1 SV=1	ENPL_HUMAN	P14625	1	1	7	2
Sodium channel protein type 10 subunit alpha OS=Homo sapiens GN=SCN10A PE=1 SV=2	SCNAA_HUMAN	Q9Y5Y9	14	2	7	1
Hemoglobin subunit delta OS=Homo sapiens GN=HBD PE=1 SV=2	HBD_HUMAN	P02042	1	1	6	3
Proline-rich protein 19 OS=Homo sapiens GN=PRR19 PE=2 SV=1	PRR19_HUMAN	A6NJB7	9	1	5	1
Tripeptidyl-peptidase 2 OS=Homo sapiens GN=TPP2 PE=1 SV=4	TPP2_HUMAN	P29144			7	2
ATP-binding cassette sub-family A member 13 OS=Homo sapiens GN=ABCA13 PE=2 SV=3	ABCAD_HUMAN	Q86UQ4	7	1	6	1
BAG family molecular chaperone regulator 3 (Fragment) OS=Homo sapiens GN=BAG3 PE=4 SV=1	C9JFK9_HUMAN	C9JFK9	11	1	7	1
Plectin OS=Homo sapiens GN=PLEC PE=1 SV=3	PLEC_HUMAN	Q15149	6	4	6	3
GTP-binding nuclear protein Ran OS=Homo sapiens GN=RAN PE=1 SV=3	RAN_HUMAN	P62826	1	1	2	1
Junction plakoglobin OS=Homo sapiens GN=JUP PE=1 SV=3	PLAK_HUMAN	P14923	30	13	16	8
Transmembrane protein 200C OS=Homo sapiens GN=TMEM200C PE=2 SV=2	T200C_HUMAN	A6NKL6	10	1	10	1
Filaggrin-2 OS=Homo sapiens GN=FLG2 PE=1 SV=1	FILA2_HUMAN	Q5D862	11	3	10	4
Ryanodine receptor 3 OS=Homo sapiens GN=RYR3 PE=1 SV=3	RYR3_HUMAN	Q15413	4	1	7	1
CAP-Gly domain-containing linker protein 1 OS=Homo sapiens GN=CLIP1 PE=1 SV=2	CLIP1_HUMAN	P30622	5	2	6	1
EF-hand calcium-binding domain-containing protein 6 OS=Homo sapiens GN=EFCAB6 PE=1 SV=1	EFCB6_HUMAN	Q5THR3	7	2	5	2
Uncharacterized protein KIAA1211 OS=Homo sapiens GN=KIAA1211 PE=1 SV=3	K1211_HUMAN	Q6ZU35	12	2	5	1
Potassium-transporting ATPase alpha chain 2 OS=Homo sapiens GN=ATP12A PE=1 SV=3	AT12A_HUMAN	P54707	5	1	5	1
Selenium-binding protein 1 OS=Homo sapiens GN=SELENBP1 PE=1 SV=2	SBP1_HUMAN	Q13228	31	18	0	0

Protein	Reference	Accession	RDM		Euge.7	
			# Total Peptides	# Unique Peptides	# Total Peptides	# Unique Peptides
Putative tyrosine-protein phosphatase TPTE OS=Homo sapiens GN=TPTE PE=2 SV=3	TPTE_HUMAN	P56180	6	1	10	1
Dermcidin OS=Homo sapiens GN=DCD PE=1 SV=2	DCD_HUMAN	P81605	8	2	7	1
Mitogen-activated protein kinase kinase kinase kinase 4 OS=Homo sapiens	M4K4_HUMAN	O95819	2	1	6	1
Probable ATP-dependent DNA helicase HFM1 OS=Homo sapiens GN=HFM1 PE=1 SV=2	HFM1_HUMAN	A2PYH4	4	1	6	1
Histone H2A type 2-B OS=Homo sapiens GN=HIST2H2AB PE=1 SV=3	H2A2B_HUMAN	Q8IUE6	4	1	5	1
Treacle protein OS=Homo sapiens GN=TCOF1 PE=1 SV=3	TCOF_HUMAN	Q13428	7	2	5	2
Heat shock 70 kDa protein 1-like OS=Homo sapiens GN=HSPA1L PE=1 SV=2	HS71L_HUMAN	P34931	4	3	4	1
Actin, aortic smooth muscle OS=Homo sapiens GN=ACTA2 PE=1 SV=1	ACTA_HUMAN	P62736	28	10	4	2
NACHT, LRR and PYD domains-containing protein 1 OS=Homo sapiens GN=NLRP1 PE=1 SV=1	NALP1_HUMAN	Q9C000	4	1	4	1
Actin, cytoplasmic 1 OS=Homo sapiens GN=ACTB PE=1 SV=1	ACTB_HUMAN	P60709	6	4	3	3
Vesicle-fusing ATPase OS=Homo sapiens GN=NSF PE=1 SV=3	NSF_HUMAN	P46459			2	2
Heat shock cognate 71 kDa protein OS=Homo sapiens GN=HSPA8 PE=1 SV=1	HSP7C_HUMAN	P11142	1	1	1	1
Probable helicase senataxin OS=Homo sapiens GN=SETX PE=1 SV=4	SETX_HUMAN	Q7Z333	6	1	13	1
Chloride channel 7, isoform CRA_c OS=Homo sapiens GN=CLCN7 PE=4 SV=1	H0Y2M6_HUMAN	H0Y2M6	9	1	11	1
Sp110 nuclear body protein OS=Homo sapiens GN=SP110 PE=1 SV=5	SP110_HUMAN	Q9HB58	6	1	10	1
1-phosphatidylinositol 4,5-bisphosphate phosphodiesterase eta-1 OS=Homo sapiens	PLCH1_HUMAN	Q4KWH8	9	2	10	1
Tyrosine-protein kinase Fes/Fps OS=Homo sapiens GN=FES PE=1 SV=3	FES_HUMAN	P07332	7	2	8	2
Fibronectin type III and SPRY domain-containing protein 2 OS=Homo sapiens GN=FSD2 PE=2 SV=1	FSD2_HUMAN	A1L4K1	1	1	6	2
Ras-related protein Rab-19 OS=Homo sapiens GN=RAB19 PE=2 SV=2	RAB19_HUMAN	A4D1S5	4	1	6	1

Protein	Reference	Accession	RDM		Euge.7	
			# Total Peptides	# Unique Peptides	# Total Peptides	# Unique Peptides
Pleckstrin homology domain-containing family H member 1 OS=Homo sapiens	E7ESY2_HUMAN	E7ESY2	0	0	5	1
Ubiquitin-60S ribosomal protein L40 OS=Homo sapiens GN=UBA52 PE=1 SV=2	RL40_HUMAN	P62987	2	2	5	3
Histone H2B type 1-A OS=Homo sapiens GN=HIST1H2BA PE=1 SV=3	H2B1A_HUMAN	Q96A08	2	2	4	2
Large neutral amino acids transporter small subunit 2 OS=Homo sapiens GN=SLC7A8 PE=1 SV=1	LAT2_HUMAN	Q9UHI5	6	1	4	1
Glyceraldehyde-3-phosphate dehydrogenase OS=Homo sapiens GN=GAPDH PE=1 SV=3	G3P_HUMAN	P04406	8	6	4	2
Peroxiredoxin-1 OS=Homo sapiens GN=PRDX1 PE=1 SV=1	PRDX1_HUMAN	Q06830	4	3	3	1
Mitogen-activated protein kinase kinase kinase kinase 4 OS=Homo sapiens GN=MAP4K4	G5E948_HUMAN	G5E948	6	1	3	1
H/ACA ribonucleoprotein complex subunit 3 OS=Homo sapiens GN=NOP10 PE=4 SV=1	H0YM60_HUMAN	H0YM60	5	1	3	1
Integrin beta-8 OS=Homo sapiens GN=ITGB8 PE=1 SV=1	ITB8_HUMAN	P26012	4	1	3	1
Dexamethasone-induced Ras-related protein 1 OS=Homo sapiens GN=RASD1 PE=1 SV=1	RASD1_HUMAN	Q9Y272			2	1
E3 SUMO-protein ligase RanBP2 OS=Homo sapiens GN=RANBP2 PE=1 SV=2	RBP2_HUMAN	P49792	9	1	11	1
Calcium-dependent secretion activator 2 OS=Homo sapiens GN=CADPS2 PE=1 SV=2	CAPS2_HUMAN	Q86UW7	1	1	9	1
1-phosphatidylinositol 4,5-bisphosphate phosphodiesterase delta-1 OS=Homo sapiens GN=PLCD1 PE=1 SV=2	PLCD1_HUMAN	P51178	8	6	8	2
Probable tRNA (uracil-O(2)-)-methyltransferase OS=Homo sapiens GN=TRMT44 PE=2 SV=2	TRM44_HUMAN	Q8IYL2	9	1	8	1
Teneurin-3 OS=Homo sapiens GN=TENM3 PE=2 SV=3	TEN3_HUMAN	Q9P273	5	1	8	1
40S ribosomal protein S18 OS=Homo sapiens GN=RPS18 PE=1 SV=3	RS18_HUMAN	P62269	7	4	7	1
rRNA/tRNA 2'-O-methyltransferase fibrillarin-like protein 1 OS=Homo sapiens	FBLL1_HUMAN	A6NHQ2	1	1	7	1

Protein	Reference	Accession	RDM		Euge.7	
			# Total Peptides	# Unique Peptides	# Total Peptides	# Unique Peptides
Protein-glutamine gamma-glutamyltransferase 4 OS=Homo sapiens GN=TGM4 PE=1 SV=2	TGM4_HUMAN	P49221	8	1	7	1
Constitutive coactivator of peroxisome proliferator-activated receptor gamma	F120B_HUMAN	Q96EK7	4	1	6	4
Solute carrier family 22 member 6 OS=Homo sapiens GN=SLC22A6 PE=1 SV=1	S22A6_HUMAN	Q4U2R8	7	1	6	1
Collectin-12 OS=Homo sapiens GN=COLEC12 PE=1 SV=3	COL12_HUMAN	Q5KU26	3	1	5	1
Annexin A2 OS=Homo sapiens GN=ANXA2 PE=1 SV=2	ANXA2_HUMAN	P07355	14	11	3	3
Spermatogenesis-associated protein 8 OS=Homo sapiens GN=SPATA8 PE=1 SV=1	SPAT8_HUMAN	Q6RVD6	3	1	2	1
Mitogen-activated protein kinase-binding protein 1 OS=Homo sapiens GN=MAPKBP1 PE=2 SV=4	MABP1_HUMAN	O60336	2	1	2	1
Thioredoxin OS=Homo sapiens GN=TXN PE=1 SV=3	THIO_HUMAN	P10599	8	2	2	2
Nucleoprotein TPR OS=Homo sapiens GN=TPR PE=1 SV=3	TPR_HUMAN	P12270			1	1
Alpha-adducin OS=Homo sapiens GN=ADD1 PE=1 SV=2	ADDA_HUMAN	P35611			1	1
T-complex protein 1 subunit delta OS=Homo sapiens GN=CCT4 PE=1 SV=4	TCPD_HUMAN	P50991	1	1	1	1
Histone H2A type 1-B/E OS=Homo sapiens GN=HIST1H2AB PE=1 SV=2	H2A1B_HUMAN	P04908			1	1
Hemoglobin subunit zeta OS=Homo sapiens GN=HBZ PE=1 SV=2	HBAZ_HUMAN	P02008			1	1
Serine/threonine-protein phosphatase 2A 65 kDa regulatory subunit A alpha isoform OS=Homo sapiens GN=PPP2R1A PE=1 SV=4	2AAA_HUMAN	P30153			1	1
Angiopoietin-4 OS=Homo sapiens GN=ANGPT4 PE=1 SV=1	ANGP4_HUMAN	Q9Y264			1	1
Zinc finger and BTB domain-containing protein 1 OS=Homo sapiens GN=ZBTB1 PE=1 SV=3	ZBTB1_HUMAN	Q9Y2K1			13	2
THAP domain-containing protein 9 OS=Homo sapiens GN=THAP9 PE=2 SV=2	THAP9_HUMAN	Q9H5L6	7	1	10	1
Zinc finger CCHC domain-containing protein 7 OS=Homo sapiens GN=ZCCHC7 PE=1 SV=2	ZCHC7_HUMAN	Q8N3Z6	7	1	10	1
Hyccin OS=Homo sapiens GN=FAM126A PE=4 SV=1	B8ZZJ1_HUMAN	B8ZZJ1	4	1	9	1

Protein	Reference	Accession	RDM		Euge.7	
			# Total Peptides	# Unique Peptides	# Total Peptides	# Unique Peptides
Heat shock protein 75 kDa, mitochondrial OS=Homo sapiens GN=TRAP1 PE=1 SV=3	TRAP1_HUMAN	Q12931	9	2	7	1
Nuclear factor 1 C-type OS=Homo sapiens GN=NFIC PE=1 SV=2	NFIC_HUMAN	P08651	8	1	7	1
Coiled-coil domain-containing protein 74A OS=Homo sapiens GN=CCDC74A PE=2 SV=1	CC74A_HUMAN	Q96AQ1	5	1	6	1
78 kDa glucose-regulated protein OS=Homo sapiens GN=HSPA5 PE=1 SV=2	GRP78_HUMAN	P11021	7	7	5	2
Cingulin OS=Homo sapiens GN=CGN PE=1 SV=2	CING_HUMAN	Q9P2M7	1	1	5	2
Nuclear factor of activated T-cells, cytoplasmic 4 OS=Homo sapiens GN=NFATC4 PE=1 SV=2	NFAC4_HUMAN	Q14934	3	1	5	2
E3 ubiquitin-protein ligase RAD18 OS=Homo sapiens GN=RAD18 PE=1 SV=2	RAD18_HUMAN	Q9NS91	5	1	5	1
Leukocyte immunoglobulin-like receptor subfamily B member 4 (Fragment) OS=Homo sapiens GN=LILRB4 PE=4 SV=1	C9JHA6_HUMAN	C9JHA6			4	1
Trinucleotide repeat-containing gene 18 protein OS=Homo sapiens GN=TNRC18 PE=1 SV=3	TNC18_HUMAN	O15417	9	2	4	1
6-phosphofructokinase, liver type OS=Homo sapiens GN=PFKL PE=1 SV=6	K6PL_HUMAN	P17858			3	3
Proline-rich protein 16 OS=Homo sapiens GN=PRR16 PE=2 SV=1	PRR16_HUMAN	Q569H4	3	1	3	1
Angiotensin-converting enzyme OS=Homo sapiens GN=ACE PE=1 SV=1	ACE_HUMAN	P12821	4	2	3	1
Desmocollin-2 OS=Homo sapiens GN=DSC2 PE=1 SV=1	DSC2_HUMAN	Q02487	2	1	3	1
Transmembrane channel-like protein 6 OS=Homo sapiens GN=TMC6 PE=1 SV=2	TMC6_HUMAN	Q7Z403	3	1	3	1
Histone-lysine N-methyltransferase ASH1L OS=Homo sapiens GN=ASH1L PE=1 SV=2	ASH1L_HUMAN	Q9NR48	7	1	3	1
Caspase-14 OS=Homo sapiens GN=CASP14 PE=1 SV=2	CASPE_HUMAN	P31944	3	2	3	3
1-phosphatidylinositol 4,5-bisphosphate phosphodiesterase eta-2 OS=Homo sapiens GN=PLCH2 PE=2 SV=3	PLCH2_HUMAN	O75038	1	1	2	1
Zinc finger and BTB domain-containing protein 40 OS=Homo sapiens GN=ZBTB40 PE=1 SV=4	ZBT40_HUMAN	Q9NUA8	2	1	2	1

Protein	Reference	Accession	RDM		Euge.7	
			# Total Peptides	# Unique Peptides	# Total Peptides	# Unique Peptides
GPI inositol-deacylase OS=Homo sapiens GN=PGAP1 PE=2 SV=1	PGAP1_HUMAN	Q75T13	3	1	2	1
Glycosyltransferase 25 family member 3 OS=Homo sapiens GN=CERCAM PE=2 SV=1	GT253_HUMAN	Q5T4B2	2	1	2	1
Ataxin-3 (Fragment) OS=Homo sapiens GN=ATXN3 PE=4 SV=1	G3V3T6_HUMAN	G3V3T6			1	1
Protein phosphatase Slingshot homolog 1 OS=Homo sapiens GN=SSH1 PE=1 SV=2	SSH1_HUMAN	Q8WYL5	1	1	1	1
Filaggrin OS=Homo sapiens GN=FLG PE=1 SV=3	FILA_HUMAN	P20930			1	1
Magnesium transporter NIPA3 OS=Homo sapiens GN=NIPAL1 PE=2 SV=1	NIPA3_HUMAN	Q6NVV3			1	1
Dynactin subunit 1 OS=Homo sapiens GN=DCTN1 PE=1 SV=3	DCTN1_HUMAN	Q14203	1	1		
Trafficking kinesin-binding protein 2 OS=Homo sapiens GN=TRAK2 PE=1 SV=2	TRAK2_HUMAN	O60296				
Histone H4-like protein type G OS=Homo sapiens GN=HIST1H4G PE=2 SV=1	H4G_HUMAN	Q99525	3	1		
Histone H2B type 1-B OS=Homo sapiens GN=HIST1H2BB PE=1 SV=2	H2B1B_HUMAN	P33778	4	3		
5' exonuclease Apollo OS=Homo sapiens GN=DCLRE1B PE=1 SV=1	DCR1B_HUMAN	Q9H816	3	1	8	1
Phosphatidylinositol 4-phosphate 5-kinase type-1 alpha OS=Homo sapiens GN=PIP5K1A PE=1 SV=1	PI51A_HUMAN	Q99755	5	1	8	2
Early endosome antigen 1 OS=Homo sapiens GN=EEA1 PE=1 SV=2	EEA1_HUMAN	Q15075			7	1
Adenylate cyclase type 5 OS=Homo sapiens GN=ADCY5 PE=1 SV=3	ADCY5_HUMAN	O95622	1	1	7	1
Inactive phospholipase C-like protein 1 OS=Homo sapiens GN=PLCL1 PE=1 SV=3	PLCL1_HUMAN	Q15111	1	1	6	2
Membrane-associated guanylate kinase, WW and PDZ domain-containing protein 1 OS=Homo sapiens GN=MAGI1 PE=1 SV=3	MAGI1_HUMAN	Q96QZ7	6	1	6	1
40S ribosomal protein S14 OS=Homo sapiens GN=RPS14 PE=1 SV=3	RS14_HUMAN	P62263	5	1	5	1
Serine protease hepsin OS=Homo sapiens GN=HPN PE=1 SV=1	HEPS_HUMAN	P05981	3	1	5	1
A-kinase anchor protein 4 OS=Homo sapiens GN=AKAP4 PE=1 SV=1	AKAP4_HUMAN	Q5JQC9			4	1

Protein	Reference	Accession	RDM		Euge.7	
			# Total Peptides	# Unique Peptides	# Total Peptides	# Unique Peptides
NAD-dependent protein deacetylase sirtuin-1 OS=Homo sapiens GN=SIRT1 PE=1 SV=2	SIR1_HUMAN	Q96EB6	1	1	4	2
Probable helicase with zinc finger domain OS=Homo sapiens GN=HELZ PE=1 SV=2	HELZ_HUMAN	P42694	2	1	4	1
Septin-1 OS=Homo sapiens GN=SEPT1 PE=1 SV=2	SEPT1_HUMAN	Q8WYJ6	2	1	4	1
Choline transporter-like protein 1 OS=Homo sapiens GN=SLC44A1 PE=1 SV=1	CTL1_HUMAN	Q8WWI5	3	2	4	1
Myotubularin-related protein 4 OS=Homo sapiens GN=MTMR4 PE=2 SV=2	MTMR4_HUMAN	Q9NYA4	4	1	4	1
F-box only protein 41 OS=Homo sapiens GN=FBXO41 PE=2 SV=5	FBX41_HUMAN	Q8TF61	7	2	4	1
Chromodomain-helicase-DNA-binding protein 3 OS=Homo sapiens GN=CHD3 PE=1 SV=3	CHD3_HUMAN	Q12873	9	2	4	1
Cytochrome P450 3A43 OS=Homo sapiens GN=CYP3A43 PE=1 SV=1	CP343_HUMAN	Q9HB55			3	1
Serine/threonine-protein phosphatase 4 regulatory subunit 4 OS=Homo sapiens GN=PPP4R4 PE=1 SV=1	PP4R4_HUMAN	Q6NUP7			3	1
Dynein heavy chain 2, axonemal OS=Homo sapiens GN=DNAH2 PE=1 SV=3	DYH2_HUMAN	Q9P225			3	2
Zinc finger protein 40 OS=Homo sapiens GN=HIVEP1 PE=1 SV=3	ZEP1_HUMAN	P15822	1	1	3	1
Histone H2A.V OS=Homo sapiens GN=H2AFV PE=1 SV=3	H2AV_HUMAN	Q71UI9	3	1	3	1
Zinc finger protein 276 OS=Homo sapiens GN=ZNF276 PE=1 SV=4	ZN276_HUMAN	Q8N554	7	1	3	1
Stress-70 protein, mitochondrial OS=Homo sapiens GN=HSPA9 PE=1 SV=2	GRP75_HUMAN	P38646			2	1
Cation channel sperm-associated protein subunit delta OS=Homo sapiens GN=CATSPERD PE=2 SV=3	CTSRD_HUMAN	Q86XM0			2	1
Solute carrier family 35 member F3 OS=Homo sapiens GN=SLC35F3 PE=2 SV=2	S35F3_HUMAN	Q8IY50			2	1
Ubiquitin-conjugating enzyme E2 T OS=Homo sapiens GN=UBE2T PE=1 SV=1	UBE2T_HUMAN	Q9NPD8			2	1
Probable ribonuclease ZC3H12B OS=Homo sapiens GN=ZC3H12B PE=2 SV=2	ZC12B_HUMAN	Q5HYM0	3	1	2	1
RNA-binding protein 48 OS=Homo sapiens GN=RBM48 PE=2 SV=1	RBM48_HUMAN	Q5RL73	3	1	2	1

Protein	Reference	Accession	RDM		Euge.7	
			# Total Peptides	# Unique Peptides	# Total Peptides	# Unique Peptides
Methylthioribose-1-phosphate isomerase OS=Homo sapiens GN=MRI1 PE=1 SV=1	MTNA_HUMAN	Q9BV20	4	1	2	1
Putative PRAME family member 24 OS=Homo sapiens GN=PRAMEF24 PE=3 SV=1	PRA24_HUMAN	A6NMC2	7	2	2	1
TBC1 domain family member 22B OS=Homo sapiens GN=TBC1D22B PE=1 SV=3	TB22B_HUMAN	Q9NU19	7	1	2	1
Potassium channel subfamily K member 15 OS=Homo sapiens GN=KCNK15 PE=1 SV=2	KCNKF_HUMAN	Q9H427	5	1	2	1
Synaptotagmin-like protein 2 OS=Homo sapiens GN=SYTL2 PE=4 SV=1	J3KP28_HUMAN	J3KP28			1	1
T-complex protein 1 subunit gamma OS=Homo sapiens GN=CCT3 PE=1 SV=4	TCPG_HUMAN	P49368			1	1
A-kinase anchor protein 6 OS=Homo sapiens GN=AKAP6 PE=1 SV=3	AKAP6_HUMAN	Q13023			1	1
Unconventional myosin-VIIb OS=Homo sapiens GN=MYO7B PE=2 SV=2	MYO7B_HUMAN	Q6PIF6			1	1
Zinc finger protein 366 OS=Homo sapiens GN=ZNF366 PE=1 SV=1	ZN366_HUMAN	Q8N895			1	1
Dynein heavy chain domain-containing protein 1 OS=Homo sapiens GN=DNHD1 PE=1 SV=2	DNHD1_HUMAN	Q96M86	1	1	1	1
Hemicentin-1 OS=Homo sapiens GN=HMCN1 PE=1 SV=2	HMCN1_HUMAN	Q96RW7	1	1	1	1
Zinc finger protein 510 OS=Homo sapiens GN=ZNF510 PE=2 SV=1	ZN510_HUMAN	Q9Y2H8	2	1	1	1
Prelamin-A/C OS=Homo sapiens GN=LMNA PE=1 SV=1	LMNA_HUMAN	P02545	6	6	1	1
Kinetochore-associated protein 1 OS=Homo sapiens GN=KNTC1 PE=1 SV=1	KNTC1_HUMAN	P50748			1	1
Laminin subunit beta-3 OS=Homo sapiens GN=LAMB3 PE=1 SV=1	LAMB3_HUMAN	Q13751			1	1
6-phosphofructokinase, muscle type OS=Homo sapiens GN=PFKM PE=1 SV=2	K6PF_HUMAN	P08237	1	1	1	1
HHIP-like protein 2 OS=Homo sapiens GN=HHIPL2 PE=2 SV=1	HIPL2_HUMAN	Q6UWX4	2	1	1	1
Ubiquitin-like modifier-activating enzyme 1 OS=Homo sapiens GN=UBA1 PE=1 SV=3	UBA1_HUMAN	P22314	1	1		
Hydroxyacylglutathione hydrolase, mitochondrial OS=Homo sapiens GN=HAGH PE=1 SV=2	GLO2_HUMAN	Q16775	1	1		

Protein	Reference	Accession	RDM		Euge.7	
			# Total Peptides	# Unique Peptides	# Total Peptides	# Unique Peptides
Protein POF1B OS=Homo sapiens GN=POF1B PE=1 SV=3	POF1B_HUMAN	Q8WVV4			1	1
Unconventional myosin-XVIIIa OS=Homo sapiens GN=MYO18A PE=1 SV=3	MY18A_HUMAN	Q92614	1	1	1	1
Neuralized-like protein 4 OS=Homo sapiens GN=NEURL4 PE=1 SV=2	NEUL4_HUMAN	Q96JN8			1	1
Serine/threonine-protein phosphatase 2A catalytic subunit alpha isoform OS=Homo sapiens GN=PPP2CA PE=1 SV=1	PP2AA_HUMAN	P67775	1	1		
Heat shock-related 70 kDa protein 2 OS=Homo sapiens GN=HSPA2 PE=1 SV=1	HSP72_HUMAN	P54652	5	4		
Band 4.1-like protein 1 OS=Homo sapiens GN=EPB41L1 PE=1 SV=2	E41L1_HUMAN	Q9H4G0	1	1		
Desmocollin-1 OS=Homo sapiens GN=DSC1 PE=1 SV=2	DSC1_HUMAN	Q08554			7	4
DNA endonuclease RBBP8 OS=Homo sapiens GN=RBBP8 PE=1 SV=2	COM1_HUMAN	Q99708	4	1	7	1
Cytoplasmic dynein 1 heavy chain 1 OS=Homo sapiens GN=DYNC1H1 PE=1 SV=5	DYHC1_HUMAN	Q14204	4	1	6	1
Receptor-type tyrosine-protein phosphatase gamma OS=Homo sapiens GN=PTPRG PE=1 SV=4	PTPRG_HUMAN	P23470			5	2
Pre-mRNA-splicing factor 18 OS=Homo sapiens GN=PRPF18 PE=1 SV=1	PRP18_HUMAN	Q99633			5	1
EF-hand domain-containing family member B OS=Homo sapiens GN=EFHB PE=2 SV=4	EFHB_HUMAN	Q8N7U6	7	2	5	1
Mediator of RNA polymerase II transcription subunit 10 OS=Homo sapiens GN=MED10 PE=1 SV=1	MED10_HUMAN	Q9BTT4			5	1

Supplemental Table 5.6. Top 200 *P. falciparum* proteins identified in all bands excised from RDM and Euge.7 oligopreciptiations.

Protein	Reference	Accession	RDM		Euge.7	
			# Total Peptides	# Unique Peptides	# Total Peptides	# Unique Peptides
Mature parasite-infected erythrocyte surface antigen OS=Plasmodium falciparum PE=4 SV=2	Q06166_PLAFA	Q06166	6	6	199	76
Knob-associated histidine-rich protein (Fragment) OS=Plasmodium falciparum PE=2 SV=1	KNOB_PLAFA	P13817	10	7	183	18
Heat shock protein 86 OS=Plasmodium falciparum GN=HSP86 PE=3 SV=1	Q25882_PLAFA	Q25882	4	4	121	31
Histone H4 (Fragment) OS=Plasmodium falciparum PE=3 SV=1	Q7JSX6_PLAFA	Q7JSX6	56	11	85	13
Heat shock protein OS=Plasmodium falciparum GN=Pfgrp PE=3 SV=1	Q07615_PLAFA	Q07615	30	2	40	11
Histone H3 OS=Plasmodium falciparum PE=3 SV=1	Q86QI3_PLAFA	Q86QI3	31	7	46	6
Histone H2B OS=Plasmodium falciparum PE=3 SV=1	Q27717_PLAFA	Q27717	19	8	41	9
Heat shock 70 kDa protein OS=Plasmodium falciparum PE=2 SV=2	HSP70_PLAFA	P11144	4	3	31	17
Putative uncharacterized protein (Fragment) OS=Plasmodium falciparum GN=PF07_0004 PE=4 SV=1	D9HMQ4_PLAFA	D9HMQ4	36	1	35	1
Histone H2A OS=Plasmodium falciparum PE=2 SV=1	H2A_PLAFA	P40282	17	3	22	3
3D7var1 (Fragment) OS=Plasmodium falciparum GN=3D7var1 PE=4 SV=1	Q25766_PLAFA	Q25766	13	5	15	6
Erythrocyte membrane protein 1 (Fragment) OS=Plasmodium falciparum GN=var-4559 PE=4 SV=1	F1DF14_PLAFA	F1DF14	24	1	15	1
Processed variable antigen (Fragment) OS=Plasmodium falciparum PE=2 SV=1	PVA_PLAFA	P08116	1	1	45	12
Elongation factor 2 (Fragment) OS=Plasmodium falciparum PE=4 SV=1	Q9NDT2_PLAFA	Q9NDT2	3	2	18	9
RIFIN (Fragment) OS=Plasmodium falciparum GN=rif PE=4 SV=1	Q2XR87_PLAFA	Q2XR87	18	2	29	1
Actin I OS=Plasmodium falciparum PE=3 SV=1	Q9U6U4_PLAFA	Q9U6U4	5	3	9	5
Polyadenylate-binding protein OS=Plasmodium falciparum PE=2 SV=1	A1EAA0_PLAFA	A1EAA0	7	4	6	3
Erythrocyte membrane protein (Fragment) OS=Plasmodium falciparum GN=var PE=4 SV=1	Q3BEX9_PLAFA	Q3BEX9	51	1	42	1

Protein	Reference	Accession	RDM		Euge.7	
			# Total Peptides	# Unique Peptides	# Total Peptides	# Unique Peptides
Glyceraldehyde-3-phosphate dehydrogenase OS=Plasmodium falciparum PE=2 SV=1	O96369_PLAFA	O96369	1	1	16	6
RhopH1/Clag3.1 OS=Plasmodium falciparum GN=rhoph1/clag3.1 PE=2 SV=1	B0M0V7_PLAFA	B0M0V7	1	1	12	9
P-type ATPase4 OS=Plasmodium falciparum GN=ATPase4 PE=3 SV=1	Q9U445_PLAFA	Q9U445	14	3	18	9
Membrane erythrocyte protein 1 (Fragment) OS=Plasmodium falciparum GN=var PE=2 SV=1	G0M6E7_PLAFA	G0M6E7	13	1	24	1
Merozoite surface protein 1 OS=Plasmodium falciparum GN=msp1 PE=4 SV=1	Q764L3_PLAFA	Q764L3	3	3	23	13
Erythrocyte membrane protein 1 (Fragment) OS=Plasmodium falciparum GN=upsAvar PE=4 SV=1	Q1KVE5_PLAFA	Q1KVE5	13	1	16	2
P-type calcium transporting ATPase OS=Plasmodium falciparum GN=serca PE=3 SV=1	E1CBY4_PLAFA	E1CBY4	5	2	10	6
78 kDa glucose-regulated protein homolog (Fragment) OS=Plasmodium falciparum PE=2 SV=1	GRP78_PLAFA	P12794	2	1	6	3
GTP-binding nuclear protein Ran OS=Plasmodium falciparum PE=2 SV=1	RAN_PLAFA	P38545	1	1	8	3
240 kDa antibody recognized protein (Fragment) OS=Plasmodium falciparum PE=4 SV=1	Q25018_PLAFA	Q25018	15	3	12	3
Spermidine synthase OS=Plasmodium falciparum GN=spds PE=2 SV=1	Q9NFS5_PLAFA	Q9NFS5	6	2	11	3
Arginase OS=Plasmodium falciparum GN=arg PE=4 SV=1	Q8WPZ7_PLAFA	Q8WPZ7	21	2	10	2
Putative uncharacterized protein (Fragment) OS=Plasmodium falciparum GN=PF07_0004 PE=4 SV=1	D9HMR4_PLAFA	D9HMR4	8	1	9	1
Normocyte binding protein 2b OS=Plasmodium falciparum GN=RBP PE=4 SV=1	Q9BK45_PLAFA	Q9BK45	7	6	9	7
EIF4A-like OS=Plasmodium falciparum PE=2 SV=1	Q2PZH3_PLAFA	Q2PZH3	1	1	8	4
Erythrocyte membrane protein (Fragment) OS=Plasmodium falciparum GN=var PE=4 SV=1	Q3BGT8_PLAFA	Q3BGT8	13	1	17	1
PfsXLX OS=Plasmodium falciparum PE=4 SV=1	Q25857_PLAFA	Q25857	8	6	14	5
Erythrocyte membrane protein 1 (Fragment) OS=Plasmodium falciparum GN=IT4_var18 PE=4 SV=1	A3R6S2_PLAFA	A3R6S2	13	8	13	7
Multi-drug resistance 1 OS=Plasmodium falciparum GN=mdr1 PE=3 SV=1	F1C8N0_PLAFA	F1C8N0	2	2	8	7

Protein	Reference	Accession	RDM		Euge.7	
			# Total Peptides	# Unique Peptides	# Total Peptides	# Unique Peptides
High molecular weight rhoptry protein-2 OS=Plasmodium falciparum GN=rhoph2 PE=2 SV=1	Q8I060_PLAFA	Q8I060	1	1	1	1
Erythrocyte membrane protein 1 OS=Plasmodium falciparum GN=var13.1 PE=4 SV=1	A1KQT2_PLAFA	A1KQT2	5	2	16	6
Erythrocyte membrane protein 1 (Fragment) OS=Plasmodium falciparum GN=var PE=2 SV=1	B5LH34_PLAFA	B5LH34	18	2	16	2
Knob-associated histidine-rich protein OS=Plasmodium falciparum GN=KAHRP PE=4 SV=1	Q9GZ06_PLAFA	Q9GZ06	3	1	15	2
EMP1 (Fragment) OS=Plasmodium falciparum GN=var PE=4 SV=1	I2CIW9_PLAFA	I2CIW9	12	3	14	6
Falcipain 2 OS=Plasmodium falciparum PE=3 SV=1	Q9NAW2_PLAFA	Q9NAW2	9	1	12	3
PfEMP2 (Fragment) OS=Plasmodium falciparum GN=PfEMP2/ MESA/ PP330 PE=4 SV=1	Q06165_PLAFA	Q06165	1	1	24	10
Rhoptry neck protein 2 (Fragment) OS=Plasmodium falciparum GN=ron2 PE=4 SV=1	B9A598_PLAFA	B9A598	12	5	10	4
Signal peptide peptidase OS=Plasmodium falciparum GN=SPP PE=2 SV=1	C0KWU7_PLAFA	C0KWU7	1	1	8	4
Equilibrative nucleoside/nucleobase transporter OS=Plasmodium falciparum GN=NT1 PE=2 SV=1	Q9NIH7_PLAFA	Q9NIH7	1	1	18	6
Myosin PfM-C (Fragment) OS=Plasmodium falciparum PE=4 SV=1	Q9U3U8_PLAFA	Q9U3U8	12	3	18	7
Phosphoribosylpyrophosphate synthetase OS=Plasmodium falciparum GN=prs PE=3 SV=1	Q27726_PLAFA	Q27726	7	1	12	3
Hexose transporter 1 OS=Plasmodium falciparum GN=ht1 PE=2 SV=1	O97467_PLAFA	O97467	2	1	11	6
Erythrocyte membrane protein 1 (Fragment) OS=Plasmodium falciparum GN=var-2361 PE=4 SV=1	F1DC19_PLAFA	F1DC19	9	1	11	2
Erythrocyte membrane protein 1 (Fragment) OS=Plasmodium falciparum GN=varO PE=1 SV=1	B7T1P0_PLAFA	B7T1P0	8	4	5	2
Multidrug resistance protein (Fragment) OS=Plasmodium falciparum GN=mdr PE=4 SV=1	Q5PZ10_PLAFA	Q5PZ10	2	2	4	3
Serine/threonine-protein kinase OS=Plasmodium falciparum GN=pfKIN PE=4 SV=1	Q26018_PLAFA	Q26018	2	2	3	3
Erythrocyte membrane protein 1 (Fragment) OS=Plasmodium falciparum GN=var-2846 PE=4 SV=1	F1DDE0_PLAFA	F1DDE0	7	1	12	1

Protein	Reference	Accession	RDM		Euge.7	
			# Total Peptides	# Unique Peptides	# Total Peptides	# Unique Peptides
Adenine nucleotide translocase OS=Plasmodium falciparum PE=2 SV=1	Q25692_PLAFA	Q25692	1		11	6
ADP-ribosylation factor 1 OS=Plasmodium falciparum GN=ARF1 PE=1 SV=3	ARF1_PLAFA	Q94650	2	1	9	5
VarP (Fragment) OS=Plasmodium falciparum GN=varP PE=4 SV=2	Q9GT78_PLAFA	Q9GT78	4	3	8	3
Mitogen-activated protein kinase 1, serine/threonine protein kinase OS=Plasmodium falciparum GN=pfmap1 PE=2 SV=1	Q94656_PLAFA	Q94656	8	3	7	3
High mobility group-like protein OS=Plasmodium falciparum GN=PS16 PE=4 SV=1	Q25870_PLAFA	Q25870	3	1	6	2
EMP1 (Fragment) OS=Plasmodium falciparum GN=var PE=4 SV=1	I2CIX6_PLAFA	I2CIX6	5	5	6	5
Proton-pumping vacuolar pyrophosphatase OS=Plasmodium falciparum GN=VP1 PE=3 SV=1	O97154_PLAFA	O97154	1		15	7
Erythrocyte membrane protein 1 (Fragment) OS=Plasmodium falciparum GN=IT4_var26 PE=4 SV=1	A3R6S8_PLAFA	A3R6S8	18	5	15	6
Normocyte-binding protein 1 OS=Plasmodium falciparum GN=NBP1 PE=4 SV=1	Q7KF73_PLAFA	Q7KF73	5	5	14	9
Erythrocyte membrane protein (Fragment) OS=Plasmodium falciparum GN=var PE=4 SV=1	Q3BFY1_PLAFA	Q3BFY1	15	2	13	2
Putative cyclin 2 (Fragment) OS=Plasmodium falciparum GN=cyc-2 PE=2 SV=2	Q8T358_PLAFA	Q8T358	13	3	12	5
Histone H3 OS=Plasmodium falciparum PE=2 SV=1	Q27718_PLAFA	Q27718	11	4	11	4
EMP1 (Fragment) OS=Plasmodium falciparum GN=var PE=4 SV=1	I2CIY0_PLAFA	I2CIY0	5	4	10	8
Erythrocyte membrane protein 1 (Fragment) OS=Plasmodium falciparum GN=upsAvar PE=4 SV=1	Q1KV85_PLAFA	Q1KV85	7	1	9	1
VAR2CSA (Fragment) OS=Plasmodium falciparum GN=var2csa PE=4 SV=1	C7FFB9_PLAFA	C7FFB9	7	1	6	1
Erythrocyte membrane protein 1 OS=Plasmodium falciparum GN=IT4_var64 PE=4 SV=1	A3R6V0_PLAFA	A3R6V0	9	7	3	3
Antigen UB05 OS=Plasmodium falciparum PE=4 SV=1	Q38G73_PLAFA	Q38G73	1	1	23	4
MB2 (Fragment) OS=Plasmodium falciparum PE=2 SV=1	Q963G7_PLAFA	Q963G7	9	4	15	2
Erythrocyte membrane protein 1 (Fragment) OS=Plasmodium falciparum GN=var-2238 PE=4 SV=1	F1DBR6_PLAFA	F1DBR6	10	1	14	1
Fibrillarin (Fragment) OS=Plasmodium falciparum GN=fib PE=3 SV=1	O15647_PLAFA	O15647	9	5	13	4

Protein	Reference	Accession	RDM		Euge.7	
			# Total Peptides	# Unique Peptides	# Total Peptides	# Unique Peptides
Var DBLalpha (Fragment) OS=Plasmodium falciparum GN=var PE=4 SV=1	C4PFA7_PLAFA	C4PFA7	11	1	13	2
Phoshoprotein 300 (Fragment) OS=Plasmodium falciparum GN=mesa PE=4 SV=1	Q86BT5_PLAFA	Q86BT5	1		12	5
Erythrocyte membrane protein 3 (Fragment) OS=Plasmodium falciparum GN=EMP3 PE=2 SV=1	Q9U8G1_PLAFA	Q9U8G1	3	2	11	7
Sodium/hydrogen exchanger (Fragment) OS=Plasmodium falciparum GN=nhe-1 PE=4 SV=1	D9IWI5_PLAFA	D9IWI5	2	1	8	5
Erythrocyte membrane protein-1 (Fragment) OS=Plasmodium falciparum GN=var PE=4 SV=1	Q8T5G0_PLAFA	Q8T5G0	6	4	8	7
Erythrocyte membrane protein 1 (Fragment) OS=Plasmodium falciparum GN=EMP1 PE=4 SV=1	G0ZT27_PLAFA	G0ZT27	8	2	8	2
PfEMP1 variant 1 of strain MC OS=Plasmodium falciparum GN=MCvar-1 PfEMP1 PE=1 SV=1	Q25733_PLAFA	Q25733	3	2	5	4
Erythrocyte membrane protein 1 (Fragment) OS=Plasmodium falciparum GN=var PE=2 SV=1	B5LGL3_PLAFA	B5LGL3	5	2	5	2
Erythrocyte membrane protein 1 (Fragment) OS=Plasmodium falciparum PE=4 SV=1	E0A3B2_PLAFA	E0A3B2	14	4	14	5
Mature parasite-infected erythrocyte surface antigen OS=Plasmodium falciparum GN=MESA PE=4 SV=1	Q9NB35_PLAFA	Q9NB35	1		13	5
Erythrocyte membrane protein 1 (Fragment) OS=Plasmodium falciparum GN=IT4_var40 PE=4 SV=1	A3R6T7_PLAFA	A3R6T7	7	2	9	3
Aquaglyceroporin OS=Plasmodium falciparum GN=AQP PE=1 SV=1	Q8WPZ6_PLAFA	Q8WPZ6	1		8	2
RabGDI protein OS=Plasmodium falciparum GN=rabGDI PE=2 SV=1	Q26001_PLAFA	Q26001	1	1	8	1
Dynamin-like protein OS=Plasmodium falciparum GN=dyn PE=2 SV=1	Q9BJC6_PLAFA	Q9BJC6	2	2	8	5
Erythrocyte membrane protein 1 (Fragment) OS=Plasmodium falciparum GN=var PE=4 SV=1	Q8T516_PLAFA	Q8T516	4	1	8	1
Hsp70-like protein (Fragment) OS=Plasmodium falciparum PE=4 SV=1	Q25881_PLAFA	Q25881	1		7	2
Variant-specific surface protein OS=Plasmodium falciparum GN=var-3 PE=4 SV=1	Q26032_PLAFA	Q26032	5	4	4	4
Gp195 surface antigen preprotein OS=Plasmodium falciparum GN=msp1 PE=2 SV=1	Q6LBT0_PLAFA	Q6LBT0	2	2	3	3

Protein	Reference	Accession	RDM		Euge.7	
			# Total Peptides	# Unique Peptides	# Total Peptides	# Unique Peptides
Exported serine/threonine protein kinase OS=Plasmodium falciparum GN=FEST PE=4 SV=1	Q94658_PLAFA	Q94658	1	1	2	2
AARP1 protein (Fragment) OS=Plasmodium falciparum GN=aarp1 PE=2 SV=2	Q94648_PLAFA	Q94648	4	2	9	7
Erythrocyte membrane protein (Fragment) OS=Plasmodium falciparum GN=var PE=4 SV=1	Q3BF55_PLAFA	Q3BF55	9	1	9	1
EMP1 (Fragment) OS=Plasmodium falciparum GN=var PE=4 SV=1	I2CIX4_PLAFA	I2CIX4	7	3	9	5
PfEMP1 (Fragment) OS=Plasmodium falciparum GN=R29R+var1 PE=4 SV=1	O15870_PLAFA	O15870	9	7	8	4
Erythrocyte membrane protein 1 Gb53var3 (Fragment) OS=Plasmodium falciparum PE=4 SV=1	Q8I987_PLAFA	Q8I987	4	1	7	1
Erythrocyte membrane protein 1 OS=Plasmodium falciparum GN=IT4_var54 PE=4 SV=1	A3R6U4_PLAFA	A3R6U4	2	2	6	2
Erythrocyte membrane protein 1 varPAM (Fragment) OS=Plasmodium falciparum PE=4 SV=1	Q6B533_PLAFA	Q6B533	4	3	6	5
Erythrocyte membrane protein 1 (Fragment) OS=Plasmodium falciparum GN=var PE=2 SV=1	B5LHE5_PLAFA	B5LHE5	1		5	1
Erythrocyte membrane protein 1 (Fragment) OS=Plasmodium falciparum GN=upsAvar PE=4 SV=1	Q1KVD7_PLAFA	Q1KVD7	1	1	5	2
DNA-directed RNA polymerase III subunit RPC1 OS=Plasmodium falciparum PE=3 SV=1	RPC1_PLAFA	P27625	1		4	1
Variant-specific surface protein OS=Plasmodium falciparum GN=var-7 PE=4 SV=1	Q26034_PLAFA	Q26034	2	2	4	4
EMP1 variant surface antigen (Fragment) OS=Plasmodium falciparum GN=var PE=2 SV=1	Q1L0A7_PLAFA	Q1L0A7	7	1	3	1
Reticulocyte binding protein 5 OS=Plasmodium falciparum PE=4 SV=1	B2L3N7_PLAFA	B2L3N7	2	1	3	1
Erythrocyte membrane protein 1 type ap (Fragment) OS=Plasmodium falciparum GN=var PE=4 SV=1	O77199_PLAFA	O77199	6	1	15	1
Asparagine-rich antigen Pfa35-2 (Fragment) OS=Plasmodium falciparum GN=Pfa35-2 PE=4 SV=1	Q03628_PLAFA	Q03628	10	1	13	2
Cysteine-rich surface protein (Fragment) OS=Plasmodium falciparum PE=4 SV=1	C5HX54_PLAFA	C5HX54	2	1	11	6
Putative Rab2 GTPase OS=Plasmodium falciparum GN=rab2 PE=2 SV=1	Q9BHT6_PLAFA	Q9BHT6	6	2	9	1

Protein	Reference	Accession	RDM		Euge.7	
			# Total Peptides	# Unique Peptides	# Total Peptides	# Unique Peptides
Merozoite capping protein-1 (Fragment) OS=Plasmodium falciparum PE=4 SV=1	O76465_PLAFA	O76465	1	1	8	2
Dihydroorotate dehydrogenase OS=Plasmodium falciparum GN=dhod PE=4 SV=1	Q54A96_PLAFA	Q54A96	4	3	8	3
Erythrocyte membrane protein 1 (Fragment) OS=Plasmodium falciparum GN=IT4_var41 PE=4 SV=1	A3R6T8_PLAFA	A3R6T8	14	3	8	4
Apicoplast Omp85-like protein OS=Plasmodium falciparum PE=2 SV=1	D6N171_PLAFA	D6N171	5	1	8	2
Cytoadherence linked asexual protein (Fragment) OS=Plasmodium falciparum GN=clag9 PE=2 SV=1	Q9GQ98_PLAFA	Q9GQ98	6	2	7	1
Erythrocyte membrane protein (Fragment) OS=Plasmodium falciparum GN=var PE=2 SV=1	Q3BF74_PLAFA	Q3BF74	10	1	7	1
Erythrocyte membrane protein 2 variant Muz12var1 (Fragment) OS=Plasmodium falciparum PE=4 SV=1	I1X0L4_PLAFA	I1X0L4	4	2	6	5
Chloroquine resistance marker protein OS=Plasmodium falciparum PE=2 SV=1	Q968T7_PLAFA	Q968T7	2	1	6	5
Erythrocyte membrane protein 1 (Fragment) OS=Plasmodium falciparum GN=var PE=4 SV=1	B1P812_PLAFA	B1P812	12	2	6	2
FCR3-varT11-1 protein (Fragment) OS=Plasmodium falciparum GN=FCR3-varT11-1 PE=4 SV=1	P90580_PLAFA	P90580	4	4	5	5
ORF 2 protein (Fragment) OS=Plasmodium falciparum GN=ORF 2 PE=2 SV=1	Q02602_PLAFA	Q02602	1		4	4
Replication factor C subunit 1 OS=Plasmodium falciparum GN=rfc1 PE=4 SV=1	Q9GQW6_PLAFA	Q9GQW6	9	3	4	1
Erythrocyte-binding antigen-175 (Fragment) OS=Plasmodium falciparum GN=EBA-175 PE=2 SV=1	Q95VT1_PLAFA	Q95VT1	7	2	3	3
Merozoite-associated tryptophan-rich antigen 2 OS=Plasmodium falciparum PE=4 SV=1	Q3HSE1_PLAFA	Q3HSE1	4	4	3	2
S-adenosylmethionine synthase OS=Plasmodium falciparum GN=MAT PE=2 SV=1	Q9GN14_PLAFA	Q9GN14	2	1	2	1
Protein kinase OS=Plasmodium falciparum GN=PK1 PE=3 SV=1	Q27739_PLAFA	Q27739	8	2	13	4
PfSNF2L OS=Plasmodium falciparum PE=2 SV=1	O00914_PLAFA	O00914	5	4	11	7
Membrane-associated histidine-rich protein OS=Plasmodium falciparum GN=mahrp1 PE=4 SV=1	Q6V0W7_PLAFA	Q6V0W7	1		10	1
P.falciparum serine-phosphoprotein PP300 DNA, 3' end. (Fragment) OS=Plasmodium	Q25996_PLAFA	Q25996	1		8	2

Protein	Reference	Accession	RDM		Euge.7	
			# Total Peptides	# Unique Peptides	# Total Peptides	# Unique Peptides
falciparum PE=4 SV=1						
EMP1 (Fragment) OS=Plasmodium falciparum GN=var PE=4 SV=1	I2CIW8_PLAFA	I2CIW8	3	3	8	7
Variant-specific surface protein OS=Plasmodium falciparum GN=var-1 PE=4 SV=1	Q26031_PLAFA	Q26031	5	4	8	4
CTRP OS=Plasmodium falciparum PE=4 SV=1	Q25757_PLAFA	Q25757	3	2	8	6
Erythrocyte membrane protein 1 (Fragment) OS=Plasmodium falciparum GN=EMP1 PE=2 SV=1	E5G525_PLAFA	E5G525	5	1	8	1
PfEMP1 DBLa (Fragment) OS=Plasmodium falciparum GN=var PE=2 SV=1	H2B3Q1_PLAFA	H2B3Q1	9	1	7	1
Erythrocyte membrane protein 1 (Fragment) OS=Plasmodium falciparum GN=var PE=2 SV=1	B5LGS8_PLAFA	B5LGS8	2	1	6	1
Erythrocyte membrane protein 1 Gb174var2 (Fragment) OS=Plasmodium falciparum PE=4 SV=1	Q8I9A1_PLAFA	Q8I9A1	3	1	6	2
Variant surface protein PfEMP1 (Fragment) OS=Plasmodium falciparum GN=var PE=4 SV=1	Q9U4A2_PLAFA	Q9U4A2	3	3	6	5
Polyubiquitin OS=Plasmodium falciparum GN=pub PE=4 SV=1	Q9U5M1_PLAFA	Q9U5M1	1	1	5	2
Variant-specific surface protein (Fragment) OS=Plasmodium falciparum GN=varph17 PE=4 SV=1	O61077_PLAFA	O61077	3	3	5	4
Erythrocyte membrane-associated giant protein antigen 332 OS=Plasmodium falciparum PE=4 SV=2	Q9U459_PLAFA	Q9U459	9	5	5	4
Transmission-blocking target antigen Pfs230 OS=Plasmodium falciparum GN=s230 PE=4 SV=1	Q9GTK4_PLAFA	Q9GTK4	3	3	5	1
Multidrug resistance-associated protein 2 OS=Plasmodium falciparum GN=mrp2 PE=2 SV=1	A7XLD6_PLAFA	A7XLD6	1		4	2
Plastidic co-chaperonin OS=Plasmodium falciparum GN=Cpn20 PE=2 SV=1	Q50JA7_PLAFA	Q50JA7	4	1	4	1
NAD(P)H-dependent glutamate synthase OS=Plasmodium falciparum GN=gltS PE=4 SV=1	O61143_PLAFA	O61143	10	7	4	4
EMP1 (Fragment) OS=Plasmodium falciparum GN=var PE=4 SV=1	I2CIX5_PLAFA	I2CIX5	5	4	4	4
Guanidine nucleotide exchange factor (Fragment) OS=Plasmodium falciparum GN=PfRCC1 PE=2 SV=1	O61072_PLAFA	O61072	2	1	4	2

Protein	Reference	Accession	RDM		Euge.7	
			# Total Peptides	# Unique Peptides	# Total Peptides	# Unique Peptides
Reticulocyte binding protein-like protein 4 OS=Plasmodium falciparum GN=rh4 PE=4 SV=1	Q8MWP1_PLAFA	Q8MWP1	1	1	3	3
Merozoite-related surface protein 5 (Fragment) OS=Plasmodium falciparum PE=4 SV=1	C5HE88_PLAFA	C5HE88	4	2	3	1
Glutamate dehydrogenase OS=Plasmodium falciparum GN=gdh PE=4 SV=1	Q9NGT0_PLAFA	Q9NGT0	3	2	3	3
Erythrocyte membrane protein 1 OS=Plasmodium falciparum GN=IT4_var22 PE=4 SV=1	A3R6S4_PLAFA	A3R6S4	4	4	3	3
Erythrocyte membrane protein 1 (Fragment) OS=Plasmodium falciparum GN=var-2639 PE=4 SV=1	F1DCS1_PLAFA	F1DCS1	9	1	3	1
Protein disulfide isomerase OS=Plasmodium falciparum GN=PDI PE=3 SV=1	Q9GRI2_PLAFA	Q9GRI2	1	1	2	2
EMP1 (Fragment) OS=Plasmodium falciparum GN=var PE=4 SV=1	I2CIW6_PLAFA	I2CIW6	1	1	2	2
Myosin D OS=Plasmodium falciparum PE=4 SV=1	Q967M4_PLAFA	Q967M4	4	3	2	1
RIFIN (Fragment) OS=Plasmodium falciparum GN=rif PE=4 SV=1	Q2XRE5_PLAFA	Q2XRE5	1		1	
Tryptophan-rich antigen 3 OS=Plasmodium falciparum PE=4 SV=1	Q5EF37_PLAFA	Q5EF37	7	1	12	2
Proton-pumping vacuolar pyrophosphatase (Fragment) OS=Plasmodium falciparum GN=VP1 PE=2 SV=1	Q9UAS4_PLAFA	Q9UAS4	1		7	3
EMP1 (Fragment) OS=Plasmodium falciparum GN=var PE=4 SV=1	C7BFE9_PLAFA	C7BFE9	4	1	7	1
Glucose-6-phosphate 1-dehydrogenase OS=Plasmodium falciparum PE=4 SV=1	Q27741_PLAFA	Q27741	7	1	7	1
Cytoadherence linked asexual protein (Fragment) OS=Plasmodium falciparum GN=clag9 PE=2 SV=1	Q9GQA1_PLAFA	Q9GQA1	4	1	5	1
Putative uncharacterized protein PF00_0003 (Fragment) OS=Plasmodium falciparum GN=PF00_0003 PE=4 SV=1	Q8IAJ8_PLAFA	Q8IAJ8	2	2	5	4
Small GTP-binding protein OS=Plasmodium falciparum GN=SAR1 PE=3 SV=1	Q9U8B7_PLAFA	Q9U8B7	1		4	3
DEAD box DNA helicase OS=Plasmodium falciparum PE=3 SV=1	Q66WQ1_PLAFA	Q66WQ1	1	1	4	4
Plasmodium falciparum (clone pNM5) ORF (Fragment) OS=Plasmodium falciparum PE=2 SV=1	Q25988_PLAFA	Q25988	1		4	2
SNARE protein OS=Plasmodium falciparum GN=PFI0515W PE=2 SV=1	Q0ZAF8_PLAFA	Q0ZAF8	1		4	2
DNA replication licensing factor MCM5 OS=Plasmodium falciparum GN=mcm5 PE=3	Q8WSL5_PLAFA	Q8WSL5	3	1	4	2

Protein	Reference	Accession	RDM		Euge.7	
			# Total Peptides	# Unique Peptides	# Total Peptides	# Unique Peptides
SV=1						
Erythrocyte membrane protein 1 (Fragment) OS=Plasmodium falciparum GN=IT4_var29 PE=4 SV=1	A3R6T1_PLAFA	A3R6T1	2	2	4	3
RhopH1/Clag3.2 OS=Plasmodium falciparum GN=rhoph1/clag3.2 PE=4 SV=1	B0M163_PLAFA	B0M163	1		3	3
Sexual stage-specific protein kinase OS=Plasmodium falciparum PE=4 SV=1	Q8WSL1_PLAFA	Q8WSL1	1		3	3
Erythrocyte membrane protein 1 (Fragment) OS=Plasmodium falciparum PE=4 SV=1	E0A3B3_PLAFA	E0A3B3	3	3	3	3
EMP1 (Fragment) OS=Plasmodium falciparum GN=var PE=4 SV=1	I2CIX9_PLAFA	I2CIX9	10	5	3	3
Erythrocyte membrane protein 1 (Fragment) OS=Plasmodium falciparum GN=var PE=2 SV=1	Q6S924_PLAFA	Q6S924	1		2	1
DNA mismatch repair enzyme (Fragment) OS=Plasmodium falciparum GN=PF00_0002 PE=3 SV=1	Q8IAJ9_PLAFA	Q8IAJ9	1	1	2	2
Erythrocyte membrane protein 1 (Fragment) OS=Plasmodium falciparum GN=var1 PE=2 SV=1	Q95W83_PLAFA	Q95W83	3	3	2	2
Erythrocyte membrane protein (Fragment) OS=Plasmodium falciparum GN=var PE=4 SV=1	Q3BGP6_PLAFA	Q3BGP6	4	1	2	1
Erythrocyte membrane protein 1 (Fragment) OS=Plasmodium falciparum PE=4 SV=1	E0A3B4_PLAFA	E0A3B4	1	1	2	2
Erythrocyte membrane protein 1 OS=Plasmodium falciparum GN=var PE=4 SV=1	Q6UDW5_PLAFA	Q6UDW5	4	3	2	2
Merozoite surface protein 3 (Fragment) OS=Plasmodium falciparum GN=msp3 PE=4 SV=1	Q9NFV9_PLAFA	Q9NFV9	1	1	2	2
Erythrocyte membrane protein 1 (Fragment) OS=Plasmodium falciparum GN=IT4_var6 PE=4 SV=1	A3R6V1_PLAFA	A3R6V1	1		1	1
Erythrocyte membrane protein 1 (Fragment) OS=Plasmodium falciparum GN=upsAvar PE=4 SV=1	Q1KVB0_PLAFA	Q1KVB0	1	1	1	1
RIFIN (Fragment) OS=Plasmodium falciparum GN=rif PE=4 SV=1	Q2XRB2_PLAFA	Q2XRB2	4	1	1	1
D13 OS=Plasmodium falciparum GN=D13 PE=4 SV=1	Q867W4_PLAFA	Q867W4	2	1	1	1
EMP1 (Fragment) OS=Plasmodium falciparum GN=var PE=4 SV=1	C7BFD9_PLAFA	C7BFD9	2	2		
Erythrocyte membrane protein 1 OS=Plasmodium falciparum GN=IT4_var19 PE=4 SV=1	A3R6S3_PLAFA	A3R6S3	10	4	12	7

Protein	Reference	Accession	RDM		Euge.7	
			# Total Peptides	# Unique Peptides	# Total Peptides	# Unique Peptides
RNA-binding protein Puf1 OS=Plasmodium falciparum PE=2 SV=1	Q8ISI8_PLAFA	Q8ISI8	4	2	10	5
Erythrocyte membrane protein 1 OS=Plasmodium falciparum GN=var PE=4 SV=1	Q6UDX0_PLAFA	Q6UDX0	1	1	9	7
96 tR antigen (Fragment) OS=Plasmodium falciparum PE=4 SV=1	Q25767_PLAFA	Q25767	1		8	3
Erythrocyte membrane protein 1 OS=Plasmodium falciparum GN=var PE=4 SV=1	Q6UDW2_PLAFA	Q6UDW2	1	1	8	3
PfEMP1 variant 2 of strain MC (Fragment) OS=Plasmodium falciparum GN=MCvar-2 PfEMP1 PE=2 SV=1	Q25734_PLAFA	Q25734	4	1	8	2
Merozoite surface protein 1 (Fragment) OS=Plasmodium falciparum GN=MSP-1 PE=4 SV=1	Q56R38_PLAFA	Q56R38	1		7	4
EMP1 (Fragment) OS=Plasmodium falciparum GN=var PE=4 SV=1	I2CIX8_PLAFA	I2CIX8	3	2	7	6
Merozoite surface protein 3 (Fragment) OS=Plasmodium falciparum GN=msp3 PE=4 SV=1	Q0KGB6_PLAFA	Q0KGB6	2	1	6	1
Erythrocyte membrane protein 1 (Fragment) OS=Plasmodium falciparum GN=var PE=2 SV=1	B5LGI9_PLAFA	B5LGI9	9	2	6	1
Erythrocyte membrane protein 1 OS=Plasmodium falciparum GN=IT4_var25 PE=4 SV=1	A3R6S7_PLAFA	A3R6S7	1		5	4
EMP1 variant surface antigen (Fragment) OS=Plasmodium falciparum GN=var PE=2 SV=1	Q1L0A0_PLAFA	Q1L0A0	2	2	5	2
Erythrocyte membrane protein 1 (Fragment) OS=Plasmodium falciparum GN=var PE=2 SV=1	B5LGI6_PLAFA	B5LGI6	1		5	1
EMP1 (Fragment) OS=Plasmodium falciparum GN=P154varH PE=2 SV=1	Q2I5J3_PLAFA	Q2I5J3	3	2	5	2
Chimeric erythrocyte-binding protein MAEBL OS=Plasmodium falciparum GN=maebl PE=4 SV=1	Q8T5C7_PLAFA	Q8T5C7	4	2	5	5
Dihydrolipoamide dehydrogenase OS=Plasmodium falciparum GN=lpd1 PE=2 SV=1	Q5VGY1_PLAFA	Q5VGY1	6	1	5	2

Chapter 6. Conclusions

Traditionally, malaria researchers have avoided directly targeting the parasite-encoded molecules on the surface of IEs for vaccination and have instead focused on merozoites or other stages in the parasite lifecycle. This is despite the fact that 1) IEs are responsible for all of the pathology associated with malaria and are a major target of naturally acquired immunity; 2) nearly all antimalarial drugs clinically established for the prevention or treatment of malaria act by killing IEs; 3) IEs are exposed to potential immune effectors in the blood for many hours during development whereas invasive forms such as merozoites are more transient. The consensus amongst investigators was that the few known parasite proteins expressed on IEs were too antigenically variable to serve as vaccine targets.

6.1 Main conclusions

Here we have generated a set of broadly reactive aptamers and employed them as molecular probes to identify PfHSP90 as a structurally conserved protein displayed on the surface of IEs. Chapter 3 describes the development of a novel aptamer technique, termed Serial-SELEX, which incorporates multiple parasite isolates as the target of *in vitro* evolution to isolate broadly binding aptamers from large randomized nucleic acid libraries. Two Serial-SELEX experiments performed in parallel enriched 11 aptamers that were synthesized and characterized further study. We found that individual aptamers recognized IEs in a sequence dependent manner with estimated dissociation constants in the nanomolar range. We confirmed that our commercially synthesized DNA SELEX libraries are sequence diverse and that enrichment of

aptamers from those libraries was not heavily influenced by the selective biases imposed by PCR, two important firsts for a technology that has been in use for over 20 years.

In Chapter 4 we screened aptamers against a large panel of *Plasmodium* isolates. Consistent with the selection pressure imposed, 10 of 11 enriched aptamers were found to be parasite selective and three of these aptamers demonstrated strain-independent binding to *P. falciparum.* Aptamer recognition extended beyond the parasites used in Serial-SELEX to other laboratory and recent field isolates. Surprisingly the same three broadly binding aptamer selected against *P. falciparum* also recognized all laboratory-adapted and clinical isolates of *P. vivax and P. knowlesi* tested, strongly supporting our hypothesis that structurally conserved molecules are present on the surface IEs.

Finally in Chapter 5, we used biochemical and imaging techniques to characterize the target of our broadly binding aptamers. First, we found that the three aptamers of interests recognized a shared target that was confirmed as an IE surface membrane protein. The pronounced and selective binding aptamers to an unprecedented range of parasites made identification of this aptamer target the highest priority. We used the broadly binding aptamers to purify and identify their binding partner, the *P. falciparum* homologue of HSP90. We showed that a broadly binding aptamer specifically interact with recombinant PfHSP90 but not human homologues and confirm that PfHSP90 is indeed displayed on the IE surface using a *falciparum*-

specific HSP90 antibody. Lastly, we explored the role of surface-displayed PfHSP90 in parasite biology and show that despite its stable display on the surface of a wide variety of circulating parasites, the aptamer binding portion of PfHSP90 is not a target of naturally acquired immunity to malaria.

6.2 Study limitations

Our study has several limitations. First, MESA was recovered from IE membrane pulldowns using Euge.4 and Euge.7 yet MESA has been consistently localized to the cytoplasmic face of the IE plasma membrane as has KAHRP. We believe KAHRP and MESA are simply in complex with PfHSP90 but it may be helpful to formally rule out MESA as a possible aptamer target using MESA deletion lines described previously (57). Second, much of our confirmatory work was done with recombinant C-terminal of PfHSP90. It is conceivable that we will obtain slightly different results with the full-length PfHSP90 protein that is currently in production. Finally, it will be important to further strengthen the observation of PfHSP90 on the IE surface by immunoblotting to examine PfHSP90 susceptibility to extracellular protease. We show that the aptamer target is cleaved by trypsin and pronase E and thus it is expected that PfHSP90 is likewise cleavable. Imaging surface PfHSP09 by indirect immunofluorescence confocal microscopy or immunoelectron microscopy would also bolster our conclusions.

6.3 PfHSP90 as a possible universal malaria vaccine target

Identification of an IE protein conserved between all strains and *P. falciparum* and *P.*

vivax and *P. knowlesi* raises the tantalizing possibility of developing a universal vaccine against human malaria. This is important because in nearly all malaria endemic areas, there exist two or more *Plasmodium* species capable of causing human disease (67, 314). Malaria vaccine development efforts are generally targeted toward a single species without regard to the complex epidemiology of *Plasmodium* or the observation that the elimination of a single species from an endemic area can result in an increase in the incidence and severity of other species (315). Moreover, the current suite of *P. falciparum* blood-stage vaccines induce strain-specific immune responses but provide little clinical protection due to parasite diversity. Targeting a wider variety of haplotypes using divalent or multivalent formulations adds complexity to vaccine manufacture and have so far yielded little clinical efficacy (106, 107). We hypothesize that antibodies induced by vaccinating against PfHSP90 will recognize a wide variety of *P. falciparum* and *P. vivax* - the two human malarias that account for over 95% of the malaria infections worldwide. Furthermore, we predict that these antibodies will be especially potent in facilitating opsonization of parasitized cells by phagocytes expressing antibody Fc receptors because they target an antigen that is stably expressed for hours over the course of parasite development independent of widespread compensatory mutations such as hemoglobin polymorphisms.

The predicted efficacy of a PfHSP90-based vaccine is supported by a series of vaccine studies in squirrel monkeys. Building on previous work showing that drug-controlled infection by *P. falciparum* induces a strong protective immunity in squirrel monkeys (316), Dubois *et al.* showed by immunochemical analysis of IgG preparations that the majority of protective immune responses was directed at an

antigen which was likely PfHSP90 and other presumptive 75-kDA parasite antigen (317). Immunization with PfHSP90-containing parasite preparations in complete Freund's adjuvant strongly protected squirrel monkeys from high-dose homologous blood-stage challenge. Specifically, 9 out of the 10 control animals showed the typical acute course of parasitemia which required quinine chemotherapy within 8 days to avoid death (309). This was in marked contrast to immunized groups where just 1 of 10 monkeys required quinine chemotherapy. Immunity was quite robust as parasitemia in all monkeys in the vaccination group became undetectable within 3 weeks of challenge and remained negative for 2 months whereas 5 of the 9 quinine-treated controls suffered recrudescence (309). These data synergize well with the observation that protection of *Aotus* monkeys against blood-stage infection by *P. falciparum* can be achieved using crude extracts of merozoites or schizonts (318–320).

It would be interesting to follow up these studies with a small PfHSP90 vaccine trial with parasite challenge. With more powerful vectors and safer adjuvants, we predict vaccination against PfHSP90 will give strong protection against both homologous and heterologous blood stage challenge. It would be important to avoid *P. chabaudi* and *P. berghei* as models for human infection because our data suggests that either HSP90 is not displayed or it is sufficiently different from PfHSP90 to avoid recognition by broadly-binding aptamers.

6.4 PfHSP90 as a target for anti-malarial drugs

PfHSP90 is essential for asexual parasite development (306, 307) and has been validated as a potential anti-malarial target *in vitro* and in the *P. berghei* mouse model using the classical HSP90 inhibitor, geldanamycin (GA). There is also evidence PfHSP90 potentiates drug resistance (321), a role for HSP90 first established in fungal systems (294, 322, 323). Treating malaria with GA is unfeasible because it has proven to be too toxic for human application (324). No less than 17 HSP90 inhibitors, many focused on the conserved N-terminal ATP-binding domain, have entered clinical trials (325) but ideally, to avoid any human toxicity, *falciparum*-specific HSP90 inhibitors should be developed. To that end, a study of the crystal structure of N-terminal ATP-binding domain of PfHSP90 reported by Corbett and Berger revealed that several unique residues resulted in a more constricted, basic, and hydrophobic pocket which may be exploited for drug discovery (326). Shahinas *et al.* now describe a naturally derived alkaloid, harmine, which selectively binds the N-terminal ATP-binding domain of PfHSP90, albeit with a micromolar affinity, and gives a small but significant potentiation of the antimalarial effect of chloroquine and artemisinin (327, 328).

The aptamers we have characterized recognize the largely uncharacterized C-terminus of PfHSP90 and efficiently discriminate hHSP90. Assuming aptamer binding inhibits PfHSP90 function, it would be beneficial to derive the aptamer into an antimalarial drug. The large size and negative charge of aptamers and lack of uptake mechanism in mature red blood cells will make cellular penetration a challenge.

Drug-quality small molecules are highly advantageous compared to nucleic acid- or biopolymer-based inhibitors both as probes of PfHSP90 function and as starting points for drug development. Recently, competitive displacement has emerged as a strategy to enable the conversion of an aptamer-protein complex into a small organic inhibitor by screening small-molecule libraries for compounds that displace the aptamer from its target and adopt its inhibitory activity. The success of this method rests on the expectation that a competitor will only elute aptamers with binding sites that overlap with it (329, 330). Others have explored this idea and shown that aptamers can be easily adapted to competitive high-throughput screens to identify functionally analogous small molecule leads (331–333). The aptamer-displacement technology is readily available to academic researchers and a detailed protocol which uses standard laboratory equipment has been published (331).

Bridging drug and vaccine development, it would be useful to co-crystalize aptamer Euge.4 with PfHSP90 to elucidate the conserved aptamer binding site. We suspect that aptamer binding to PfHSP90 induces structural rearrangements not accurately predicted by simple protein or nucleic acid folding programs. Finally, experiments testing competition between aptamers and a prototypic inhibitor of the C-terminal HSP90, novobiocin (334), should reveal whether aptamers target previously unrecognized druggable site.

6.4 Using Serial-SELEX to probe for additional conserved IE determinants

It is curious that all three broadly binding aptamers from our two independent selections recognize PfHSP90. While it may be tempting to conclude that PfHSP90 is the only conserved parasite determinant expressed on the IE surface it is important to note that SELEX libraries are known to converge on a single target even when presented with a complex mixture of possible targets (211, 215). Oligodominance may be a nonrandom phenomenon because it has been shown that repeated selection with the same library enriches for aptamers against the same dominant target (335). We now present data showing that different libraries will produce aptamers against the same dominant target.

Removing the oligodominant protein from a mixture of possible targets allows for the enrichment of aptamers against other targets (211), however, PfHSP90 is essential for parasite growth and likely cannot be deleted. It may be possible to simply mask PfHSP90 with specific antibody or a non-amplifiable aptamer. The role of these masking agents within the selection mixture is to out-compete any PfHSP90 binding sequences, thus allowing aptamers against other targets to be selected more efficiently. Repeating the Serial-SELEX experiment against IEs with naïve LV and LIC libraries spiked with a version of Euge.4 that lacks the primer region for PCR amplification should allow us to better test whether other conserved targets are displayed on IEs. Because it is unclear whether Euge.1 and Euge.7 bind sites identical or partially overlapping with Euge.4, it would be advantageous to include all three broadly binding aptamers in our masking strategy. By extension, we should suppress the enrichment of all 11 tested aptamers since their binding pattern to IEs have already been characterized. We hypothesize that repeating Serial-SELEX with

this masking strategy should enrich a second generation of aptamers, some of which may target novel conserved IEs determinants.

6.5 Other applications of Serial-SELEX

A priori identification of conserved proteins within complex targets by Serial-SELEX and other aptamer based techniques hold great promise for the discovery of proteins not previously associated with a disease state. An obvious extension of our studies would be to probe for conserved targets on other stages in the malaria parasite lifecycle. For example, very little is known about the complement of proteins exposed on the surface of early developing gametocytes and there is growing interest in targeting these proteins for transmission-blocking vaccines. Serial-SELEX and other aptamer-based screens could also prove useful in increasing our understanding of other infectious diseases and neoplasias. For example, cancer cells are incredibly heterogeneous between patients and even within a patient where the different layers of solid tumors represent an increasing lack of cell-cycle regulation from the inside out. With the appropriate use of healthy tissue for counterselection, one could envision Serial-SELEX experiments designed to isolate tumor antigens common between patients or a differential SELEX aimed at identifying early markers of cell-cycle dysregulation.

6.6 Final remarks

Reverse vaccinology, a vaccine development strategy that uses bioinformatics and other tools to identify potential vaccine targets from pathogenic genomes, has

produced a number of promising bacterial vaccine candidates over the past decade (336). The seminal work of Pizza *et al.* took a brute force approach in expressing hundreds of predicted proteins and screening them in a robust surrogate of protection assay (337, 338). Improvements of the technique build on the observation that protective antigens are generally secreted or surface-exposed components and thus subsequent studies have used extracellular proteolysis (339) or intrinsic secretory mechanisms (340, 341) to collect and characterize protective surface determinants. The work described in this thesis provides an important proof of concept that reverse vaccinology approaches can be applied to complex pathogens such as *Plasmodium* and that such screens can be streamlined to target conserved surface determinants, regardless of the whether the pathogen evades immune detection and/or exhibits extensive genetic variability. Our work contributes to a growing body of antigen discovery, vector, and adjuvant work that may help usher in a new era of vaccine development.

Chapter 7. Bibliography

1. World Malaria Report 2011 (2011) *World Heal Organ*.

2. Sachs J, Malaney P (2002) The economic and social burden of malaria. *Nature* 415:680–5.

3. O'Meara WP, Mangeni JN, Steketee R, Greenwood B (2010) Changes in the burden of malaria in sub-Saharan Africa. *Lancet Infect Dis* 10:545–555.

4. Murray CJL et al. (2012) Global malaria mortality between 1980 and 2010: a systematic analysis. *Lancet* 379:413–31.

5. Marsh K (2010) Research priorities for malaria elimination. *Lancet* 6736:7–8.

6. Nzila A, Mwai L (2010) In vitro selection of Plasmodium falciparum drug-resistant parasite lines. *J Antimicrob Chemother* 65:390–8.

7. Noedl H et al. (2008) Evidence of artemisinin-resistant malaria in western Cambodia. *N Engl J Med* 359:2619–20.

8. Malaria Vaccine Technology Roadmap (2006) *PATH Malar Vaccine Initiat*.

9. Alonso PL et al. (2011) A research agenda to underpin malaria eradication. *PLoS Med* 8:e1000406.

10. Sternberg GM (1886) The Malarial Germ of Laveran. *Science* 7:297–9.

11. Smith D, Sanford L (1985) Laveran's germ: the reception and use of a medical discovery. *Am J Trop Med Hyg* 34:2–20.

12. Ross R (1897) Observations on a Condition Necessary to the Transformation of the Malaria Crescent. *BMJ* 1:251–255.

13. Grassi, B., Bignami, A., and Bastianelli G (1899) Ulteriore ricerche sul ciclo dei parassiti malarici umani sul corpo del zanzarone. *Atti R Accad Lincei* 8:21–28.

14. The Nobel Prize in Physiology or Medicine 1902 *Nobelprize.org*.

15. Jin Y, Kebaier C, Vanderberg J (2007) Direct microscopic quantification of dynamics of Plasmodium berghei sporozoite transmission from mosquitoes to mice. *Infect Immun* 75:5532–9.

16. Ménard R (2000) The journey of the malaria sporozoite through its hosts: two parasite proteins lead the way. *Microbes Infect* 2:633–42.

17. Kappe S, Buscaglia C, Nussenzweig V (2004) Plasmodium sporozoite molecular cell biology. *Annu Rev Cell Dev Biol* 20:29–59.

18. Kappe S, Bruderer T, Gantt S (1999) Conservation of a gliding motility and cell invasion machinery in Apicomplexan parasites. *J Cell Biol ...* 147:937–943.

19. Baum J et al. (2006) A conserved molecular motor drives cell invasion and gliding motility across malaria life cycle stages and other apicomplexan parasites. *J Biol Chem* 281:5197–208.

20. Amino R et al. (2006) Quantitative imaging of Plasmodium transmission from mosquito to mammal. *Nat Med* 12:220–4.

21. Voza T, Miller JL, Kappe SHI, Sinnis P (2012) Extrahepatic exoerythrocytic forms of rodent malaria parasites at the site of inoculation: clearance after immunization, susceptibility to primaquine, and contribution to blood-stage infection. *Infect Immun* 80:2158–64.

22. Yamauchi LM, Coppi A, Snounou G, Sinnis P (2007) Plasmodium sporozoites trickle out of the injection site. *Cell Microbiol* 9:1215–22.

23. Cockburn IA et al. (2011) Dendritic cells and hepatocytes use distinct pathways to process protective antigen from plasmodium in vivo. *PLoS Pathog* 7:e1001318.

24. Gueirard P et al. (2010) Development of the malaria parasite in the skin of the mammalian host. *Proc Natl Acad Sci U S A* 107:18640–5.

25. Van de Sand C et al. (2005) The liver stage of Plasmodium berghei inhibits host cell apoptosis. *Mol Microbiol* 58:731–42.

26. Graewe S et al. (2011) Hostile takeover by Plasmodium: reorganization of parasite and host cell membranes during liver stage egress. *PLoS Pathog* 7:e1002224.

27. Singh AP et al. (2007) Plasmodium circumsporozoite protein promotes the development of the liver stages of the parasite. *Cell* 131:492–504.

28. Miller LH, Baruch DI, Marsh K, Doumbo OK (2002) The pathogenic basis of malaria. *Nature* 415:673–9.

29. Cowman AF, Berry D, Baum J (2012) The cellular and molecular basis for

malaria parasite invasion of the human red blood cell. *J Cell Biol* 198:961–71.

30. Duraisingh MT et al. (2003) Phenotypic variation of Plasmodium falciparum merozoite proteins directs receptor targeting for invasion of human erythrocytes. *EMBO J* 22:1047–57.

31. Sim BK, Chitnis CE, Wasniowska K, Hadley TJ, Miller LH (1994) Receptor and ligand domains for invasion of erythrocytes by Plasmodium falciparum. *Science* 264:1941–4.

32. Mayer DCG et al. (2009) Glycophorin B is the erythrocyte receptor of Plasmodium falciparum erythrocyte-binding ligand, EBL-1. *Proc Natl Acad Sci U S A* 106:5348–52.

33. Maier AG et al. (2003) Plasmodium falciparum erythrocyte invasion through glycophorin C and selection for Gerbich negativity in human populations. *Nat Med* 9:87–92.

34. Tham W-H et al. (2010) Complement receptor 1 is the host erythrocyte receptor for Plasmodium falciparum PfRh4 invasion ligand. *Proc Natl Acad Sci U S A* 107:17327–17332.

35. Awandare G a et al. (2011) Plasmodium falciparum field isolates use complement receptor 1 (CR1) as a receptor for invasion of erythrocytes. *Mol Biochem Parasitol* 177:57–60.

36. Douglas AD et al. (2011) The blood-stage malaria antigen PfRH5 is susceptible to vaccine-inducible cross-strain neutralizing antibody. *Nat Commun* 2:601.

37. Crosnier C et al. (2011) Basigin is a receptor essential for erythrocyte invasion by Plasmodium falciparum. *Nature* 480:534–7.

38. Hayton K et al. (2008) Erythrocyte binding protein PfRH5 polymorphisms determine species-specific pathways of Plasmodium falciparum invasion. *Cell Host Microbe* 4:40–51.

39. Baum J et al. (2009) Reticulocyte-binding protein homologue 5 - an essential adhesin involved in invasion of human erythrocytes by Plasmodium falciparum. *Int J Parasitol* 39:371–80.

40. Bustamante LY et al. (2012) A full-length recombinant Plasmodium falciparum PfRH5 protein induces inhibitory antibodies that are effective across common PfRH5 genetic variants. *Vaccine* 31:373–379.

41. Williams AR et al. (2012) Enhancing Blockade of Plasmodium falciparum Erythrocyte Invasion: Assessing Combinations of Antibodies against PfRH5 and Other Merozoite Antigens. *PLoS Pathog* 8:e1002991.

42. De Koning-Ward TF et al. (2009) A newly discovered protein export machine in malaria parasites. *Nature* 459:945–9.

43. Marti M, Good RT, Rug M, Knuepfer E, Cowman AF (2004) Targeting malaria virulence and remodeling proteins to the host erythrocyte. *Science* 306:1930–3.

44. Hiller NL et al. (2004) A host-targeting signal in virulence proteins reveals a secretome in malarial infection. *Science* 306:1934–7.

45. Russo I et al. (2010) Plasmepsin V licenses Plasmodium proteins for export into the host erythrocyte. *Nature* 463:632–6.

46. Boddey J a et al. (2010) An aspartyl protease directs malaria effector proteins to the host cell. *Nature* 463:627–31.

47. Lingelbach K (1997) Protein trafficking in the Plasmodium-falciparum-infected erythrocyte--from models to mechanisms. *Ann Trop Med Parasitol* 91:543–9.

48. Trelka DP, Schneider TG, Reeder JC, Taraschi TF (2000) Evidence for vesicle-mediated trafficking of parasite proteins to the host cell cytosol and erythrocyte surface membrane in Plasmodium falciparum infected ertythrocytes. *Mol Biochem Parasitol* 106:131–145.

49. Acharya P, Chaubey S, Grover M, Tatu U (2012) An exported heat shock protein 40 associates with pathogenesis-related knobs in Plasmodium falciparum infected erythrocytes. *PLoS One* 7:e44605.

50. Bullen HE et al. (2012) Biosynthesis, localization, and macromolecular arrangement of the Plasmodium falciparum translocon of exported proteins (PTEX). *J Biol Chem* 287:7871–84.

51. Ansorge I, Benting J, Bhakdi S, Lingelbach K (1996) Protein sorting in Plasmodium falciparum-infected red blood cells permeabilized with the pore-forming protein streptolysin O. *Biochem J* 315 (Pt 1:307–14.

52. Maier AG, Cooke BM, Cowman AF, Tilley L (2009) Malaria parasite proteins that remodel the host erythrocyte. *Nat Rev Microbiol* 7:341–54.

53. Newbold C et al. (1999) Cytoadherence, pathogenesis and the infected red cell surface in Plasmodium falciparum. *Int J Parasitol* 29:927–37.

54. Viebig NK et al. (2005) A single member of the Plasmodium falciparum var multigene family determines cytoadhesion to the placental receptor chondroitin sulphate A. *EMBO Rep* 6:775–81.

55. Baruch DI, Ma XC, Pasloske B, Howard RJ, Miller LH (1999) CD36 peptides that block cytoadherence define the CD36 binding region for Plasmodium falciparum-infected erythrocytes. *Blood* 94:2121–7.

56. Maier AG et al. (2008) Exported proteins required for virulence and rigidity of Plasmodium falciparum-infected human erythrocytes. *Cell* 134:48–61.

57. Cooke BM, Glenister FK, Mohandas N, Coppel RL (2002) Assignment of functional roles to parasite proteins in malaria-infected red blood cells by competitive flow-based adhesion assay. *Br J Haematol* 117:203–11.

58. Glenister FK (2002) Contribution of parasite proteins to altered mechanical properties of malaria-infected red blood cells. *Blood* 99:1060–1063.

59. Kyes S, Horrocks P, Newbold C (2001) Antigenic variation at the infected red cell surface in malaria. *Annu Rev Microbiol* 55:673–707.

60. Dvorin JD et al. (2010) A Plant-Like Kinase in Plasmodium falciparum Regulates Parasite Egress from Erythrocytes. *Science (80-)* 328:910–912.

61. Arastu-Kapur S et al. (2008) Identification of proteases that regulate erythrocyte rupture by the malaria parasite Plasmodium falciparum. *Nat Chem*

Biol 4:203–13.

62. Millholland MG et al. (2013) A Host GPCR Signaling Network Required for the Cytolysis of Infected Cells Facilitates Release of Apicomplexan Parasites. *Cell Host Microbe* 13:15–28.

63. Niaré O et al. (2002) Genetic loci affecting resistance to human malaria parasites in a West African mosquito vector population. *Science* 298:213–6.

64. Menge DM et al. (2006) Quantitative trait loci controlling refractoriness to Plasmodium falciparum in natural Anopheles gambiae mosquitoes from a malaria-endemic region in western Kenya. *Genetics* 173:235–41.

65. Cirimotich CM et al. (2011) Natural microbe-mediated refractoriness to Plasmodium infection in Anopheles gambiae. *Science* 332:855–8.

66. Krotoski WA et al. (1982) Demonstration of hypnozoites in sporozoite-transmitted Plasmodium vivax infection. *Am J Trop Med Hyg* 31:1291–3.

67. Gething PW et al. (2012) A long neglected world malaria map: Plasmodium vivax endemicity in 2010. *PLoS Negl Trop Dis* 6:e1814.

68. Miller LH, Mason SJ, Dvorak J a, McGinniss MH, Rothman IK (1975) Erythrocyte receptors for (Plasmodium knowlesi) malaria: Duffy blood group determinants. *Science* 189:561–3.

69. Miller LH, Mason SJ, Clyde DF, McGinniss MH (1976) The resistance factor to Plasmodium vivax in blacks. The Duffy-blood-group genotype, FyFy. *N Engl J Med* 295:302–4.

70. Ménard D et al. (2010) Plasmodium vivax clinical malaria is commonly observed in Duffy-negative Malagasy people. *Proc Natl Acad Sci U S A* 107:5967–71.

71. Mendes C et al. (2011) Duffy negative antigen is no longer a barrier to Plasmodium vivax--molecular evidences from the African West Coast (Angola and Equatorial Guinea). *PLoS Negl Trop Dis* 5:e1192.

72. Hay SI, Guerra CA, Tatem AJ, Noor AM, Snow RW (2004) The global distribution and population at risk of malaria: past, present, and future. *Lancet Infect Dis* 4:327–36.

73. Snow RW, Guerra CA, Noor AM, Myint HY, Hay SI (2005) The global distribution of clinical episodes of Plasmodium falciparum malaria. *Nature* 434:214–7.

74. Mueller I et al. (2013) Natural acquisition of immunity to Plasmodium vivax: epidemiological observations and potential targets. *Adv Parasitol* 81:77–131.

75. Hay SI, Guerra CA, Tatem AJ, Atkinson PM, Snow RW (2005) Urbanization, malaria transmission and disease burden in Africa. *Nat Rev Microbiol* 3:81–90.

76. White NJ (1996) The treatment of malaria. *N Engl J Med* 335:800–6.

77. Bejon P et al. (2007) Defining childhood severe falciparum malaria for intervention studies. *PLoS Med* 4:e251.

78. Marsh K et al. (1995) Indicators of life-threatening malaria in African children. *N Engl J Med* 332:1399–404.

79. Marsh K, Kinyanjui S (2006) Immune effector mechanisms in malaria. *Parasite Immunol* 28:51–60.

80. Struik SS, Riley EM (2004) Does malaria suffer from lack of memory? *Immunol Rev* 201:268–90.

81. Gupta S, Snow RW, Donnelly C a, Marsh K, Newbold C (1999) Immunity to non-cerebral severe malaria is acquired after one or two infections. *Nat Med* 5:340–3.

82. Pacheco ND, McConnell E, Beaudoin RL (1979) Duration of immunity following a single vaccination with irradiated sporozoites of Plasmodium berghei. *Bull World Health Organ* 57:159–63.

83. Nussenzweig R, Vanderberg J, Most H, Orton C (1967) Protective Immunity produced by the Injection of X-irradiated Sporozoites of Plasmodium berghei. *Nature* 216:160–162.

84. Nussenzweig V, Nussenzweig RS (1986) Development of a sporozoite malaria vaccine. *Am J Trop Med Hyg* 35:678–88.

85. Kumar KA et al. (2006) The circumsporozoite protein is an immunodominant protective antigen in irradiated sporozoites. *Nature* 444:937–40.

86. Trieu A et al. (2011) Sterile protective immunity to malaria is associated with a panel of novel P. falciparum antigens. *Mol Cell Proteomics* 10:6958–63.

87. Agnandji ST et al. (2011) First results of phase 3 trial of RTS,S/AS01 malaria vaccine in African children. *N Engl J Med* 365:1863–75.

88. Agnandji ST et al. (2012) A phase 3 trial of RTS,S/AS01 malaria vaccine in African infants. *N Engl J Med* 367:2284–95.

89. Olotu A et al. (2013) Four-Year Efficacy of RTS,S/AS01E and Its Interaction with Malaria Exposure. *N Engl J Med* 368:1111–1120.

90. Guinovart C et al. (2009) Insights into Long-Lasting Protection Induced by RTS , S / AS02A Malaria Vaccine : Further Results from a Phase IIb Trial in Mozambican Children. *Vaccine* 4.

91. Bejon P et al. (2013) Efficacy of RTS,S malaria vaccines: individual-participant pooled analysis of phase 2 data. *Lancet Infect Dis* 13:319–327.

92. Stoute JA et al. (1997) A preliminary evaluation of a recombinant circumsporozoite protein vaccine against Plasmodium falciparum malaria. RTS,S Malaria Vaccine Evaluation Group. *N Engl J Med* 336:86–91.

93. Kester KE et al. (2009) Randomized, Double-Blind, Phase 2a Trial of Falciparum Malaria Vaccines RTS,S/AS01B and RTS,S/AS02A in Malaria-Naive Adults: Safety, Efficacy, and Immunologic Associates of Protection. *J Infect Dis* 200:337–346.

94. Kester KE et al. (2008) Phase 2a trial of 0, 1, and 3 month and 0, 7, and 28 day immunization schedules of malaria vaccine RTS,S/AS02 in malaria-naïve adults at the Walter Reed Army Institute of Research. *Vaccine* 26:2191–202.

95. Genton B et al. (2010) Randomized double-blind controlled Phase I/IIa trial to assess the efficacy of malaria vaccine PfCS102 to protect against challenge

with P. falciparum. *Vaccine* 28:6573–80.

96. Walther M et al. (2006) Safety, immunogenicity, and efficacy of prime-boost immunization with recombinant poxvirus FP9 and modified vaccinia virus Ankara encoding the full-length Plasmodium falciparum circumsporozoite protein. *Infect Immun* 74:2706–16.

97. Walther M et al. (2005) Safety, immunogenicity and efficacy of a pre-erythrocytic malaria candidate vaccine, ICC-1132 formulated in Seppic ISA 720. *Vaccine* 23:857–64.

98. Cummings JF et al. (2010) Recombinant Liver Stage Antigen-1 (LSA-1) formulated with AS01 or AS02 is safe, elicits high titer antibody and induces IFN-gamma/IL-2 CD4+ T cells but does not protect against experimental Plasmodium falciparum infection. *Vaccine* 28:5135–44.

99. Ewer KJ et al. (2013) Protective CD8+ T-cell immunity to human malaria induced by chimpanzee adenovirus-MVA immunisation. *Nat Commun* 4:2836.

100. Sabchareon a et al. (1991) Parasitologic and clinical human response to immunoglobulin administration in falciparum malaria. *Am J Trop Med Hyg* 45:297–308.

101. Cohen S, McGregor IA, Carrington S (1961) Gamma-globulin and acquired immunity to human malaria. *Nature* 192:733–7.

102. Logie DE, McGregor IA, Rowe DS, Billewicz WZ (1973) Plasma immunoglobulin concentrations in mothers and newborn children with special reference to placental malaria: Studies in the Gambia, Nigeria, and

Switzerland. *Bull World Health Organ* 49:547–54.

103. Graves P, Gelband H (2006) Vaccines for preventing malaria (blood-stage). *Cochrane Database Syst Rev*:CD006199.

104. Goodman AL, Draper SJ (2010) Blood-stage malaria vaccines - recent progress and future challenges. *Ann Trop Med Parasitol* 104:189–211.

105. Takala SL et al. (2009) Extreme polymorphism in a vaccine antigen and risk of clinical malaria: implications for vaccine development. *Sci Transl Med* 1:2ra5.

106. Duan J et al. (2008) Population structure of the genes encoding the polymorphic Plasmodium falciparum apical membrane antigen 1: implications for vaccine design. *Proc Natl Acad Sci U S A* 105:7857–62.

107. Miura K et al. (2013) Overcoming allelic specificity by immunization with five allelic forms of Plasmodium falciparum apical membrane antigen 1. *Infect Immun* 81:1491–501.

108. Thera M a et al. (2011) A field trial to assess a blood-stage malaria vaccine. *N Engl J Med* 365:1004–13.

109. Lensen AH et al. (1992) Transmission blocking antibody of the Plasmodium falciparum zygote/ookinete surface protein Pfs25 also influences sporozoite development. *Parasite Immunol* 14:471–9.

110. Mendis KN, Munesinghe YD, de Silva YN, Keragalla I, Carter R (1987) Malaria transmission-blocking immunity induced by natural infections of Plasmodium vivax in humans. *Infect Immun* 55:369–72.

111. Bousema JT et al. (2006) Rapid onset of transmission-reducing antibodies in javanese migrants exposed to malaria in papua, indonesia. *Am J Trop Med Hyg* 74:425–31.

112. Saul A (2008) Efficacy model for mosquito stage transmission blocking vaccines for malaria. *Parasitology* 135:1497–506.

113. Wu Y et al. (2008) Phase 1 trial of malaria transmission blocking vaccine candidates Pfs25 and Pvs25 formulated with montanide ISA 51. *PLoS One* 3:e2636.

114. Gregory J a et al. (2012) Algae-produced Pfs25 elicits antibodies that inhibit malaria transmission. *PLoS One* 7:e37179.

115. Da DF et al. (2013) Anti-Pfs25 Human Plasma Reduces Transmission of Plasmodium falciparum Isolates That Have Diverse Genetic Backgrounds. *Infect Immun* 81:1984–9.

116. Bull P, Lowe B, Kortok M, Molyneux C (1998) Parasite antigens on the infected red cell surface are targets for naturally acquired immunity to malaria. *Nat Med* 5:358–360.

117. Mackintosh CL et al. (2008) Failure to respond to the surface of Plasmodium falciparum infected erythrocytes predicts susceptibility to clinical malaria amongst African children. *Int J Parasitol* 38:1445–54.

118. Langhorne J, Ndungu FM, Sponaas A-M, Marsh K (2008) Immunity to malaria: more questions than answers. *Nat Immunol* 9:725–32.

119. Dodoo D et al. (2001) Antibodies to Variant Antigens on the Surfaces of Infected Erythrocytes Are Associated with Protection from Malaria in Ghanaian Children. *Infect Immun* 69:3713–3718.

120. Grun JL, Weidanz WP (1983) Antibody-independent immunity to reinfection malaria in B-cell-deficient mice. *Infect Immun* 41:1197–204.

121. McMorran BJ et al. (2009) Platelets kill intraerythrocytic malarial parasites and mediate survival to infection. *Science* 323:797–800.

122. McMorran BJ et al. (2012) Platelet factor 4 and Duffy antigen required for platelet killing of Plasmodium falciparum. *Science* 338:1348–51.

123. Pombo DJ et al. (2002) Immunity to malaria after administration of ultra-low doses of red cells infected with Plasmodium falciparum. *Lancet* 360:610–7.

124. Pinzon-Charry A et al. (2010) Low doses of killed parasite in CpG elicit vigorous CD4+ T cell responses against blood-stage malaria in mice. *J Clin Invest* 120:2967–78.

125. Baruch DI et al. (1995) Cloning the P. falciparum gene encoding PfEMP1, a malarial variant antigen and adherence receptor on the surface of parasitized human erythrocytes. *Cell* 82:77–87.

126. Smith JD et al. (1995) Switches in expression of Plasmodium falciparum var genes correlate with changes in antigenic and cytoadherent phenotypes of infected erythrocytes. *Cell* 82:101–110.

127. Su XZ et al. (1995) The large diverse gene family var encodes proteins

involved in cytoadherence and antigenic variation of Plasmodium falciparum-infected erythrocytes. *Cell* 82:89–100.

128. David PH, Hommel M, Miller LH, Udeinya IJ, Oligino LD (1983) Parasite sequestration in Plasmodium falciparum malaria: spleen and antibody modulation of cytoadherence of infected erythrocytes. *Proc Natl Acad Sci U S A* 80:5075–9.

129. Rowe JA, Claessens A, Corrigan R a, Arman M (2009) Adhesion of Plasmodium falciparum-infected erythrocytes to human cells: molecular mechanisms and therapeutic implications. *Expert Rev Mol Med* 11:e16.

130. Kyes S, Taylor H, Craig a, Marsh K, Newbold C (1997) Genomic representation of var gene sequences in Plasmodium falciparum field isolates from different geographic regions. *Mol Biochem Parasitol* 87:235–8.

131. Taylor HM, Kyes SA, Newbold CI (2000) Var gene diversity in Plasmodium falciparum is generated by frequent recombination events. *Mol Biochem Parasitol* 110:391–7.

132. Voss TS et al. (2006) A var gene promoter controls allelic exclusion of virulence genes in Plasmodium falciparum malaria. *Nature* 439:1004–8.

133. Kyes S et al. (2007) Plasmodium falciparum var gene expression is developmentally controlled at the level of RNA polymerase II-mediated transcription initiation. *Mol Microbiol* 63:1237–47.

134. Brancucci NMB, Witmer K, Schmid CD, Flueck C, Voss TS (2012) Identification of a cis-acting DNA-protein interaction implicated in singular var

gene choice in Plasmodium falciparum. *Cell Microbiol* 14:1836–48.

135. Duraisingh MT et al. (2005) Heterochromatin silencing and locus repositioning linked to regulation of virulence genes in Plasmodium falciparum. *Cell* 121:13–24.

136. Tonkin CJ et al. (2009) Sir2 paralogues cooperate to regulate virulence genes and antigenic variation in Plasmodium falciparum. *PLoS Biol* 7:e84.

137. Chookajorn T et al. (2007) Epigenetic memory at malaria virulence genes. *Proc Natl Acad Sci U S A* 104:899–902.

138. Merrick CJ, Duraisingh MT (2006) Heterochromatin-mediated control of virulence gene expression. *Mol Microbiol* 62:612–20.

139. Roberts DJ et al. (1992) Rapid switching to multiple antigenic and adhesive phenotypes in malaria. *Nature* 357:689–92.

140. Recker M et al. (2011) Antigenic variation in Plasmodium falciparum malaria involves a highly structured switching pattern. *PLoS Pathog* 7:e1001306.

141. Bull PC et al. (2005) Plasmodium falciparum antigenic variation: relationships between in vivo selection, acquired antibody response, and disease severity. *J Infect Dis* 192:1119–26.

142. Gamain B, Smith JD, Viebig NK, Gysin J, Scherf A (2007) Pregnancy-associated malaria: parasite binding, natural immunity and vaccine development. *Int J Parasitol* 37:273–83.

143. Rogerson SJ, Hviid L, Duffy PE, Leke RFG, Taylor DW (2007) Malaria in

pregnancy: pathogenesis and immunity. *Lancet Infect Dis* 7:105–17.

144. Khunrae P et al. (2010) Full-length recombinant Plasmodium falciparum VAR2CSA binds specifically to CSPG and induces potent parasite adhesion-blocking antibodies. *J Mol Biol* 397:826–34.

145. Avril M et al. (2011) Antibodies to a Full-Length VAR2CSA Immunogen Are Broadly Strain-Transcendent but Do Not Cross-Inhibit Different Placental-Type Parasite Isolates. *PLoS One* 6:e16622.

146. Fried M, Duffy PE (1996) Adherence of Plasmodium falciparum to chondroitin sulfate A in the human placenta. *Science (80-)* 272:1502.

147. Singh K et al. (2008) Structure of the DBL3x domain of pregnancy-associated malaria protein VAR2CSA complexed with chondroitin sulfate A. *Nat Struct Mol Biol* 15:932–938.

148. Salanti A et al. (2003) Selective upregulation of a single distinctly structured var gene in chondroitin sulphate A-adhering Plasmodium falciparum involved in pregnancy-associated malaria. *Mol Microbiol* 49:179–191.

149. Jensen ATR et al. (2004) Plasmodium falciparum associated with severe childhood malaria preferentially expresses PfEMP1 encoded by group A var genes. *J Exp Med* 199:1179–90.

150. Claessens A et al. (2012) A subset of group A-like var genes encodes the malaria parasite ligands for binding to human brain endothelial cells. *Proc Natl Acad Sci U S A* 109:E1772–81.

151. Avril M et al. (2012) A restricted subset of var genes mediates adherence of Plasmodium falciparum-infected erythrocytes to brain endothelial cells. *Proc Natl Acad Sci U S A* 109:E1782–90.

152. Lavstsen T et al. (2012) Plasmodium falciparum erythrocyte membrane protein 1 domain cassettes 8 and 13 are associated with severe malaria in children. *Proc Natl Acad Sci U S A* 109:E1791–800.

153. Cholera R et al. (2008) Impaired cytoadherence of Plasmodium falciparum-infected erythrocytes containing sickle hemoglobin. *Proc Natl Acad Sci U S A* 105:991–6.

154. Fairhurst RM et al. (2005) Abnormal display of PfEMP-1 on erythrocytes carrying haemoglobin C may protect against malaria. *Nature* 435:1117–21.

155. Cyrklaff M et al. (2011) Hemoglobins S and C interfere with actin remodeling in Plasmodium falciparum-infected erythrocytes. *Science* 334:1283–6.

156. Overmann R. (1948) Reversible cellular permeability alterations in disease. In vivo studies on sodium, potassium and chloride concentrations in erythrocytes of the malarious monkey. *Am J Physiol* 152:112–121.

157. Elford BC, Cowan G, Ferguson D (1995) Parasite-regulated membrane transport processes and metabolic control in malaria-infected erythrocytes. *Biochem J* 308:361.

158. Sherman I (2008) New Permeability Pathways and Transport. *Adv Parasitol* 67:151–170.

159. Staines HM et al. (2007) Electrophysiological studies of malaria parasite-infected erythrocytes: current status. *Int J Parasitol* 37:475–82.

160. Desai S a, Bezrukov SM, Zimmerberg J (2000) A voltage-dependent channel involved in nutrient uptake by red blood cells infected with the malaria parasite. *Nature* 406:1001–5.

161. Martin RE, Kirk K (2007) Transport of the essential nutrient isoleucine in human erythrocytes infected with the malaria parasite Plasmodium falciparum. *Blood* 109:2217–2224.

162. Cobbold S a, Martin RE, Kirk K (2010) Methionine transport in the malaria parasite Plasmodium falciparum. *Int J Parasitol* 41:125–135.

163. Elford BC, Haynes JD, Chulay JD, Wilson RJM (1985) Selective Stage-specific Changes in the Permeablity to Human Erythrocytes infected with Plasmodium Falciparum. *Mol Biochem Parasitol* 16:43–60.

164. Saliba KJ, Horner HA, Kirk K (1998) Transport and metabolism of the essential vitamin pantothenic acid in human erythrocytes infected with the malaria parasite Plasmodium falciparum. *J Biol Chem* 273:10190–5.

165. Saliba K, Ferru I, Kirk K (2005) Provitamin B 5 (Pantothenol) Inhibits Growth of the Intraerythrocytic Malaria Parasite. *Antimicrob Agents Chemother* 49:632–637.

166. Kirk K, Horner HA, Elford BC, Ellory JC, Newbold CI (1994) Transport of diverse substrates into malaria-infected erythrocytes via a pathway showing functional characteristics of a chloride channel. *J Biol Chem* 269:3339–47.

167. Lisk G, Kang M, Cohn J V, Desai SA (2006) Specific inhibition of the plasmodial surface anion channel by dantrolene. *Eukaryot Cell* 5:1882–93.

168. Staines H (2004) Furosemide analogues as potent inhibitors of the new permeability pathways of Plasmodium falciparum-infected human erythrocytes. *Mol Biochem Parasitol* 133:315–318.

169. Kang M, Lisk G, Hollingworth S, Baylor SM, Desai SA (2005) Malaria Parasites Are Rapidly Killed by Dantrolene Derivatives Specific for the Plasmodial Surface Anion Channel. *Mol Pharmacol* 68:34–40.

170. Nguitragool W, Bokhari A, Pillai A (2011) Malaria Parasite clag3 Genes Determine Channel-Mediated Nutrient Uptake by Infected Red Blood Cells. *Cell* 145:665–677.

171. Comeaux C a, Coleman BI, Bei AK, Whitehurst N, Duraisingh MT (2011) Functional analysis of epigenetic regulation of tandem RhopH1/clag genes reveals a role in Plasmodium falciparum growth. *Mol Microbiol* 80:378–90.

172. Scherf A, Lopez-Rubio JJ, Riviere L (2008) Antigenic variation in Plasmodium falciparum. *Annu Rev Microbiol* 62:445–70.

173. Bengtsson D et al. (2008) A method for visualizing surface-exposed and internal PfEMP1 adhesion antigens in Plasmodium falciparum infected erythrocytes. *Malar J* 7:101.

174. Kaviratne M, Khan SM, Jarra W, Preiser PR (2002) Small variant STEVOR antigen is uniquely located within Maurer's clefts in Plasmodium falciparum-infected red blood cells. *Eukaryot Cell* 1:926–35.

175. Niang M, Yan Yam X, Preiser PR (2009) The Plasmodium falciparum STEVOR multigene family mediates antigenic variation of the infected erythrocyte. *PLoS Pathog* 5:e1000307.

176. Crabb BS et al. (1997) Targeted gene disruption shows that knobs enable malaria-infected red cells to cytoadhere under physiological shear stress. *Cell* 89:287–96.

177. Wickham ME et al. (2001) Trafficking and assembly of the cytoadherence complex in Plasmodium falciparum-infected human erythrocytes. *EMBO J* 20:5636–49.

178. Waller KL et al. (2003) Mature parasite-infected erythrocyte surface antigen (MESA) of Plasmodium falciparum binds to the 30-kDa domain of protein 4.1 in malaria-infected red blood cells. *Blood* 102:1911–4.

179. Da Silva E et al. (1994) The Plasmodium falciparum protein RESA interacts with the erythrocyte cytoskeleton and modifies erythrocyte thermal stability. *Mol Biochem Parasitol* 66:59–69.

180. Pei X et al. (2007) The ring-infected erythrocyte surface antigen (RESA) of Plasmodium falciparum stabilizes spectrin tetramers and suppresses further invasion. *Blood* 110:1036–42.

181. Mills JP et al. (2007) Effect of plasmodial RESA protein on deformability of human red blood cells harboring Plasmodium falciparum. *Proc Natl Acad Sci U S A* 104:9213–7.

182. Waterkeyn JG et al. (2000) Targeted mutagenesis of Plasmodium falciparum

erythrocyte membrane protein 3 (PfEMP3) disrupts cytoadherence of malaria-infected red blood cells. *EMBO J* 19:2813–23.

183. Pei X, Guo X, Coppel R, Mohandas N, An X (2007) Plasmodium falciparum erythrocyte membrane protein 3 (PfEMP3) destabilizes erythrocyte membrane skeleton. *J Biol Chem* 282:26754–8.

184. Trager W, Jensen JB (1976) Human malaria parasites in continuous culture. *Science* 193:673–5.

185. Gardner MJ et al. (2002) Genome sequence of the human malaria parasite Plasmodium falciparum. *Nature* 419:498–511.

186. Sargeant TJ et al. (2006) Lineage-specific expansion of proteins exported to erythrocytes in malaria parasites. *Genome Biol* 7:R12.

187. Wu Y, Craig A (2006) Comparative proteomic analysis of metabolically labelled proteins from Plasmodium falciparum isolates with different adhesion properties. *Malar J* 5:67.

188. Florens L et al. (2002) A proteomic view of the Plasmodium falciparum life cycle. *Nature* 419:520–6.

189. Fontaine A et al. (2012) Plasmodium falciparum infection-induced changes in erythrocyte membrane proteins. *Parasitol Res* 110:545–56.

190. Sharling L, Sowa KM, Thompson J, Kyriacou HM, Arnot DE (2007) Rapid and specific biotin labelling of the erythrocyte surface antigens of both cultured and ex-vivo Plasmodium parasites. *Malar J* 6:66.

191. Cech TR, Zaug AJ, Grabowski PJ (1981) In vitro splicing of the ribosomal RNA precursor of tetrahymena: Involvement of a guanosine nucleotide in the excision of the intervening sequence. *Cell* 27:487–496.

192. Guerrier-Takada C, Gardiner K, Marsh T, Pace N, Altman S (1983) The RNA moiety of ribonuclease P is the catalytic subunit of the enzyme. *Cell* 35:849–57.

193. Pyle AM (1993) Ribozymes: a distinct class of metalloenzymes. *Science* 261:709–14.

194. Mandal M, Boese B, Barrick JE, Winkler WC, Breaker RR (2003) Riboswitches control fundamental biochemical pathways in Bacillus subtilis and other bacteria. *Cell* 113:577–86.

195. Memczak S et al. (2013) Circular RNAs are a large class of animal RNAs with regulatory potency. *Nature* 495:333–338.

196. Hansen TB et al. (2013) Natural RNA circles function as efficient microRNA sponges. *Nature* 495:384–388.

197. Gilbert W (1986) Origin of life: The RNA world. *Nature* 319:618–618.

198. Oliphant AR, Brandl CJ, Struhl K (1989) Defining the sequence specificity of DNA-binding proteins by selecting binding sites from random-sequence oligonucleotides: analysis of yeast GCN4 protein. *Mol Cell Biol* 9:2944–9.

199. Tuerk C, Gold L (1990) Systematic evolution of ligands by exponential enrichment: RNA ligands to bacteriophage T4 DNA polymerase. *Science*

249:505–10.

200. Ellington AD, Szostak JW (1990) In vitro selection of RNA molecules that bind specific ligands. *Nature* 346:818–22.

201. Glanville J et al. (2009) Precise determination of the diversity of a combinatorial antibody library gives insight into the human immunoglobulin repertoire. *Proc Natl Acad Sci U S A* 106:20216–21.

202. Eda S, Sherman IW (2005) Selection of peptides recognized by human antibodies against the surface of Plasmodium falciparum-infected erythrocytes. *Parasitology* 130:1–11.

203. Barfod A, Persson T, Lindh J (2009) In vitro selection of RNA aptamers against a conserved region of the Plasmodium falciparum erythrocyte membrane protein 1. *Parasitol Res* 105:1557–66.

204. Weissbuch I, Leiserowitz L (2008) Interplay between malaria, crystalline hemozoin formation, and antimalarial drug action and design. *Chem Rev* 108:4899–914.

205. Kapishnikov S et al. (2012) Oriented nucleation of hemozoin at the digestive vacuole membrane in Plasmodium falciparum. *Proc Natl Acad Sci U S A*:1–6.

206. Sullivan DJ, Gluzman IY, Russell DG, Goldberg DE (1996) On the molecular mechanism of chloroquine's antimalarial action. *Proc Natl Acad Sci U S A* 93:11865–70.

207. Niles JC, Derisi JL, Marletta M a (2009) Inhibiting Plasmodium falciparum

growth and heme detoxification pathway using heme-binding DNA aptamers. *Proc Natl Acad Sci U S A* 106:13266–71.

208. White R et al. (2001) Generation of Species Cross-reactive Aptamers Using " Toggle " SELEX. *Gene Ther* 4:567–573.

209. Bock LC, Griffin LC, Latham JA, Vermaas EH, Toole JJ (1992) selection of single-stranded dna molecules that bind and inhibit human thrombin. *Group*.

210. Long SB, Long MB, White RR, Sullenger BA (2008) Crystal structure of an RNA aptamer bound to thrombin. *RNA* 14:2504–12.

211. Fitter S, James R (2005) Deconvolution of a complex target using DNA aptamers. *J Biol Chem* 280:34193.

212. Jenison RD, Gill SC, Pardi a, Polisky B (1994) High-resolution molecular discrimination by RNA. *Science* 263:1425–9.

213. Homann M, Göringer HU (1999) Combinatorial selection of high affinity RNA ligands to live African trypanosomes. *Nucleic Acids Res* 27:2006–14.

214. Homann M, Lorger M, Engstler M, Zacharias M, Göringer HU (2006) Serum-stable RNA aptamers to an invariant surface domain of live African trypanosomes. *Comb Chem High Throughput Screen* 9:491–9.

215. Morris KN, Jensen KB, Julin CM, Weil M, Gold L (1998) High affinity ligands from in vitro selection: complex targets. *Proc Natl Acad Sci U S A* 95:2902–7.

216. Ramos E et al. (2007) A DNA aptamer population specifically detects Leishmania infantum H2A antigen. *Lab Invest* 87:409–16.

217. Parekh P, Tang Z, Turner PC, Moyer RW, Tan W (2010) Aptamers recognizing glycosylated hemagglutinin expressed on the surface of vaccinia virus-infected cells. *Anal Chem* 82:8642–9.

218. Shangguan D et al. (2006) Aptamers evolved from live cells as effective molecular probes for cancer study. *Proc Natl Acad Sci USA* 103:11838–11843.

219. Mi J et al. (2010) In vivo selection of tumor-targeting RNA motifs. *Nat Chem Biol* 6:22–4.

220. Cheng C, Chen YH, Lennox K a, Behlke M a, Davidson BL (2013) In vivo SELEX for Identification of Brain-penetrating Aptamers. *Mol Ther Nucleic Acids* 2:e67.

221. Hicke BJ et al. (2001) Tenascin-C aptamers are generated using tumor cells and purified protein. *J Biol Chem* 276:48644–54.

222. Blank M, Weinschenk T, Priemer M, Schluesener H (2001) Systematic evolution of a DNA aptamer binding to rat brain tumor microvessels. selective targeting of endothelial regulatory protein pigpen. *J Biol Chem* 276:16464–8.

223. Shangguan D et al. (2008) Cell-specific aptamer probes for membrane protein elucidation in cancer cells. *J Proteome Res* 7:2133–9.

224. Wu Y, Sefah K, Liu H, Wang R, Tan W (2010) DNA aptamer-micelle as an efficient detection/delivery vehicle toward cancer cells. *Proc Natl Acad Sci U S A* 107:5–10.

225. Shi H et al. (2011) Activatable aptamer probe for contrast-enhanced in vivo

cancer imaging based on cell membrane protein-triggered conformation alteration. *Proc Natl Acad Sci U S A* 108:3900–5.

226. Douglas SM, Bachelet I, Church GM (2012) A logic-gated nanorobot for targeted transport of molecular payloads. *Science* 335:831–4.

227. Rothemund PWK (2006) Folding DNA to create nanoscale shapes and patterns. *Nature* 440:297–302.

228. Willis MC et al. (1998) Liposome-anchored vascular endothelial growth factor aptamers. *Bioconjug Chem* 9:573–82.

229. Drolet DW et al. (2000) Pharmacokinetics and safety of an anti-vascular endothelial growth factor aptamer (NX1838) following injection into the vitreous humor of rhesus monkeys. *Pharm Res* 17:1503–10.

230. Pieken WA, Olsen DB, Benseler F, Aurup H, Eckstein F (1991) Kinetic characterization of ribonuclease-resistant 2’-modified hammerhead ribozymes. *Science* 253:314–7.

231. Jellinek D et al. (1995) Potent 2’-amino-2'-deoxypyrimidine RNA inhibitors of basic fibroblast growth factor. *Biochemistry* 34:11363–72.

232. Chelliserrykattil J, Ellington AD (2004) Evolution of a T7 RNA polymerase variant that transcribes 2’-O-methyl RNA. *Nat Biotechnol* 22:1155–60.

233. Rhodes a et al. (2000) The generation and characterization of antagonist RNA aptamers to human oncostatin M. *J Biol Chem* 275:28555–61.

234. Beigelman L et al. (1995) Chemical modification of hammerhead ribozymes.

Catalytic activity and nuclease resistance. *J Biol Chem* 270:25702–8.

235. Larocca A et al. (2008) Defibrotide: a review on clinical use and future development. *Expert Opin Biol Ther* 8:1201–12.

236. Ng EWM et al. (2006) Pegaptanib, a targeted anti-VEGF aptamer for ocular vascular disease. *Nat Rev Drug Discov* 5:123–32.

237. Nimjee SM, Rusconi CP, Sullenger BA (2005) Aptamers: an emerging class of therapeutics. *Annu Rev Med* 56:555–83.

238. Keefe AD, Pai S, Ellington A (2010) Aptamers as therapeutics. *Nat Rev Drug Discov* 9:537–50.

239. Nimjee SM et al. (2012) Rapidly regulating platelet activity in vivo with an antidote controlled platelet inhibitor. *Mol Ther* 20:391–7.

240. Oney S et al. (2009) Development of universal antidotes to control aptamer activity. *Nat Med* 15:1224–8.

241. Ostroff RM et al. (2010) Unlocking biomarker discovery: large scale application of aptamer proteomic technology for early detection of lung cancer. *PLoS One* 5:e15003.

242. Gold L et al. (2010) Aptamer-based multiplexed proteomic technology for biomarker discovery. *PLoS One* 5:e15004.

243. Ribaut C et al. (2008) Concentration and purification by magnetic separation of the erythrocytic stages of all human Plasmodium species. *Malar J* 7:45.

244. Aley SB (1984) Knob-positive and knob-negative Plasmodium falciparum differ in expression of a strain-specific malarial antigen on the surface of infected erythrocytes. *J Exp Med* 160:1585–1590.

245. Amaratunga C et al. (2012) Artemisinin-resistant Plasmodium falciparum in Pursat province, western Cambodia: a parasite clearance rate study. *Lancet Infect Dis* 12:851–8.

246. Miura K et al. (2013) Relationship between malaria incidence and IgG levels to Plasmodium falciparum merozoite antigens in Malian children: impact of hemoglobins S and C. *PLoS One* 8:e60182.

247. Boyle MJ et al. (2010) Isolation of viable Plasmodium falciparum merozoites to define erythrocyte invasion events and advance vaccine and drug development. *Proc Natl Acad Sci U S A* 107:14378–83.

248. Ifediba T, Vanderberg JP (1981) Complete in vitro maturation of Plasmodium falciparum gametocytes. *Nature* 294:364–366.

249. Smilkstein M, Sriwilaijaroen N (2004) Simple and Inexpensive Fluorescence-Based Technique for High-Throughput Antimalarial Drug Screening. *Antimicrob Agents Chemother* 48:1803–1806.

250. Murphy M, Fuller S, Richardson P (2003) An improved method for the in vitro evolution of aptamers and applications in protein detection and purification. *Nucleic Acids* 31:1–8.

251. Shangguan D et al. (2008) Identification of liver cancer-specific aptamers using whole live cells. *Anal Chem* 80:721–8.

252. R: A language and environment for statistical computing (2011) *R Found Stat Comput*:Vienna, Austria.

253. Kriek N et al. (2003) Characterization of the pathway for transport of the cytoadherence-mediating protein, PfEMP1, to the host cell surface in malaria parasite-infected erythrocytes. *Mol Microbiol* 50:1215–1227.

254. Zimmermann B, Gesell T, Chen D, Lorenz C, Schroeder R (2010) Monitoring genomic sequences during SELEX using high-throughput sequencing: neutral SELEX. *PLoS One* 5:e9169.

255. Zhao Z et al. (2009) Recognition of subtype non-small cell lung cancer by DNA aptamers selected from living cells. *Analyst* 134:1808–14.

256. Goyal D et al. Modifications to MerMade 192 High Throughput synthesizers for Efficient Aptamer Synthesis. *Screen*:2129–2129.

257. Thiel WH et al. (2011) Nucleotide bias observed with a short SELEX RNA aptamer library. *Nucleic Acid Ther* 21:253–63.

258. Macaya RF, Schultze P, Smith FW, Roe J a, Feigon J (1993) Thrombin-binding DNA aptamer forms a unimolecular quadruplex structure in solution. *Proc Natl Acad Sci U S A* 90:3745–9.

259. Weiss S et al. (1997) RNA aptamers specifically interact with the prion protein PrP. *J Virol* 71:8790–7.

260. Li Y, Geyer CR, Sen D (1996) Recognition of anionic porphyrins by DNA aptamers. *Biochemistry* 35:6911–22.

261. Pologe LG (1994) Aberrant transcription and the failure of Plasmodium falciparum to differentiate into gametocytes. *Mol Biochem Parasitol* 68:35–43.

262. Day K, Karamalis F (1993) Genes necessary for expression of a virulence determinant and for transmission of Plasmodium falciparum are located on a 0.3-megabase region of chromosome 9. *Proc Natl Acad Sci USA* 90:7–11.

263. Looareesuwan S, White N, Bunnag D (1987) High rate of Plasmodium vivax relapse following treatment of falciparum malaria in Thailand. *Lancet* 2:1052–1054.

264. Xu L, Pei X, Berzins K, Chaudhuri A (2007) Plasmodium yoelii: experimental evidences for the conserved epitopes between mouse and human malaria parasite, Plasmodium falciparum. *Exp Parasitol* 116:214–24.

265. Douradinha B, Mota MM, Luty AJF, Sauerwein RW (2008) Cross-species immunity in malaria vaccine development: two, three, or even four for the price of one? *Infect Immun* 76:873–8.

266. Collins WE, Jeffery GM (2002) A retrospective examination of sporozoite-induced and trophozoite-induced infections with Plasmodium ovale: development of parasitologic and clinical immunity during primary infection. *Am J Trop Med Hyg* 66:492–502.

267. Lee M, Lambros C (1988) The ELISA-U: an enzyme-linked immunosorbent assay using urease as the enzyme marker for rapid detection of Plasmodium falciparum antibody in human serum. *Am J Trop Med Hyg* 39:421–6.

268. Bracho C, Perez H (1992) An immunocytochemical test for the diagnosis of

antibodies to Plasmodium vivax. *Parasite Immunol* 14:481–7.

269. Kumar N, Folgar JP, Lubega P (1992) Recognition of Plasmodium falciparum asexual stage antigens by antibodies in sera from people exposed to Plasmodium vivax. *Am J Trop Med Hyg* 47:422–8.

270. Wipasa J et al. (2010) Long-lived antibody and B Cell memory responses to the human malaria parasites, Plasmodium falciparum and Plasmodium vivax. *PLoS Pathog* 6:e1000770.

271. Igonet S et al. (2007) Cross-reactivity studies of an anti-Plasmodium vivax apical membrane antigen 1 monoclonal antibody: binding and structural characterisation. *J Mol Biol* 366:1523–37.

272. Maitland K et al. (1996) The interaction between Plasmodium falciparum and P. vivax in children on Espiritu Santo island, Vanuatu. *Trans R Soc Trop Med Hyg* 90:614–20.

273. Bruce MC, Day KP (2003) Cross-species regulation of Plasmodium parasitemia in semi-immune children from Papua New Guinea. *Trends Parasitol* 19:271–277.

274. Gunewardena DM, Carter R, Mendis KN (1994) Patterns of acquired anti-malarial immunity in Sri Lanka. *Mem Inst Oswaldo Cruz* 89 Suppl 2:63–5.

275. Maitland K, Williams T, Newbold C (1997) Plasmodium vivax and P. falciparum: Biological interactions and the possibility of cross-species immunity. *Parasitol Today* 13.

276. Portugal S et al. (2011) Host-mediated regulation of superinfection in malaria. *Nat Med* 17:732–7.

277. Yewdell JW (2006) Confronting complexity: real-world immunodominance in antiviral CD8+ T cell responses. *Immunity* 25:533–43.

278. Yewdell JW, Bennink JR (1999) Immunodominance in major histocompatibility complex class I-restricted T lymphocyte responses. *Annu Rev Immunol* 17:51–88.

279. Zichel R, Chearwae W, Pandey GS, Golding B, Sauna ZE (2012) Aptamers as a sensitive tool to detect subtle modifications in therapeutic proteins. *PLoS One* 7:e31948.

280. Black CG et al. (2008) In vivo studies support the role of trafficking and cytoskeletal-binding motifs in the interaction of MESA with the membrane skeleton of Plasmodium falciparum-infected red blood cells. *Mol Biochem Parasitol* 160:143–7.

281. Erkeller-Yüksel FM, Isenberg D a, Dhillon VB, Latchman DS, Lydyard PM (1992) Surface expression of heat shock protein 90 by blood mononuclear cells from patients with systemic lupus erythematosus. *J Autoimmun* 5:803–14.

282. Becker B et al. (2004) Induction of Hsp90 protein expression in malignant melanomas and melanoma metastases. *Exp Dermatol* 13:27–32.

283. El Hamidieh A, Grammatikakis N, Patsavoudi E (2012) Cell surface Cdc37 participates in extracellular HSP90 mediated cancer cell invasion. *PLoS One* 7:e42722.

284. Gopal U et al. (2011) A novel extracellular Hsp90 mediated co-receptor function for LRP1 regulates EphA2 dependent glioblastoma cell invasion. *PLoS One* 6:e17649.

285. Rojas P a et al. (2000) Expression of a cDNA encoding a Toxoplasma gondii protein belonging to the heat-shock 90 family and analysis of its antigenicity. *FEMS Microbiol Lett* 190:209–13.

286. Eustace B, Jay D (2005) Functional Proteomics Using Direct Protein Inactivation. *Curr Proteomics* 2:103–107.

287. Péroval M, Péry P, Labbé M (2006) The heat shock protein 90 of Eimeria tenella is essential for invasion of host cell and schizont growth. *Int J Parasitol* 36:1205–15.

288. Banumathy G, Singh V, Tatu U (2002) Host chaperones are recruited in membrane-bound complexes by Plasmodium falciparum. *J Biol Chem* 277:3902–12.

289. Picard D (2002) Heat-shock protein 90, a chaperone for folding and regulation. *Cell Mol Life Sci* 59:1640–8.

290. Walsh N et al. (2011) RNAi knockdown of Hop (Hsp70/Hsp90 organising protein) decreases invasion via MMP-2 down regulation. *Cancer Lett* 306:180–9.

291. Su XZ, Wellems TE (1994) Sequence, transcript characterization and polymorphisms of a Plasmodium falciparum gene belonging to the heat-shock protein (HSP) 90 family. *Gene* 151:225–30.

292. Pavithra SR, Banumathy G, Joy O, Singh V, Tatu U (2004) Recurrent fever promotes Plasmodium falciparum development in human erythrocytes. *J Biol Chem* 279:46692–9.

293. Mahalingam D et al. (2009) Targeting HSP90 for cancer therapy. *Br J Cancer* 100:1523–9.

294. Cowen LE, Lindquist S (2005) Hsp90 potentiates the rapid evolution of new traits: drug resistance in diverse fungi. *Science* 309:2185–9.

295. Shiau AK, Harris SF, Southworth DR, Agard D a (2006) Structural Analysis of E. coli hsp90 reveals dramatic nucleotide-dependent conformational rearrangements. *Cell* 127:329–40.

296. Pearl LH, Prodromou C (2006) Structure and mechanism of the Hsp90 molecular chaperone machinery. *Annu Rev Biochem* 75:271–94.

297. Kumar R, Pavithra SR, Tatu U (2007) Three-dimensional structure of heat shock protein 90 from Plasmodium falciparum: molecular modelling approach to rational drug design against malaria. *J Biosci* 32:531–6.

298. Freeman BC, Myers MP, Schumacher R, Morimoto RI (1995) Identification of a regulatory motif in Hsp70 that affects ATPase activity, substrate binding and interaction with HDJ-1. *EMBO J* 14:2281–92.

299. Akide-Ndunge OB et al. (2009) Co-ordinated stage-dependent enhancement of Plasmodium falciparum antioxidant enzymes and heat shock protein expression in parasites growing in oxidatively stressed or G6PD-deficient red blood cells. *Malar J* 8:113.

300. Acharya P, Kumar R, Tatu U (2007) Chaperoning a cellular upheaval in malaria: heat shock proteins in Plasmodium falciparum. *Mol Biochem Parasitol* 153:85–94.

301. Sidera K, Samiotaki M, Yfanti E, Panayotou G, Patsavoudi E (2004) Involvement of cell surface HSP90 in cell migration reveals a novel role in the developing nervous system. *J Biol Chem* 279:45379–88.

302. Tsutsumi S et al. (2008) A small molecule cell-impermeant Hsp90 antagonist inhibits tumor cell motility and invasion. *Oncogene* 27:2478–87.

303. Matthews RC, Burnie JP, Tabaqchali S (1987) Isolation of immunodominant antigens from sera of patients with systemic candidiasis and characterization of serological response to Candida albicans. *J Clin Microbiol* 25:230–7.

304. Pachl J et al. (2006) A randomized, blinded, multicenter trial of lipid-associated amphotericin B alone versus in combination with an antibody-based inhibitor of heat shock protein 90 in patients with invasive candidiasis. *Clin Infect Dis* 42:1404–13.

305. Horrocks P, Muhia D (2005) Pexel/VTS: a protein-export motif in erythrocytes infected with malaria parasites. *Trends Parasitol* 21:396–9.

306. Banumathy G, Singh V, Pavithra SR, Tatu U (2003) Heat shock protein 90 function is essential for Plasmodium falciparum growth in human erythrocytes. *J Biol Chem* 278:18336–45.

307. Pallavi R et al. (2010) Heat shock protein 90 as a drug target against protozoan infections: biochemical characterization of HSP90 from Plasmodium

falciparum and Trypanosoma evansi and evaluation of its inhibitor as a candidate drug. *J Biol Chem* 285:37964–75.

308. Mahlknecht G et al. (2013) Aptamer to ErbB-2/HER2 enhances degradation of the target and inhibits tumorigenic growth. *Proc Natl Acad Sci U S A* 110:8170–5.

309. Dubois P et al. (1984) Protective immunization of the squirrel monkey against asexual blood stages of Plasmodium falciparum by use of parasite protein fractions. *Proc Natl Acad Sci U S A* 81:229–32.

310. Jendoubi M, Dubois P, Da Silva LP (1985) Characterization of one polypeptide antigen potentially related to protective immunity against the blood infection by Plasmodium falciparum in the squirrel monkey. *J Immunol* 134:1941–5.

311. Wider D, Péli-Gulli M-P, Briand P-A, Tatu U, Picard D (2009) The complementation of yeast with human or Plasmodium falciparum Hsp90 confers differential inhibitor sensitivities. *Mol Biochem Parasitol* 164:147–152.

312. Zhang M et al. (2001) Antibodies specific for heat shock proteins in human and murine malaria. *Microbes Infect* 3:363–7.

313. Pashov A et al. (2002) Autoantibodies to heat shock protein 90 in the human natural antibody repertoire. *Int Immunol* 14:453–61.

314. Guerra C a, Snow RW, Hay SI (2006) Mapping the global extent of malaria in 2005. *Trends Parasitol* 22:353–8.

315. Mayxay M, Pukrittayakamee S, Newton PN, White NJ (2004) Mixed-species

malaria infections in humans. *Trends Parasitol* 20:233–40.

316. Gysin J, Fandeur T, Pereira da Silva L Kinetics of the humoral immune response to blood-induced falciparum malaria in the squirrel monkey Saimiri sciureus. *Ann Immunol (Paris)* 133D:95–102.

317. Gysin J, Dubois P, Pereira da Silva L (1982) Protective antibodies against erythrocytic stages of Plasmodium falciparum in experimental infection of the squirrel monkey, Saimiri sciureus. *Parasite Immunol* 4:421–30.

318. Kan SC, Yamaga KM, Kramer KJ, Case SE, Siddiqui W a (1984) Plasmodium falciparum: protein antigens identified by analysis of serum samples from vaccinated Aotus monkeys. *Infect Immun* 43:276–82.

319. Siddiqui WA (1977) An effective immunization of experimental monkeys against a human malaria parasite, Plasmodium falciparum. *Science* 197:388–9.

320. Siddiqui W a, Taylor DW, Kan SC, Kramer K, Richmond-Crum S (1978) Partial protection of Plasmodium falciparum-vaccinated Aotus trivirgatus against a challenge of a heterologous strain. *Am J Trop Med Hyg* 27:1277–8.

321. Shahinas D, Folefoc A, Pillai D (2013) Targeting Plasmodium falciparum Hsp90: Towards Reversing Antimalarial Resistance. *Pathogens* 2:33–54.

322. Cowen LE et al. (2009) Harnessing Hsp90 function as a powerful, broadly effective therapeutic strategy for fungal infectious disease. *Proc Natl Acad Sci U S A* 106:2818–23.

323. Cowen LE (2009) Hsp90 orchestrates stress response signaling governing

fungal drug resistance. *PLoS Pathog* 5:e1000471.

324. Dey A, Cederbaum AI (2007) Geldanamycin, an inhibitor of Hsp90 increases cytochrome P450 2E1 mediated toxicity in HepG2 cells through sustained activation of the p38MAPK pathway. *Arch Biochem Biophys* 461:275–86.

325. Neckers L, Workman P (2012) Hsp90 molecular chaperone inhibitors: are we there yet? *Clin Cancer Res* 18:64–76.

326. Corbett KD, Berger JM (2010) Structure of the ATP-binding domain of Plasmodium falciparum Hsp90. *Proteins* 78:2738–44.

327. Shahinas D, Macmullin G, Benedict C, Crandall I, Pillai DR (2012) Harmine is a potent antimalarial targeting Hsp90 and synergizes with chloroquine and artemisinin. *Antimicrob Agents Chemother* 56:4207–13.

328. Shahinas D, Liang M, Datti A, Pillai DR (2010) A repurposing strategy identifies novel synergistic inhibitors of Plasmodium falciparum heat shock protein 90. *J Med Chem* 53:3552–7.

329. Ulrich H, Magdesian MH, Alves MJM, Colli W (2002) In vitro selection of RNA aptamers that bind to cell adhesion receptors of Trypanosoma cruzi and inhibit cell invasion. *J Biol Chem* 277:20756–62.

330. Bridonneau P, Chang YF, Buvoli a V, O'Connell D, Parma D (1999) Site-directed selection of oligonucleotide antagonists by competitive elution. *Antisense Nucleic Acid Drug Dev* 9:1–11.

331. Hafner M et al. (2008) Displacement of protein-bound aptamers with small

molecules screened by fluorescence polarization. *Nat Protoc* 3:579–87.

332. Yamazaki S et al. (2007) Aptamer displacement identifies alternative small-molecule target sites that escape viral resistance. *Chem Biol* 14:804–12.

333. Bill A et al. (2010) Cytohesins Are Cytoplasmic ErbB Receptor Activators. *Cell* 143:201–11.

334. Marcu MG, Chadli a, Bouhouche I, Catelli M, Neckers LM (2000) The heat shock protein 90 antagonist novobiocin interacts with a previously unrecognized ATP-binding domain in the carboxyl terminus of the chaperone. *J Biol Chem* 275:37181–6.

335. Sefah K et al. (2010) DNA aptamers as molecular probes for colorectal cancer study. *PLoS One* 5:e14269.

336. Sette A, Rappuoli R (2010) Reverse vaccinology: developing vaccines in the era of genomics. *Immunity* 33:530–41.

337. Pizza M (2000) Identification of Vaccine Candidates Against Serogroup B Meningococcus by Whole-Genome Sequencing. *Science (80-)* 287:1816–1820.

338. Grifantini R et al. (2002) Previously unrecognized vaccine candidates against group B meningococcus identified by DNA microarrays. *Nat Biotechnol* 20:914–21.

339. Rodríguez-Ortega MJ et al. (2006) Characterization and identification of vaccine candidate proteins through analysis of the group A Streptococcus

surface proteome. *Nat Biotechnol* 24:191–7.

340. Ferrari G et al. (2006) Outer membrane vesicles from group B Neisseria meningitidis delta gna33 mutant: proteomic and immunological comparison with detergent-derived outer membrane vesicles. *Proteomics* 6:1856–66.

341. Giuliani MM et al. (2006) A universal vaccine for serogroup B meningococcus. *Proc Natl Acad Sci U S A* 103:10834–9.